Chem Soc Rev

REVIEW ARTICLE

View Article Online
View Journal | View Issue

Cite this: *Chem. Soc. Rev.*, 2025, **54**, 4353

Insights into the mechanism of 3d transition-metal-catalyzed directed C(sp^3)–H bond functionalization reactions

Andrés García-Viada, [a] Juan C. Carretero, [abc] Javier Adrio *[abc] and Nuria Rodríguez *[abc]

Received 14th October 2024

DOI: 10.1039/d4cs00657g

rsc.li/chem-soc-rev

The growing interest in the catalytic activity of earth-abundant 3d transition-metals has led to the development of new and more sustainable methods for C–H bond functionalization reactions. However, this is an emerging field which involves considerable mechanistic complexity as the mode of action of 3d transition metals differs markedly from the well-studied mechanisms of precious metals. In this review, we present an overview of the research efforts in Ni-, Cu-, Fe- and Co-catalyzed directed C(sp^3)–H bond functionalization reactions, covering design principles and mechanistic discussions, along with potential applications and limitations. To conclude, the unresolved challenges and future viewpoints are highlighted. We aspire for this review to serve as a relevant and valuable reference for researchers in this swiftly progressing field, helping to inspire the development of more original and innovative strategies.

1. Introduction

Transition-metal-catalyzed C–H bond functionalization has changed the mindset about the "inactivity" of these bonds, opening new retrosynthetic pathways that sidestep the need for pre-activated compounds.[1–4] This breakthrough minimizes synthetic steps and reduces the production of undesired by-products in total synthesis.[5–10] However, attaining site selectivity for the target C–H bond among numerous others in the substrate remains a significant challenge in C–H functionalization.[11–25] Often, this problem is solved using directing groups (DGs). A DG is a basic functional group able to coordinate the metal catalyst, bringing it in proximity to the desired C–H bond, facilitating its regioselective activation and subsequent functionalization.[26–35]

[a] *Dpto. de Química Orgánica, Facultad de Ciencias, Universidad Autónoma de Madrid (UAM), Cantoblanco, 28049, Madrid, Spain. E-mail: javier.adrio@uam.es, n.rodriguez@uam.es*
[b] *Institute for Advanced Research in Chemical Sciences (IAdChem), UAM, 28049 Madrid, Spain*
[c] *Center for Innovation in Advanced Chemistry (ORFEO-CINQA), Madrid, Spain*

Andrés García-Viada

Andrés García-Viada obtained his BSc in Chemistry in 2019 from Universidad Autónoma de Madrid and his MSc in 2020 at the same university. He is currently doing his PhD at the Universidad Autónoma de Madrid under the supervision of Prof. Juan Carlos Carretero and Prof. Nuria Rodríguez. His research focuses on the selective functionalization of aliphatic C–H bonds using directing groups as structural tool for the control of the selectivity.

Juan C. Carretero

Juan Carlos Carretero received his PhD from the Universidad Autónoma de Madrid (UAM) in 1985 with Prof. José L. García Ruano. After postdoctoral studies at the Université Catholique de Louvain (Belgium) with Prof. Léon Ghosez, he joined the Department of Organic Chemistry of the UAM and became Associate Professor in 1988 and Professor of Organic Chemistry in 2000. His research interests are focused on developing new methodologies in asymmetric catalysis, C–H functionalization and stereocontrolled metal-catalyzed processes.

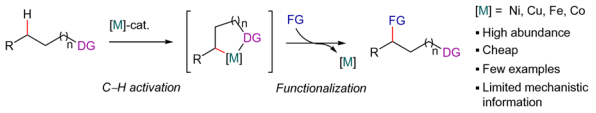

Scheme 1 3d TM-catalyzed directed C(sp^3)–H bond functionalization reactions.

Directed C(sp^3)–H functionalization is notably challenging due to the greater conformational flexibility and less favourable orbital interactions between the σ* orbitals of the C–H bonds and the metal's d orbitals, in contrast to the more favourable interactions observed with sp^2 centers.[36–43] However, direct functionalization of sp^3 centers is of great interest in many areas, including the increase in the three-dimensional character of pharmacological compounds to improve their selectivity and efficiency.[8–10,44–47]

To date, this is an area in which catalysis with noble metal-based complexes has dominated, with palladium standing out among them mainly because of its low activation barrier during the change of redox state and its compatibility with many different ligands and oxidants.[48–55] In the past decade, however, chemists have pursued sustainable methods for C(sp^3)–H bond functionalization using abundant and cost-effective 3d transition metal catalysts (Scheme 1).[29,40,56–60] This leap to the use of 3d transition-metals holds considerable mechanistic complexity, as the mode of action of 3d transition metals may differ from the well-studied mechanisms of precious metals. Therefore, innovation in this arena goes hand in hand with progress in the analysis and understanding of the mechanistic peculiarities that govern these processes.

Recently published reviews have addressed specific aspects of the evolution of 3d transition-metal-catalyzed directed C(sp^3)–H bond functionalization reactions.[40,43,61–64] While these reports offer valuable insights, they do not provide broad mechanistic discussions. Covering this aspect, this article aims to present a thorough review of these methodologies, encompassing their scope, limitations and digging into the reaction mechanisms by highlighting key catalytic systems and integrating mechanistic insights. For example, a description of the oxidation states of the metal centers in the intermediate species, the role of additives and/or co-catalysts, isolated intermediates, deuterium scrambling experiments, KIE studies, and DFT calculations.

The content has been organized according to the metal employed (Ni, Cu, Fe and Co) and the nature of the bond formed (C–C, C–N, C–O and C–S). Although significant advances have been made in Mn catalysis,[65–67] progress in Mn-catalyzed functionalization of inert C(sp^3)–H bonds is beyond the scope of this review of directed transformations.

By understanding these recent advances and underlying principles, we hope that this review will be handy for researchers to further expand the potential of organic synthesis, ultimately contributing to the development of novel, sustainable, and efficient 3d-transition metal-catalyzed synthetic methodologies.

2. Ni-catalysis

Nickel, a group 10 metal located just above palladium, represents one of the most prominent alternatives for replacing noble metals.[68] Inherent advantages of nickel-catalysis include a wide range of catalytically active oxidation states (ranging from 0 to +4), high abundance in the earth's crust and comparatively low cost.

Its ability to activate C–H bonds was first demonstrated in the 1960s by Dubeck *et al.* in their study of the cyclometalation of azobenzene with Cp_2Ni.[69] However, it was not until the early 2000s that nickel-catalyzed chelation-assisted C–H functionalization

Javier Adrio

Javier Adrio completed his PhD in Organic Chemistry at the Universidad Autónoma de Madrid under the supervision of Prof. Juan Carlos Carretero. From 2001 to 2003 he worked as a senior scientist on PharmaMar. During this period, he also pursued postdoctoral studies at the University of Pennsylvania under the supervision of Professor Madeleine Joullié. He returned to UAM as a Ramón y Cajal researcher, a position he held until his appointment as Associate Professor in 2010 and subsequently as Professor in 2022. Throughout his career, he has undertaken several short research stays as a Visiting Scholar at the University of Pennsylvania, collaborating with Professor Patrick Walsh's lab. His research interest focus on metal-catalyzed reactions, C–H functionalization processes and catalytic asymmetric methodologies.

Nuria Rodríguez

Nuria Rodríguez was born in 1978 in Valencia (Spain). She received her D. Chem. in 2006 from the Department of Organic Chemistry at the University of Valencia (Spain) under the guidance of Professors G. Asensio and M. Medio-Simón. After spending about five years with Professor L. J. Gooßen at the Technische University of Kaiserslautern (Germany), in 2011 she took up a Ramón y Cajal researcher position at the University of Madrid (Spain), where she remains active as Associate Professor. Her major research goals now are the direct and selective functionalization of inert carbon–hydrogen bonds.

began to emerge as a prominent alternative, especially with regard to C(sp^2)–H bond functionalization.[64,70–73] In contrast, the functionalization of unactivated aliphatic C–H bonds remains in its early stages. The following sections highlight key contributions, covering mechanistic discussions and potential applications.[63]

2.1. C–C bond formation

2.1.1. Arylation processes. In a pioneering contribution in 2014, Chatani *et al.* reported the 8-aminoquinoline (8-AQ)-assisted nickel(II)-catalyzed direct arylation of β-C(sp^3)–H bonds in aliphatic amides using aryl iodides as coupling partners (Scheme 2).[74] The reaction efficiently occurred in the presence of $Ni(OTf)_2$ as catalyst precursor, the sterically bulky 2,4,6-trimethylbenzoic acid ($MesCO_2H$) as additive and Na_2CO_3 as base, in DMF at 140 °C for 24 h. Under these conditions, electronically diverse *para*-substituted aryl iodides gave good to excellent yields, even in the presence of sensitive free amino and iodide groups. Among them, electron-rich aryl iodides typically lead to slightly higher yields compared to their electron-poor counterparts. However, *ortho*-substituted aryl iodides were unreactive. The reaction was sensitive to the structure of the amides; while aliphatic amides quaternized at the α-position reacted efficiently, yields from α-tertiary propanamides were significantly lower and no reactivity was observed with simple propanamide derivatives. In most cases, the reaction proceeded exclusively at the methyl group, and methylene and aryl C–H bonds were not arylated. Nonetheless, the reaction of cycloheptane derivative gave a mixture of mono-arylated and biarylated products, the latter involving the arylation at the cyclic methylene C–H bond. Likewise, the β-methylene C–H arylation in 1-phenylcyclobutyl and 1-phenylcyclopentyl derivatives occurred smoothly, giving mixtures of mono- and diarylated products.

Parallel to this work, You *et al.* published a similar reactivity using aryl iodides and bromides as coupling partners (Scheme 3).[75] In this case, $Ni(OTf)_2$ was also used as catalyst precursor, along with pivalic acid (PivOH) as additive, Na_2CO_3 as base and PPh_3 as ligand, in DMSO/1,4-dioxane solvent mixture at 160 °C for 36 h. Remarkably, this methodology was suitable for the functionalization of both α-quaternary and α-tertiary propanamides. The system was selective for the

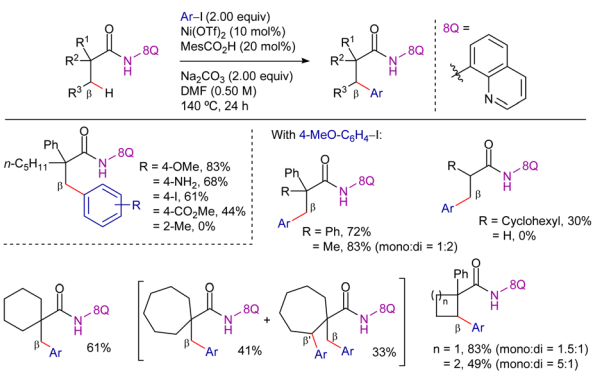

Scheme 2 β-C(sp^3)–H arylation of amides with iodoarenes.

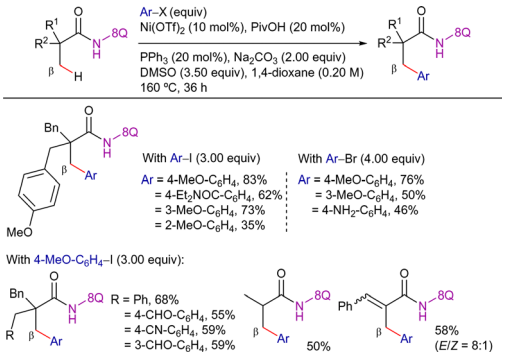

Scheme 3 Ni-cat. β-C(sp^3)–H arylation of aliphatic amides with aryl halides.

β-CH_3 functionalization, maintaining this selectivity even in the case of 2-methyl-3-phenylacrylamide derivative.

Regarding the reaction mechanism, Chatani *et al.* conducted deuterium-labeling experiments and observed H/D exchange in both the product and the recovered amide (Scheme 4). Based on these findings, the C–H bond cleavage is presumably reversible and occurs rapidly, preceding the addition of the aryl halide. Furthermore, the addition of 2,2,6,6-tetramethyl-1-piperidinoxyl (TEMPO) did not inhibit the reaction, suggesting that a single-electron transfer (SET) mechanism is not involved. On this basis, Chatani proposed the Ni^{II}/Ni^{IV} catalytic cycle depicted in Scheme 4. The process starts with the *N*,*N*-coordination of the amide derivative to the nickel(II)-catalyst followed by the reversible C(sp^3)–H bond cleavage *via* a base-assisted concerted metalation-deprotonation mechanism (CMD), forming the nickel(II)-cyclometalated intermediate **II**. Subsequently, oxidative addition of the aryl halide leads to the highly oxidized nickel(IV)-complex **III**, from which the β-arylated product is formed through reductive elimination and protodemetalation, closing thus the catalytic cycle. This

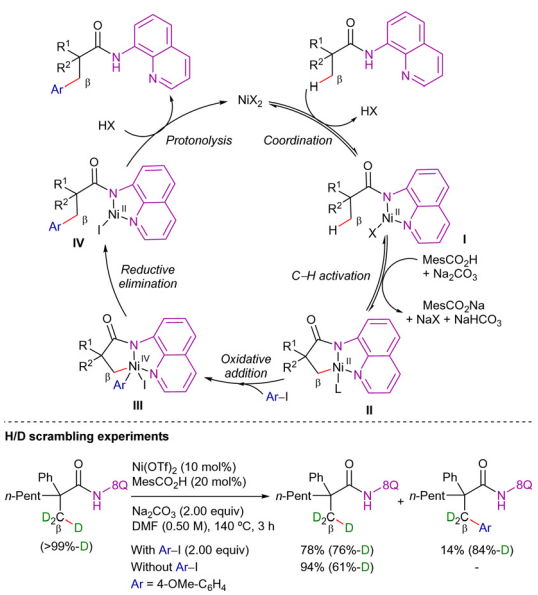

Scheme 4 β-C(sp^3)–H arylation with aryl halides. Mechanistic hypothesis.

mechanistic pathway closely resembles those proposed for heavier metal catalysts.[50,76]

Moreover, this pathway was further supported by the computational studies conducted by Liu and Sunoj.[77,78] Both authors discarded a radical pathway involving Ni^{III} due to the inherent instability of phenyl radicals, highlighting certain distinctions from Pd chemistry. According to their computational studies, the formation of the nickelacycle **II** seems to be thermodynamically less favourable than the corresponding C–H metalation process with a palladium(II)-catalyst (with a difference of 1.6 kcal mol^{-1}). The optimized transition state geometries suggest a later transition state in the metalation step with the nickel catalyst compared to palladium, which aligns with the predictions of the Hammond postulate. Furthermore, while the C–H metalation step with the palladium catalyst is most likely the *r.d.s.* step, in nickel arylation, the C–H metalation step is reversible and the subsequent oxidative addition step with the aryliodide is the *r.d.s.* Nonetheless, the barrier of the oxidative addition (~14.3 kcal mol^{-1} for PhI) did not justify experimentally requiring high temperatures (140–160 °C).

Shedding light on this point, mechanistic studies reported by Johnson *et al.*[79] showed that the intermediates prior to C–H activation and after functionalization were not diamagnetic but paramagnetic nickel(II)-species. Moreover, both the C–H activation and oxidative addition steps occurred stoichiometrically at 80 °C, a temperature much lower than the temperatures required for catalysis. On this basis, the authors postulated that under the original catalytic conditions employing Na_2CO_3 as a base, the deprotonation and binding of the substrate to the nickel-center was possibly the *r.d.s.* due to the insufficient basicity of Na_2CO_3. In fact, using Na^tBuO as base, the reaction occurred at only 100 °C rather than 140–160 °C required when Na_2CO_3 was used. Nevertheless, catalysis proceeded smoothly at higher temperatures, and the use of 10 equivalents of Na^tBuO resulted in a 94% conversion to the triarylated product (Scheme 5).

Complementing the structural versatility of Chatani's and You's methodologies, Xu and Qiu disclosed the 8-AQ-assisted nickel(II)-catalyzed β-C(sp^3)–H heteroarylation of aliphatic amides using heteroaryl bromides as coupling partners (Scheme 6).[80] The reaction proceeded efficiently using $NiBr_2$ as the catalyst precursor, $MesCO_2H$ and tetrabutylammonium iodide (TBAI) as additives, Na_2CO_3 as base, in DMF at 160 °C for 24 h. Overall, the reactivity pattern resembled that observed in previous couplings with aryl bromides,[75] with electron-rich heteroarenes demonstrating better reactivity than their electron-deficient counterparts. Interestingly, in this work, the

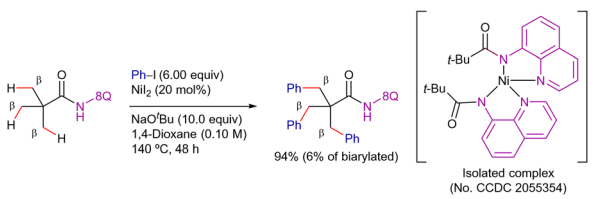

Scheme 5 β-C(sp^3)–H tri-arylation of pivalamide derivative.

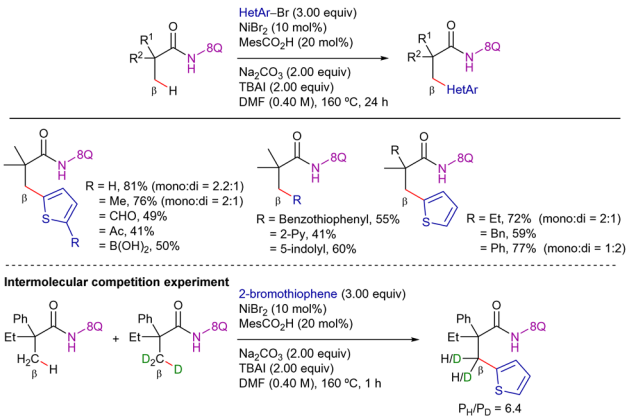

Scheme 6 Ni-cat. β-C(sp^3)–H arylation with heteroarylbromides.

authors proposed a Ni^{II}/Ni^{IV} catalytic cycle involving diamagnetic mononuclear intermediates but pointing that in the coupling with heteroaryl bromides, the C–H bond cleavage seemed to be the *r.d.s.* (KIE = 6.4). The efficient removal of the 8-AQ moiety under basic conditions enhanced the practicability of the method (Scheme 7).

Alternatively, Chatani *et al.* demonstrated the viability of the 8-AQ-assisted nickel-catalyzed β-C(sp^3)–H arylation of aliphatic amides with diaryliodonium salts as electrophilic coupling partners (Scheme 8).[81] In this case, the optimal reaction conditions were $Ni(OTf)_2$ as catalyst precursor, Na_2CO_3 as base in 4-methyltetrahydro-2*H*-pyran (MTHP) at 140 °C for 24 h. Although diaryliodonium salts can decompose into aryl iodides and aryl triflates under these basic conditions at high temperatures, the authors showed that neither of them was suitable coupling partners in this process. Consequently, the diaryliodonium salts

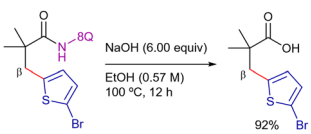

Scheme 7 Removal of the 8-AQ with sodium hydroxide.

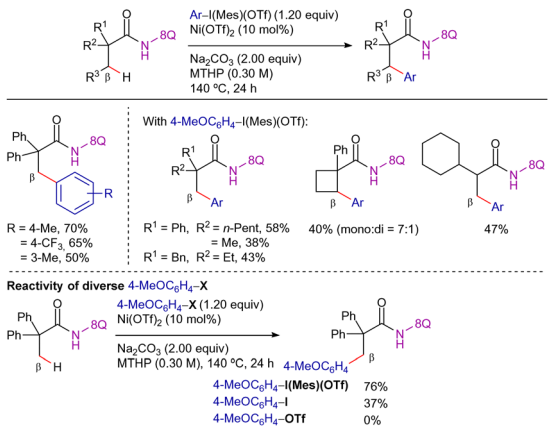

Scheme 8 β-C(sp^3)–H arylation with diaryliodonium salts.

acted as both coupling partners and oxidants. Interestingly, the method was suitable for the functionalization of methyl and methylene positions in α,α- and α-substituted propanamide derivatives.

In this work, H/D scrambling experiments showed deuterium incorporation at the *β*-position, suggesting that the C–H bond cleavage was reversible (Scheme 9). Moreover, as the H/D scrambling in the absence of the hypervalent iodide was higher than in its presence, the authors proposed that the oxidative addition step would take place after the C–H activation step. Furthermore, the addition of TEMPO to the reaction did not have much effect, suggesting that radical species were not involved in the reaction pathway.

Along these studies, the authors proposed the Ni^{II}/Ni^{IV} catalytic cycle disclosed in Scheme 9.[82] This hypothesis was closely related to the mechanism suggested for the coupling with aryl halides. The cycle consists of (i) AQ-directed C–H activation leading to metallacycle **II**, (ii) oxidative addition of the diaryliodonium salt to form the cationic nickel(IV) intermediate **V**, and (iii) C–C bond-forming reductive elimination, followed by protonolysis to yield the functionalized product.

Taking this mechanism as reference, Sanford *et al.* disclosed a ligand design strategy to isolate a cyclometallated nickel(IV) complex similar to the key intermediate proposed in the aforementioned processes (Scheme 10).[83] The reaction of the anionic nickel(II)-picolinate with the diaryliodonium salt resulted in the formation of a stable nickel(IV) σ-aryl complex at room temperature. This complex subsequently underwent $C(sp^3)$–$C(sp^2)$ bond-coupling *via* reductive elimination in almost quantitative yield under mild conditions (70 °C, 120 min). The authors suggested that the high temperatures required for the catalytic reaction may be due to slow $C(sp^3)$–H activation and/or to the formation of off-cycle Ni-species. Note that in these studies, no diamagnetic Ni-intermediates were detected by ^{1}H-NMR spectroscopy under any conditions.

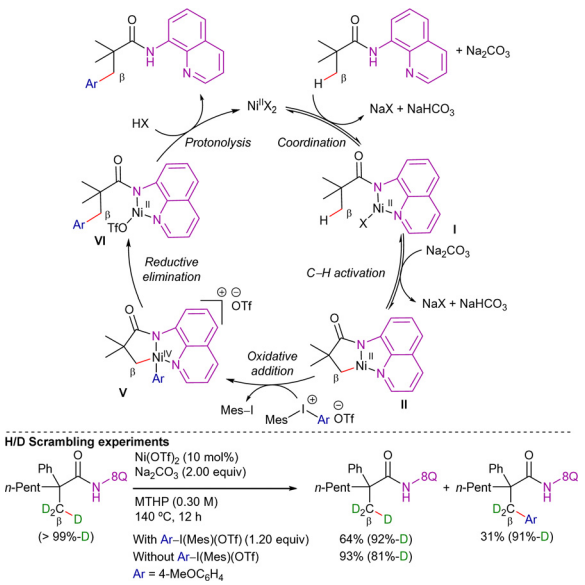

Scheme 9 β-$C(sp^3)$–H arylation with iodonium salts. Mechanistic hypothesis.

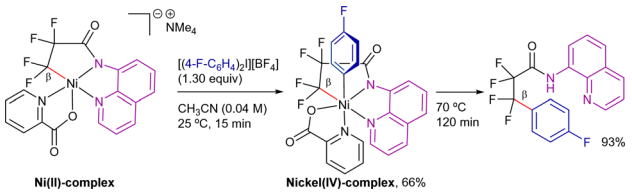

Scheme 10 Nickel(IV)-intermediates in 8-AQ-directed $C(sp^3)$–$C(sp^2)$ coupling.

As an alternative strategy for $C(sp^3)$–H arylation, Xia and Yin reported the Ni-catalyzed oxidative C–H/C–H cross-dehydrogenative coupling (CDC) reaction as an straightforward methodology to construct various highly functionalized alkyl (aryl)-substituted thiophenes (Scheme 11).[84] Under optimized conditions ($Ni(OTf)_2$ as catalyst source, Ag_2CO_3 as oxidant, $MesCO_2H$ and TBAB as additives, and KH_2PO_4 as base in DMSO at 160 °C for 24 h), a variety of alkyl-aryl substituted thiophenes were obtained in high yields *via* double C–H bond cleavage without affecting the C–Br or C–I bonds. Other heteroaryl groups, such as thiazole, benzofuran and furyl derivatives also participated in the reaction showing similar reactivity.

In this work, the KIE experiments suggested that the $C(sp^3)$–H bond cleavage could be involved in the *r.d.s* (KIE value = 4.6) but not the activation of the aromatic position (KIE value = 1.1) (Scheme 12). Moreover, the addition of TEMPO or 1,4-benzoquinone (1,4-BQ) did not inhibit the reactivity, supporting a non-radical pathway. On the other hand, DFT calculations verified the importance of KH_2PO_4 as an additive for generating $Ni(H_2PO_4)_2$ as the predominant active catalytic nickel(II)-species and promoting the $C(sp^3)$–H bond cleavage. The mechanistic proposal is depicted in Scheme 12: (i) nickel(II)-mediated 8-AQ-directed C–H activation to form metallacycle **II**, (ii) Ag-mediated oxidation to nickel(III)-intermediate **VII**, (iii) metalation of the thiophene to form the nickel(III)-intermediate **VIII**, and finally, (iv) C–C bond-forming reductive elimination to release the functionalized product. Subsequently, Ag-mediated reoxidation of the generated nickel(I)-species would regenerate the active nickel(II)-catalyst.

Following a similar strategy, You *et al.* reported the 8-AQ-assisted Ni-catalyzed oxidative heteroarylation of unactivated $C(sp^3)$–H bonds with benzothiazoles (Scheme 13).[85] In this case, the optimal conditions consisted on $Ni(OAc)_2{\cdot}H_2O$ as catalyst source, PPh_3 as ligand, Ag_2CO_3 as oxidant, 1-adamantanecarboxylic acid (1-$AdCO_2H$) as additive in ClPh at 160 °C for

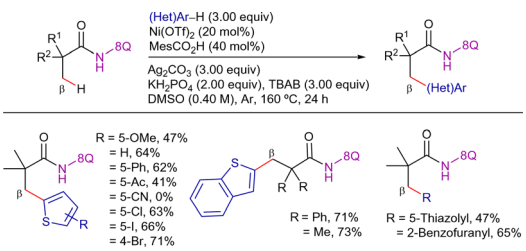

Scheme 11 β-$C(sp^3)$–H arylation with heteroaryls through a CDC process.

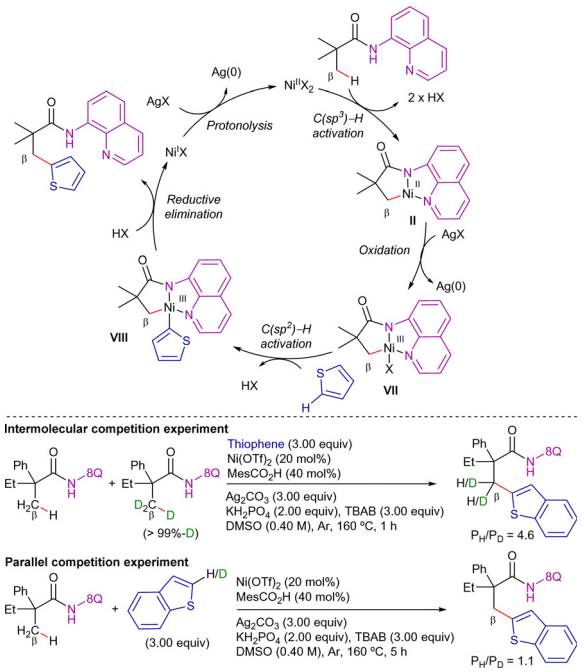

Scheme 12 Proposed catalytic cycle for the Ni-catalyzed CDC.

24 h. The method was limited to aliphatic amides quaternized at the α-position. In this work, the elimination of the DG was achieved efficiently, accessing carboxylic acid under basic conditions or carboxylate ester using $BF_3{\cdot}Et_2O$ (Scheme 14).

2.1.2. Alkenylation processes. In 2015, You *et al.* reported the 8-AQ-assisted nickel(II)-catalyzed alkenylation of β-C–H bonds of aliphatic amides with both symmetrical and unsymmetrical internal alkynes (Scheme 15).[86] The optimal reaction conditions involved $Ni(OAc)_2$ as catalyst and PPh_3 as ligand in toluene/isopropanol solvent mixture at 170 °C for 24 h. Under these conditions, a broad set of aliphatic amides were readily alkenylated in moderate to good yields albeit mixtures of *E*/*Z* isomers were isolated. Remarkably, a methyl adjacent to an α-tertiary carbon center also underwent the C(sp^3)–H bond alkenylation in good yield. The practicability of the method was further shown by the removal of the DG to access γ-butyrolactone scaffolds (Scheme 16).

In this work, deuterium labeling experiments suggested that the C–H activation step was reversible and not involved in the *r.d.s.* (KIE = 1.0), whereas the insertion of the alkyne was likely

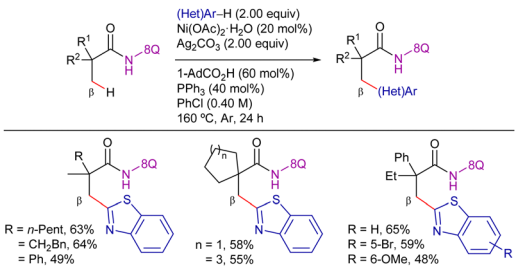

Scheme 13 β-C(sp^3)–H arylation with benzothiazoles through a CDC process.

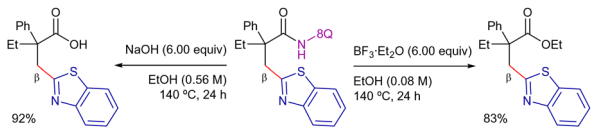

Scheme 14 Selective removal of the DG.

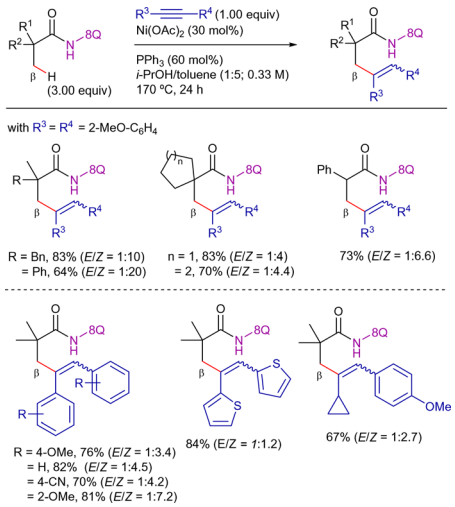

Scheme 15 β-C(sp^3)–H alkenylation with internal alkynes.

to occur a posteriori. The authors proposed the catalytic cycle depicted in Scheme 17, which involves: (i) reversible nickel(II)-mediated 8-AQ-directed C–H activation to form metallacycle **II**, (ii) coordination of the alkyne to form complex **IX**, and its subsequent migratory insertion to form the seven-membered metallacycle intermediate **X**, and (iii) final protonation of **X**, delivering the alkenylated product and the nickel(II) active species to close the catalytic cycle. In principle, the protonolysis step tends to generate the (*Z*)-isomer. However, under the reaction conditions, isomerization to the thermodynamically more stable (*E*)-isomer may occur, which accounts for the *E*/*Z* mixtures observed in the reaction.

Interestingly, in the same year, Maiti *et al.* also published an improved methodology for this process, showing that by changing the solvent mixture of toluene/isopropanol to either DMF or NMP, the temperature could be decreased to 140 °C while maintaining similar reactivity (Scheme 18).[87] The system was selective for the β-CH_3 functionalization, observing this selectivity even in the case of methylacrylamide derivative. Moreover, the conditions were optimal for the decarboxylative coupling with phenyl propionic acid, yielding the alkenylated product in moderate yield and with complete regio- and stereoselectivity.

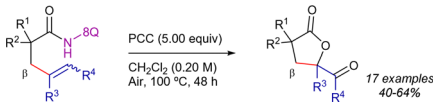

Scheme 16 Synthesis of γ-butyrolactone scaffolds.

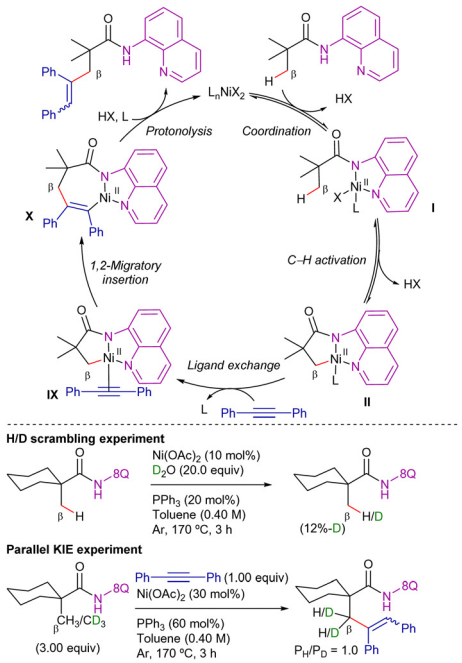

Scheme 17 β-C(sp^3)–H alkenylation with internal alkynes. Proposed mechanism.

Adding to these contributions, in 2017, Zhang *et al.* reported a new set of conditions for the reaction with terminal alkynes (Scheme 19).[88] The reaction was performed in the presence of

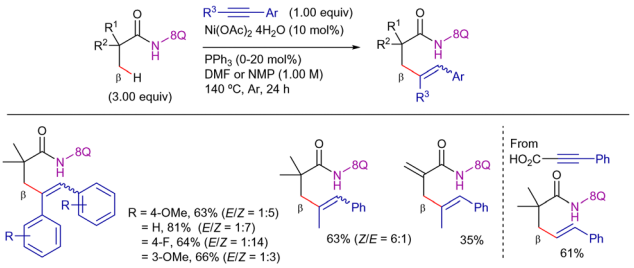

Scheme 18 Ni-catalyzed β-C(sp^3)–H alkenylation with internal alkynes.

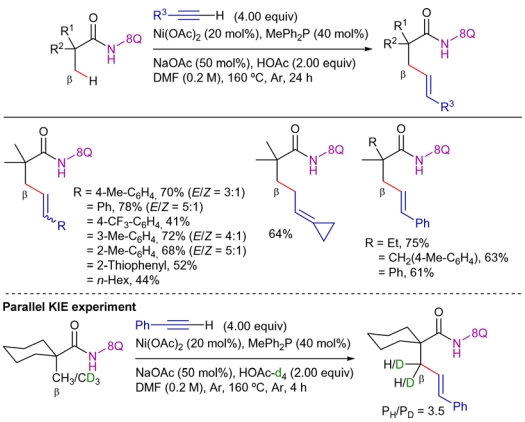

Scheme 19 β-C(sp^3)–H alkenylation with terminal alkynes.

$Ni(OAc)_2$ as precatalyst, $MePh_2P$ as ligand, and the appropriate combination of NaOAc with AcOH in DMF at 160 °C for 24 h. Under these conditions, the reaction displayed excellent functional group tolerance with respect to both aliphatic amides and terminal alkynes, being possible to apply less activated aliphatic alkynes. Remarkably, removal of the DG was achieved upon treatment with $BF_3{\cdot}Et_2O$ and sodium hydroxide (Scheme 20).

Mechanistic experiments revealed that the reaction did not involve radical species and that the C–H activation step was presumably irreversible. Moreover, parallel KIE experiments provided a value of 3.5, while the intermolecular KIE value was 4.6, indicating that the C–H activation step was presumably involved in the *r.d.s.* The authors proposed a mechanistic hypothesis similar to that depicted in Scheme 17, which involves the following sequence: (i) nickel(II)-amide coordination, (ii) C–H bond cleavage, (iii) alkyne migratory insertion to generate a seven-membered nickelacycle, and (iv) protonolysis, yielding the alkenylated product.

Terminal alkynes have not only been employed in alkenylation processes but also in alkynylation/annulation sequences. Thus, in 2016, Zhang *et al.* described the 8-AQ-assisted nickel(II)-catalyzed synthesis of structurally diverse five-membered lactams from aliphatic amides and terminal acetylenes (Scheme 21).[89] The optimized reaction conditions involved the use of $(Cy_3P)_2NiCl_2$ as precatalyst, Ag_2CO_3 as oxidant, Na_2CO_3 as a base and TBAI as additive, in toluene at 150 °C for 24 h. Using this system, a broad range of terminal acetylenes and aliphatic amides were efficient coupling partners, furnishing the corresponding *E*-ethylidene-pyrrolidinones in good yields. Interestingly, amides with prochiral β-CH_3 positions led to a mixture of diastereomers generated by the presence of the chiral C3 and the axial chirality of the lactam ring.

In this work, the authors suggested that the transformation presumably proceeds through an oxidative alkynylation process, followed by an Ag/TBAI-mediated intramolecular annulation reaction, ultimately leading to the thermodynamically

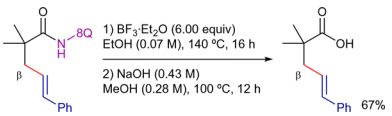

Scheme 20 Removal of the 8-AQ DG under basic conditions.

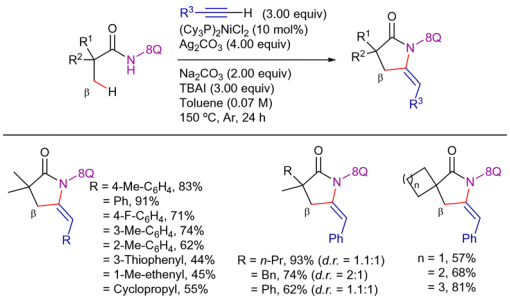

Scheme 21 β-C(sp^3)–H alkynylation/annulation with terminal alkynes.

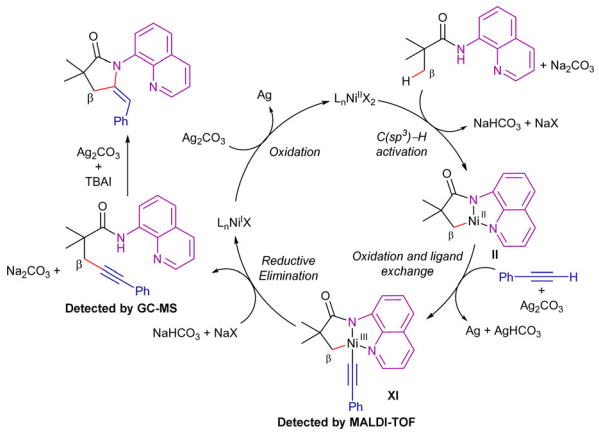

Scheme 22 Sequential β-C(sp^3)–H alkynylation/annulation with terminal alkynes. Proposed mechanism.

favoured (*E*)-ethylidene-pyrrolidinones (Scheme 22). The addition of TEMPO or BHT (2,6-di-*tert*-butyl-4-methylphenol) did not influence the reactivity, and therefore the intervention of radical species in the process was ruled out. It is proposed that the catalytic cycle starts by the C–H bond cleavage for the formation of the nickel(II)-cyclometallated intermediate **II**. Then, silver-mediated single electron-oxidation and ligand exchange generate intermediate **XI**, which was detected by MALDI-TOF analysis. From here, reductive elimination leads to the formation of the β-alkynylated product, which, in the presence of Ag/TBAI, undergoes *in situ* cyclization to generate the γ-lactams. On the other hand, the nickel(I) complex generated in the reductive elimination step would be re-oxidized to nickel(II) species by the remaining Ag-salt.

In 2020, Shen *et al.* expanded this methodology to the nickel-catalyzed annulation of aliphatic amides with alkynylsilanes (Scheme 23).[90] The method was effective in promoting the process with aryl, heteroaryl, and alkyl acetylenes, as well as with enynes. The authors suggested a mechanistic proposal like that of terminal alkynes (Scheme 22): the transformation is likely to occur *via* an oxidative alkynylation process, which is then followed by an intramolecular annulation reaction mediated by Ag/TBAI generating the thermodynamically favoured (*E*)-ethylidene-pyrrolidinones. The possibility of a mechanism involving radical intermediates was excluded since the addition of TEMPO did not affect the reaction.

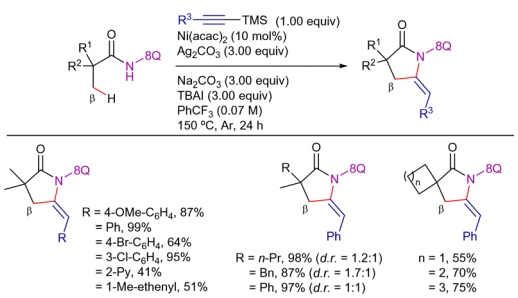

Scheme 23 Sequential β-C(sp^3)–H alkynylation/annulation with trimethylsilyl alkynes.

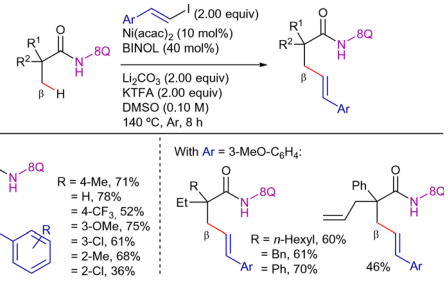

Scheme 24 β-C(sp^3)–H alkenylation with aryl vinyl iodides.

On the other hand, Shi *et al.* disclosed the efficient 8-AQ-assisted nickel(II)-catalyzed alkenylation of β-methyl C(sp^3)–H bonds of a broad range of α-quaternary aliphatic carboxamides using *trans*-vinyl iodides as coupling partners (Scheme 24).[91] The catalytic system comprised the air-stable Ni(acac)$_2$ as catalyst, BINOL as ligand, and the combination of KTFA and Li_2CO_3 as basic additives in DMSO at 140 °C for 8 h. The scope of carboxamides revealed that a wide variety of carboxamides bearing both linear and cyclic chains were compatible with this protocol, showing a preference for functionalization of aliphatic β-methyl than β-methylene and γ-C(sp^2)–H bonds.

2.1.3. Carbonylation processes. In 2015, Ge *et al.* published the direct aerobic carbonylation of C(sp^3)–H bonds through Ni/Cu synergistic catalysis using DMF as the carbonyl source and 8-AQ as DG (Scheme 25).[92] The addition of tetrabutylammonium hexafluorophosphate ($TBAPF_6$) was necessary presumably to facilitate the solubility of intermediates and reagents. This method was compatible with a wide range of aliphatic propanamide derivatives lacking a hydrogen at the α-position. In addition, the 8-AQ auxiliary could be removed under acidic conditions and the corresponding succinic derivative was accessed in good yield (Scheme 26).

As in previously reported examples, the authors proposed the nickel(II) mediated C(sp^3)–H cleavage to afford the cyclometallated intermediate **II** (Scheme 27). Subsequent nucleophilic addition to the iminium ion intermediate **a**, generated *in situ* from DMF and copper species, forms intermediate **XII** that after

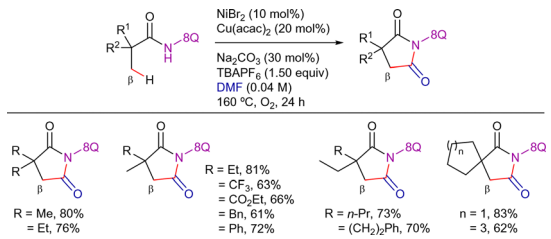

Scheme 25 Ni/Cu synergistic catalyzed β-C(sp^3)–H carbonylation with DMF.

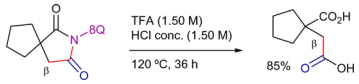

Scheme 26 Post-synthetic modification to obtain 1,4-dicarbonyl compounds.

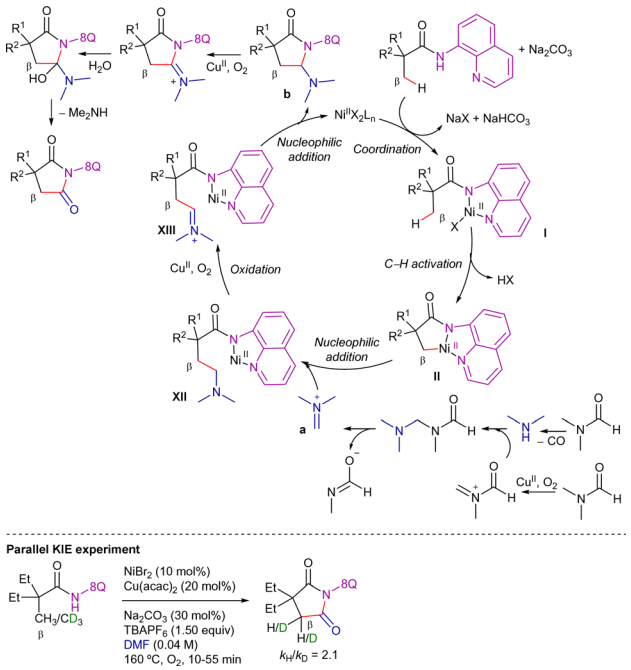

Scheme 27 Proposed catalytic cycle for the β-C(sp^3)–H carbonylation with DMF.

oxidation, intramolecular nucleophilic addition and hydrolysis, liberates intermediate **b**. Finally, oxidation and hydrolysis of the resulting iminium intermediate generates the succinimide derivative. Agreeing with this mechanistic proposal, ^{13}C-labeling studies confirmed that the carbonyl group inserted would not come directly from the carbonyl group of DMF. Instead, the incorporated carbonyl group mainly comes from the methyl group. Moreover, deuterium labeling and KIE experiments seemed to indicate that the C–H activation step was irreversible and involved in the *r.d.s.* (KIE = 2.1).

2.1.4. Alkylation processes. In 2014, Ge *et al.* reported the 8-AQ-assisted nickel(II)-catalyzed β-C–H alkylation of aliphatic amides with alkyl halides (Scheme 28).[93] The reaction conditions consisted on Ni(acac)$_2$ as catalyst precursor, 1,2-bis(diphenylphosphino)benzene (dppbz) as ligand and either Cs_2CO_3 or CsI as base, in toluene at 150 °C for 24 h. Under these conditions, the reaction showed a great preference for C(sp^3)–H bonds of methyl groups over methylene C–H bonds, showing good functional group tolerance. However, in line with previous reports, a quaternary α-carbon was also necessary for the success of this

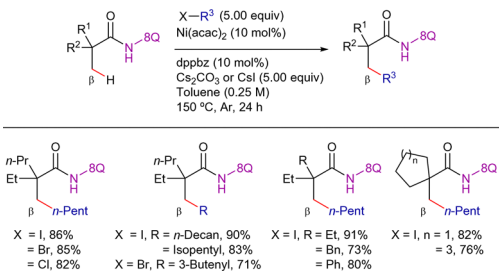

Scheme 28 Ni-cat. β-C(sp^3)–H alkylation with alkyl halides.

reaction. Interestingly, this reaction displayed a preference for the activation of methyl C–H bonds through five-membered ring intermediates in the cyclometalation step, rather than C(sp^2)–H bonds of arenes, which would proceed *via* six-membered ring intermediates.

In this work, intermolecular competition KIE experiments provided a value of 4.1, indicating that the C–H bond cleavage was involved in the *r.d.s.* Furthermore, the reaction in the presence of TEMPO resulted in a great decrease in the yield, but not its inhibition, and a product derived from the coupling between TEMPO and alkyl halides was isolated. Therefore, radical alkyl species might be generated in the reaction and might be involved in the mechanism. The authors suggested two possible reaction pathways: (i) a Ni^{II}/Ni^{IV} catalytic cycle (path a) or (ii) a Ni^{II}/Ni^{III}/Ni^{I} route (path b) (Scheme 29). Both routes have in common the initial formation of the nickel(II)-cyclometallated intermediate **II**. From this point, path a involves oxidative addition of the alkyl halide, generating the nickel(IV)-intermediate **XIV**, which, by subsequent reductive elimination and protonolysis, releases the alkylated product and nickel(II) species to accomplish the catalytic cycle. On the other hand, if path b is considered, the next step would be the alkyl radical addition to intermediate **II**, forming the nickel(III) intermediate **XVI**, followed by reductive elimination and nitrogen protonation to release the final product and nickel(I) species. Alkyl halide single electron oxidation of nickel(I) species would regenerate the active nickel(II) species, generating also an alkyl radical.

In addition to these contributions, Chatani's work described one example of Ni-catalyzed 8-AQ-assisted β-C(sp^3)–H methylation of aliphatic amides using phenyltrimethylammonium iodide as methyl source (Scheme 30).[94] The reaction proceeds

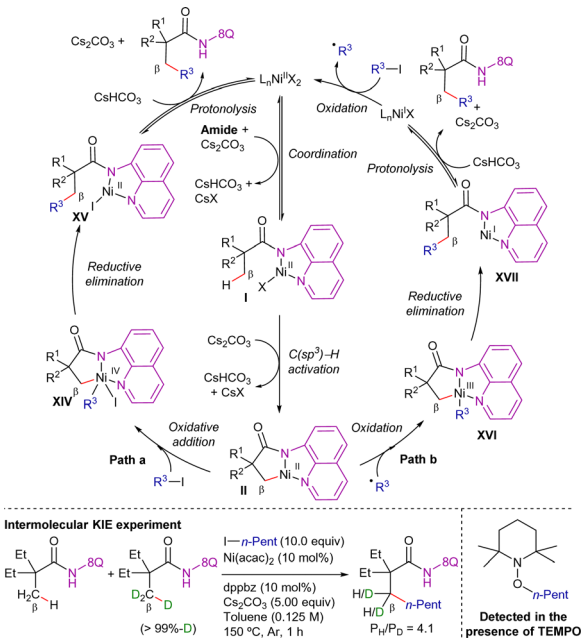

Scheme 29 Mechanistic proposals for β-C(sp^3)–H alkylation with alkyl halides.

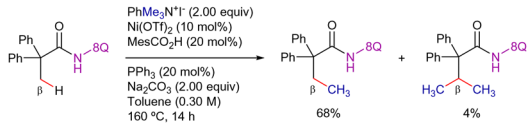

Scheme 30 β-C(sp^3)–H alkylation with phenyltrimethylammonium salts.

with high regiocontrol, providing the mono-functionalized product in 68% yield along with traces of the di-alkylated product.

As an alternative to the use of alkyl halides (or *pseudo*-halides), Maiti *et al.* disclosed the nickel-catalyzed insertion of electron-deficient olefins into unactivated C(sp^3)–H bonds using also the 8-AQ as optimal DG (Scheme 31).[87] The reaction conditions consisted on $Ni(OAc)_2{\cdot}4H_2O$ as catalyst precursor, PPh_3 as ligand, in DMSO at 140 °C for 24 h. This system displayed excellent linear selectivity. The authors proposed a mechanistic hypothesis similar to alkynes (Scheme 17), involving the following sequence: (i) nickel(II)-amide coordination, (ii) C–H bond cleavage, (iii) alkene migratory insertion, leading to the formation of a seven-membered nickelacycle, and (iv) protonolysis, yielding the alkylated product. To the best of our understanding, the acetate counteranion facilitates the C–H activation step and acts as a proton shuttle, thereby contributing to the closure of the catalytic cycle. At no time do the authors mention having detected the alkenylation product, the formation of which could have been more favoured in the presence of basic additives.

The method was sensitive to the structure of both reagents, obtaining the best results with alkyl substitution at the amide substrate with alkyl acrylates and acrylonitrile.

2.1.5. Alkynylation processes. The introduction of alkynes into organic molecules has been an important synthetic target due to its versatility as building block and its presence in many organic frameworks with biological properties and material science.[95,96] Among the traditional approaches, it is worth highlighting the coupling of alkynyl-metal species and carbonyl or alkyl halides, the nucleophilic addition to electrophilic alkynyl species, or metal-catalyzed radical pathways.[97] A more straightforward approach would be the direct insertion of alkynes into aliphatic C–H bonds. The high efficiency of Ni-based catalysts to promote C(sp^3)–C(sp^3) and C(sp^3)–C(sp^2) bond- forming reactions pushed the search for C(sp^3)–C(sp)

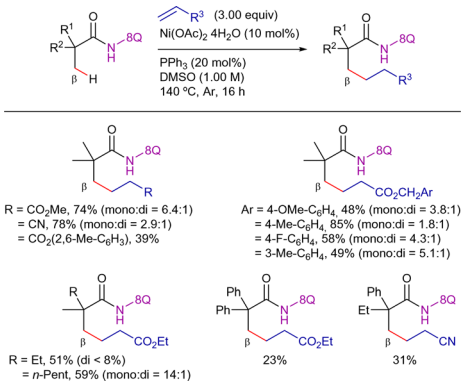

Scheme 31 β-C(sp^3)–H alkylation with activated olefins.

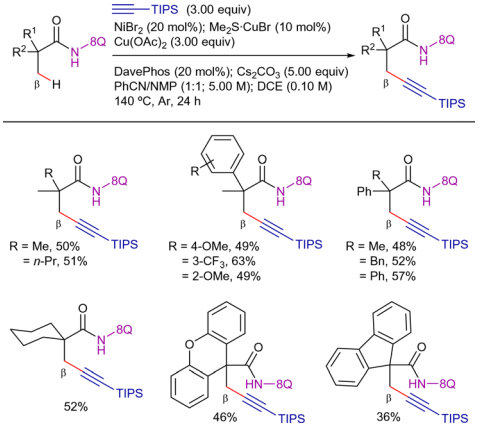

Scheme 32 β-C(sp^3)–H alkynylation with trimethylsilylacetylene.

bond- forming reactions or other oxidative C–C couplings that have been previously described for the direct functionalization of C(sp^2)–H bonds.[98] In this regard, the group of Shi *et al.* disclosed a procedure for the β-C(sp^3)–C(sp) bond formation by using trimethylsilylacetylene as coupling partner, taking advantage of the well-known directing ability of the 8-AQ (Scheme 32).[99] The optimized reaction conditions for this transformation are the following: $NiBr_2$ as catalyst precursor, DavePhos as ligand, $Me_2S{\cdot}CuBr$ as transmetalating reagent, $Cu(OAc)_2$ as oxidant and Cs_2CO_3 as base in a benzonitrile/NMP/DCE solvent mixture at 140 °C for 24 h. The incorporation of the triisopropylsilyl acetylide was achieved in reasonable yields using α,α-disubstituted propanamide derivatives with high regioselectivity to primary positions. The method could be expanded to the functionalization of highly complex structures such as 9*H*-fluorene and 9*H*-xanthene derivatives (46% and 36% yields respectively). Control experiments showed the essentiality of all components, except $Me_2S{\cdot}CuBr$. The practicability of the method was expanded by eliminating the 8-AQ auxiliary under NaOH/EtOH conditions.

To gain mechanistic data about the transformation, the authors analysed the reactivity of 1-(methyl-d_3)cyclohexanoic acid derivative under the standard conditions, in the absence of the alkyne, and adding 1.00 mL of H_2O. The starting material was recovered unaltered and fully deuterated at the β-position. Moreover, the intermolecular competition KIE experiment provided a 2.03 value, while the parallel KIE experiment gave a 2.28 value. These results indicated, therefore, that the C–H activation step was irreversible and was involved in the *r.d.s.* Finally, the addition of TEMPO had a significant effect, suggesting the formation of radical species in the process.

Based on these results, the authors proposed the catalytic cycle depicted in Scheme 33. First coordination of the amide to the catalytically active nickel(II) species, followed by the β-C(sp^3)–H bond cleavage would generate intermediate **XIX**. From this point, two pathways were proposed: (a) Cu-mediated single electron oxidation of nickel(II) to nickel(III), followed by transmetalation with the alkynyl cupper(I) species generated *in situ* by reaction between Cu^I and terminal alkynes, leading to intermediate **XXI** (path a); (b) single electron oxidation by alkynyl radical species generated by the homolytic cleavage of

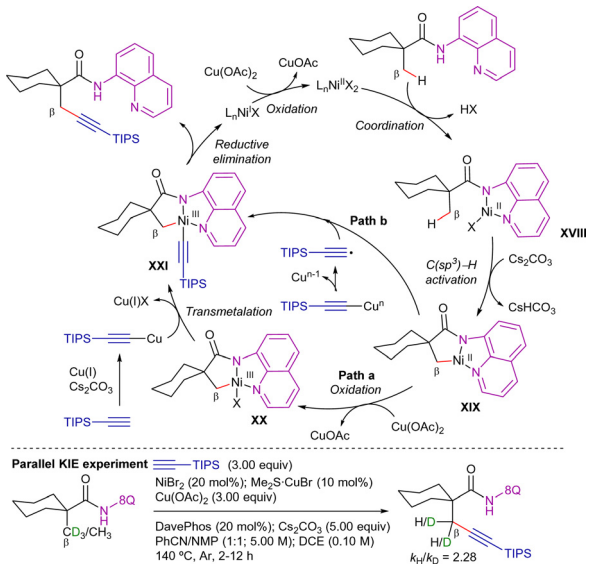

Scheme 33 Proposed catalytic cycle for β-C(sp^3)–H alkynylation with trimethylsilylacetylene.

alkynyl cupper species to generate intermediate **XXI** (path b). From intermediate **XXI**, the subsequent reductive elimination step would generate the alkynylated product and nickel(I) species. Then Cu-mediated oxidation would further re-oxidize the nickel(I) species to the catalytically active nickel(II) species.

2.2. C-Heteroatom bond formation

2.2.1. C–N bond formation. Nitrogen-containing compounds are ubiquitous motifs in biologically active natural products, pharmaceutical drugs, and agrochemicals.[100] One of the most straightforward and atom-economical approaches for the construction of a C–N bond is the dehydrogenative C–H/N–H cross-coupling.[101]

In a seminal contribution, Ge *et al.* reported the intramolecular dehydrogenative cyclization of aliphatic amides by a nickel-catalyzed C(sp^3)–H bond functionalization process with the assistance of 8-AQ as a bidentate DG (Scheme 34).[102] The reaction favoured the C–H bonds of β-methyl groups over the γ-methyl or β-methylene groups, as well as the β-methyl C–H bonds over aromatic C(sp^2)–H bonds. Additionally, this process enabled the efficient functionalization of secondary benzylic C–H bonds with complete regioselectivity when there were no accessible β-methyl positions. The authors showed that

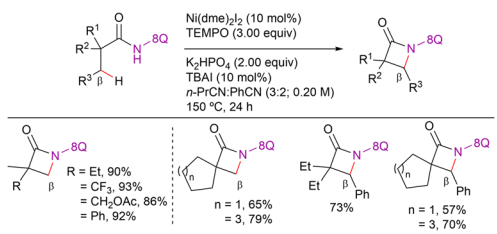

Scheme 34 Ni-catalyzed β-C(sp^3)–H intramolecular dehydrogenative cyclization.

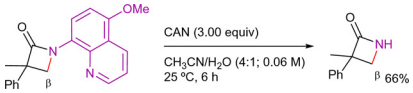

Scheme 35 Removal of the 8-amino-5-methoxyquinoline group.

the 8-amino-5-methoxyquinoline was as effective as the 8-AQ and could be removed under oxidative conditions to afford the desired NH-β-lactam product (Scheme 35).

The proposed catalytic cycle is depicted in Scheme 36. The reaction starts with the coordination of the amide to nickel(II)-species and subsequent ligand exchange process under basic conditions, leading to the formation of the nickel complex **XXII**. Subsequent C(sp^3)–H nickellation generates the nickel(II) complex **XXIII**, which is then oxidized to the nickel(III) species **XXIV** by TEMPO. Finally, reductive elimination from intermediate **XXIV** generates the desired product and a nickel(I)-species that would be re-oxidized by TEMPO closing the catalytic cycle.

Years later, Chatani *et al.* disclosed a methodology for the Ni-catalyzed synthesis of β-lactams from aliphatic amides employing the 8-amino-5-chloroquinoline as optimal DG (Scheme 37).[103] The reaction occurred in the presence of Ni(OTf)$_2$ as catalyst

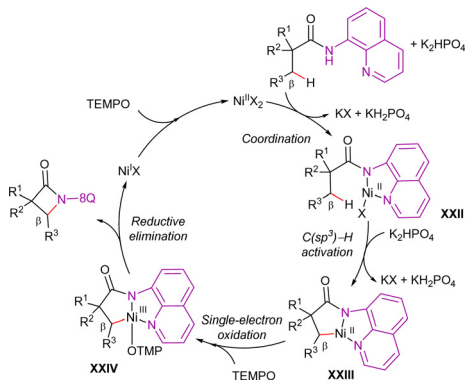

Scheme 36 Proposed catalytic cycle for β-C(sp^3)–H intramolecular amidation.

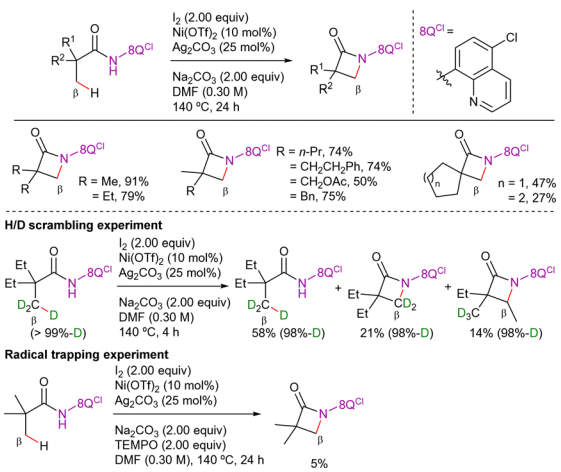

Scheme 37 β-C(sp^3)–H cyclization in the presence of I$_2$.

precursor, Na_2CO_3 as a base, catalytic amounts of Ag_2CO_3 and an excess of I_2, in DMF at 140 °C for 24 h.

In this work, the authors proposed that the reaction might occur through a direct pathway, in which the β-lactam would be formed by (i) nickel(II)-cyclometalation after the C–H activation step, and (ii) C–N bond reductive elimination from a nickel(III) or a nickel(IV) intermediate generated by iodine single-electron or oxidative addition oxidations, respectively. Nonetheless, their findings seemed to indicate that a stepwise pathway was also feasible, involving the direct β-iodination of the aliphatic amide and a facile subsequent intramolecular cyclization to form the β-lactam. Deuterium-labeling experiments revealed that the C(sp^3)–H bond cleavage was irreversible and presumably the *r.d.s.* in this reaction. The addition of radical scavengers, such as TEMPO and BHT, completely inhibited the reaction, suggesting that radical intermediates may play a role in the process. However, the involvement of a background reaction in which radical scavengers react with I_2 cannot be ruled out. Such a reaction could consume most of the I_2, potentially influencing the observed inhibition.

Shedding light on this point, Sanford *et al.* synthesize a σ-alkyl nickelacycle complex that undergo intramolecular C(sp^3)–N bond-forming at room temperature to form a β-lactam product (Scheme 38a).[104] Moreover, this complex proved to be catalytically active under the previously reported reaction conditions by Chatani, which suggested its involvement in the reaction (Scheme 38b). In contrast, when a nickel(III)-complex was tested, no reactivity was observed, indicating that it is not a competent catalyst for the C–H amination process.

On the other hand, in 2021, Baik's and Chang's group reported a DG-assisted Ni-catalyzed intermolecular C(sp^3)–H amidation using organic sulfonylazides as nitrene precursors (Scheme 39).[105] In this transformation, 8-amino-5-trifluoromethyl quinoline was proved to be the optimal DG. The external oxidant-free conditions enabled the selective intermolecular amidation to outcompete an intramolecular counterpart. A complete chemoselectivity toward the β-methyl C(sp^3)–H bond suggested that the inner-sphere mechanism was operative. The method provided amidated products with low to good yields, observing better reactivities with electron-rich aryl azides. In addition, alkyl azides were also compatible with the reaction conditions. Nevertheless, the method was less effective with α-substituted propanamide derivatives or for the functionalization of β-methylene positions.

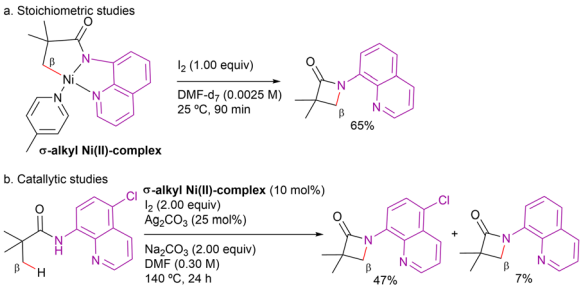

Scheme 38 Nickel(II)-intermediates in 8-AQ-directed C(sp^3)–N coupling in the presence of I_2.

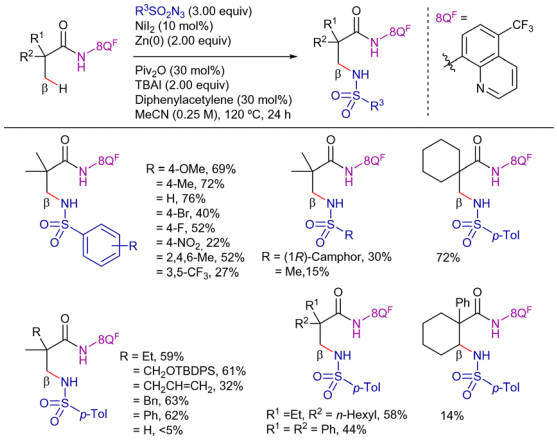

Scheme 39 β-C(sp^3)–H intermolecular amidation with sulfonylazides.

Based on theoretical calculations, the authors suggested the catalytic cycle shown in Scheme 40. The reaction would start with the *in situ* reduction of nickel(II) species to nickel(0), followed by pivalic anhydride oxidation through a highly exothermic step to generate nickel(II) species.[106,107] Subsequent amide coordination to generate intermediate **XXV** and irreversible C–H metalation (*via* CMD mechanism, intermediate **XVI**) followed by ligand exchange gives the azide-nickel(II) cyclometallated intermediate **XXVII**. Extrusion of N_2 forms a nitrene-nickel(III) intermediate **XXVII**, that undergoes favourable inner-sphere C–N

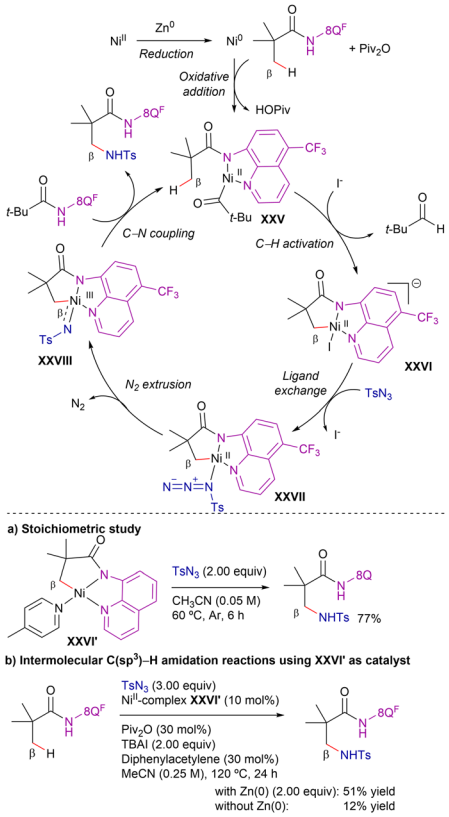

Scheme 40 Proposed catalytic cycle for β-C(sp^3)–H intermolecular amidation.

coupling to release the aminated product. Attending to the energy profile of the reaction, the azide coordination-N_2 extrusion goes through the highest energy barrier (29.8 kcal mol^{-1}), indicating that this step is the *r.d.s*. Moreover, DFT calculations showed that the substitution in the quinoline ring did not significantly affect the C–H activation step, but it influenced the efficiency of the aminated product release and regeneration of intermediate **XXV**. While this process was calculated to be only 13.4 kcal mol^{-1} uphill with an electron-withdrawing CF_3 group at the quinoline core, the presence of an electron-donating methoxy functionality increases the energy requirement to 15.4 kcal mol^{-1}.

To evaluate the feasibility of the above nickel(II/III) catalytic cycle proposed by computational studies, the authors performed stoichiometric amidation reactions using a C–H-activated nickel(II) complex (**XXVI′**, Scheme 40a), which exhibits structural similarity to the hypothesized Ni(II) intermediate **XXVI**. When the Ni^{II}–C complex **XXVI′** was combined solely with TsN_3 in acetonitrile at 60 °C, the desired intermolecular C(sp^3)–H amidation proceeded efficiently (77% yield). This result indicates that nickel(II) serves as an active species in the amidation process and that the putative Ni^{III}-nitrenoid species, responsible for C–N bond formation, originates from the nickel(II) intermediate.

To gain further mechanistic insights into the catalytic system, the authors employed the Ni^{II}–C complex **XXVI′** as catalyst precursor under the amidation conditions (Scheme 40b). Under standard reaction conditions, the desired amidation product was obtained with a 51% yield; however, in the absence of Zn, the reaction efficiency significantly dropped (12%). Given that catalytic turnover was hindered by the absence of Zn, unlike in the stoichiometric amidation scenario, the authors inferred that while Zn does not participate in the key amidation step, it plays a crucial role in facilitating the regeneration of the active catalyst.

2.2.2. C–O bond formation. Group 10 late metals has demonstrated efficiency in promoting C(sp^3)–H oxygenation with the assistance of monodentate and bidentate DGs.[108] In 2022, You and co-workers reported the only example using nickel catalysis, which involves a aminoxylation of C(sp^3)–H bonds with stable nitroxyl radicals under air (Scheme 41).[109] This method was sensible to the substitution patterns in both the amide and nitroxyl structures. Additionally, this protocol provided a feasible one-pot synthetic approach to α-formyl acid derivatives (Scheme 42).

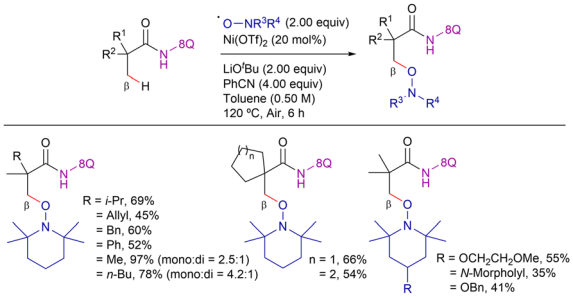

Scheme 41 β-C(sp^3)–H alkoxylation with TEMPO and analogues.

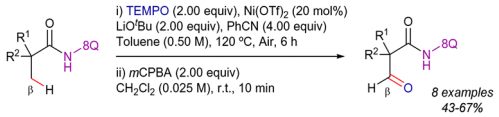

Scheme 42 One-pot synthesis of α-formyl acid derivatives.

The proposed catalytic cycle is depicted in Scheme 43. Initially, bidentate chelation of the amide to the nickel(II) species forms the nickel(II) complex **I**, accompanied by the generation of HX, which is captured by Li^{t}BuO. Subsequently, the β-C–H bond undergoes irreversible cleavage, resulting in the formation of the nickel(II) cyclometallated intermediate **II**. Next, oxidative addition of **II** with the nitroxyl radical leads to intermediate **XXIX**. Finally, reductive elimination and protonation deliver the desired product along with the generation of nickel(I) species. Oxidation to nickel(II) species by either the stable nitroxyl radical or oxygen in air furnishes the catalytic cycle. Mechanistic insights suggested that the C–H activation step was presumably irreversible and was involved in the *r.d.s*. (KIE = 2.4).

2.2.3. C–S and C–Se bond formation. The development of new catalytic approaches for the introduction of sulfur moieties in organic frameworks has been a constant hurdle due to the strong binding of sulfur species to transition metals.[110] In fact, the direct transformation of a C–H bond into a C–S bond remains, in general, underdeveloped.[111]

In 2015, Zhang,[112] Qiu, Xu and Yin,[113] and Shi[114] reported different protocols for the 8-AQ-assisted Ni-catalyzed β-C–H thioetherification of aliphatic amides using disulfides as coupling partners (Scheme 44). The three reaction conditions were rather similar, requiring the use of a nickel(II)-salt as catalyst precursor ($Ni(OTf)_2$, $NiBr_2$ or $(dppp)NiCl_2$), a carboxylic acid or biaryl-type ligand (*N*-acetylglycine, $MesCO_2H$ or BINOL), a base (Na_2CO_3 or KTFA) and the use of a coordinating polar solvent (DMF or DMSO) at high reaction temperatures (140–160 °C).

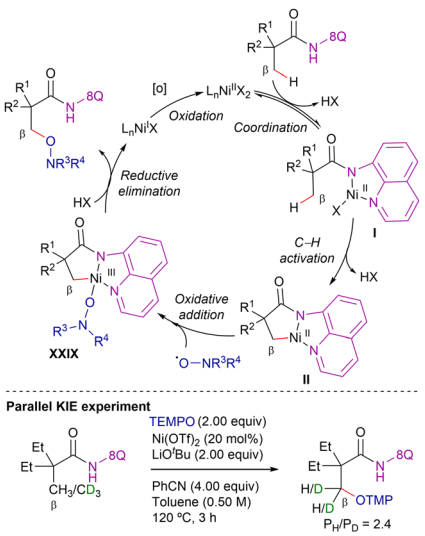

Scheme 43 Proposed catalytic cycle for the β-C(sp^3)–H alkoxylation.

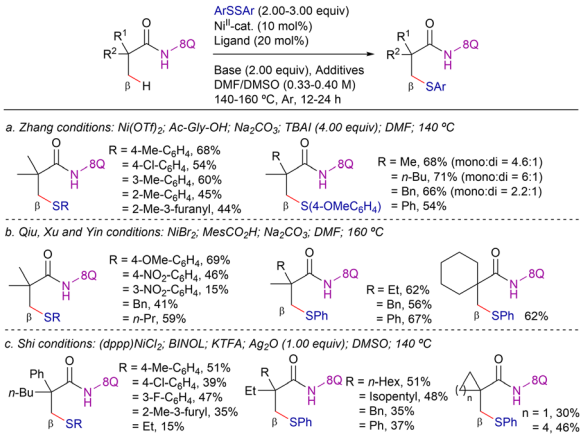

Scheme 44 β-C(sp^3)–H thiolation with disulfides.

In addition, the work of Zhang required the use of TBAI as an extra additive (Scheme 44a), while the work of Shi used Ag_2O (Scheme 44c). Analyzing the scope of these contributions, in general, electron-rich diaryl disulfides were more efficient than electron-withdrawing and the substituents at *para*-positions provided better yields than *meta* and *ortho*. Notably, the method of Qiu, Xu and Yin could be applied to challenging aliphatic disulfides, achieving the desired products in good yields (Scheme 44b).[113]

Regarding the mechanistic studies disclosed in these papers, the addition of radical scavengers such as TEMPO or BHT did not affect the reactivity in any case. Therefore, radical species were presumably not involved in the reaction. Deuterium labeling experiments at short reaction times performed by Zhang indicated that the C–H bond cleavage was reversible while KIE experiments performed by Qiu, Xu and Yin, indicated that the C–H activation step was involved in the *r.d.s.* (KIE = 5.7).

With all the mechanistic data, a combined proposed catalytic cycle based on the ones proposed in each work is presented in Scheme 45. Firstly, coordination of nickel(II) species to the amide followed by base-assisted N–H deprotonation leads to intermediate **I**, which then undergoes C–H metalation to generate intermediate **II**. Then, oxidative addition of PhSSPh generates nickel(IV) intermediate **XXX**, which then evolves through a reductive elimination step to generate the new C–S bond and the nickel(II) intermediate **XXXI**. Finally, the presence of silver, sodium or potassium would capture the thiol ligand that has not been inserted in the activated carbon, facilitating the release of the final product and the regeneration of the catalytically active nickel(II) species.

On the other hand, Zhang (Scheme 46a),[112] and Qiu, Xu and Yin (Scheme 46b)[113] showed that diphenyl diselenide also reacted, rendering the β-phenylselenated product in 40% and 27% yield, respectively (Scheme 46).

In parallel, Shi and co-workers reported a complementary method for the direct thiolation of β-C(sp^3)–H bonds in α,α-disubstituted propanamide derivatives with disulfides and thiols as coupling partners (Scheme 47).[115] The key to achieving good reactivities with thiols was to carry out the reaction under air.

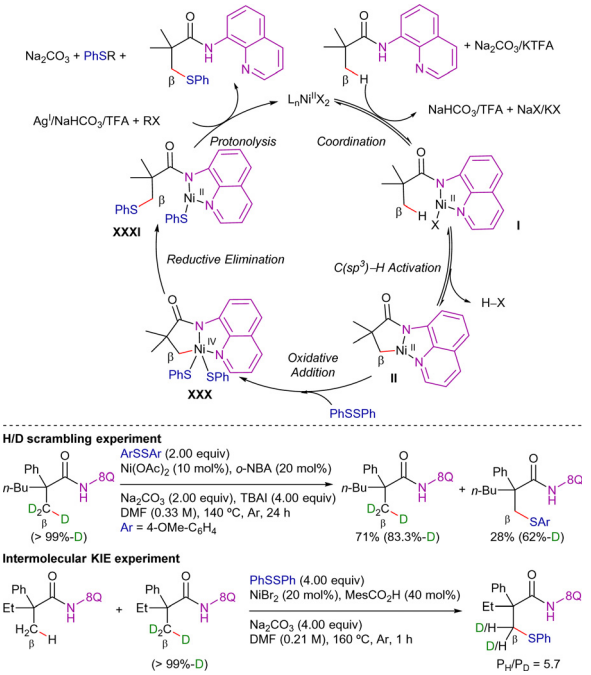

Scheme 45 Proposed catalytic cycle for Ni-cat. β-C(sp^3)–H thiolation with disulfides.

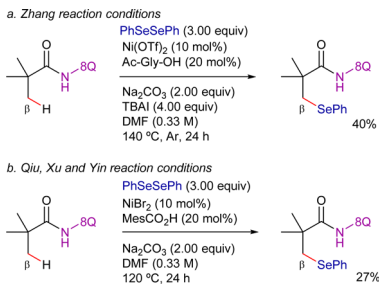

Scheme 46 β-C(sp^3)–H functionalization with diselenides.

This could be due to the *in situ* generation of the disulfide from the thiol.[116] The reaction was compatible with a wide range of aromatic thiols and lineal or cyclic carboxamides, providing the thiolated products in moderate to good yields.

Later, Weng, Lu and co-workers reported a novel method for C–H thiolation with disulfides by using a 2-pyridyl hydrazine

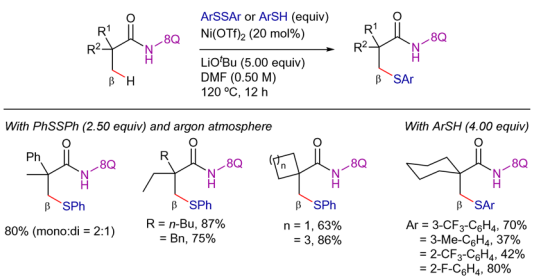

Scheme 47 β-C(sp^3)–H thiolation with disulfides and thiols.

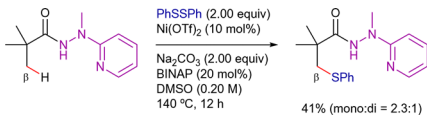

Scheme 48 Hydrazine-directed β-C(sp^3)–H thiolation with disulfides.

moiety as DG (Scheme 48).[117] A mixture of mono- and di-thiolated products was isolated in 41% overall yield and 2.3 : 1 ratio.

2.3. Exploring organometallic nickel intermediates

In all the contributions mentioned in the previous sections, the generally accepted mechanism would be that in which the activation of the C–H bond would take place at a low-valent Ni^{II}-center leading to the formation of a Ni^{II}-(σ-alkyl) intermediate. Its subsequent oxidative functionalization would release the desired product and regenerate the Ni^{II}-catalyst. In general, this mechanistic view has been shown to be valid for the functionalization of C(sp^3)–H bonds proximal to AQ-type DGs.

However, the substrate scope of Ni-catalyzed C–H functionalization is currently more limited compared to similar transformations using Pd. Additionally, most Ni-catalyzed C–H functionalization reactions necessitate harsh conditions (typically temperatures above 130 °C). These limitations are, at least in part, due to the C–H activation step, which is known to be significantly more challenging in Ni^{II} than in analogous Pd^{II} centers. Shedding light on this point, the group of Schafer and Love demonstrated that the C(sp^3)–H activation in urea scaffolds took place in nickel(II) species under mild conditions, and was easier at β-methyl rather than β-methylene positions (Scheme 49).[118] In fact, these studies showed that increasing the steric hindrance around the *β*-position with alkyl substituents resulted in lower reaction rates, not observing the formation of the nickelacycle with the substrate wearing a tertiary isopropyl group. These results agreed with the computational study reported by Omer and Lui.[77] In contrast, with benzyl substitution, the reaction rates increased, favoured with electron-donating rather than with electron-withdrawing substitution. More recently, they also observed that the kinetic for the C–H

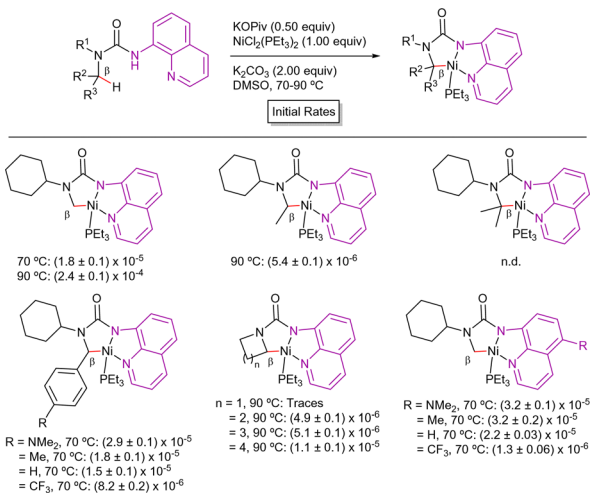

Scheme 49 Isolated thiourea nickel(II)-cyclometallated species.

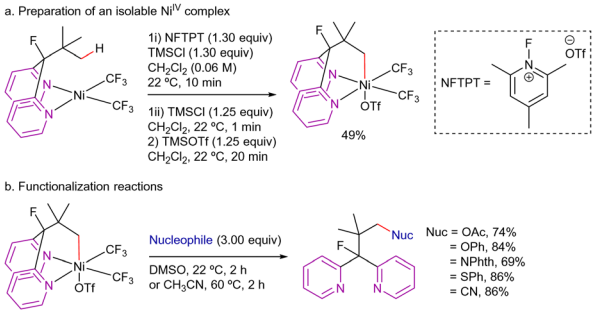

Scheme 50 C(sp^3)–H functionalization at high-valent Ni-centers.

activation step was modified by introducing substituents at the C5 position of the quinoline ring.[119] Thus, with electron-rich substituents, the reaction rates were higher. However, despite these studies, no report has demonstrated the viability of functionalizing the *β*-position in urea moieties.

On the other hand, Sanford *et al.* have demonstrated that unactivated C(sp^3)–H bonds could be cleaved and subsequently functionalized at high-valent Ni-centers with both heteroatom- and carbon-based nucleophiles under relatively mild conditions (Scheme 50).[120] Moreover, these two steps were combined to demonstrate a proof-of-principle catalytic transformation for converting a C(sp^3)–H bond into a C(sp^3)–N bond. Unfortunately, the competing decomposition of the oxidant limited the catalyst turnover in this transformation. DFT studies revealed two possible mechanisms for the C–H activation process, involving triflate-assisted C–H activation at either a Ni^{IV} or Ni^{III} intermediate. The former pathway was slightly favoured over the latter, with a difference of approximately 3 kcal mol^{-1}.

3. Cu-catalysis

The low price and toxicity of copper have awakened chemist interest in exploring its potential in organic synthesis.[121] Since the discovery of the Ullmann and Golberg couplings,[122] multiple radical relay transformations,[123] cross-coupling reactions,[124–126] Wacker-type oxidations[127] or C–H oxidation processes,[128–130] among others, have clearly shown the multidisciplinary of copper to promote reactions.[131–133] Following the general trend, the directed C–H functionalization *via in situ* formation of Cu metallacyclic intermediates has predominantly been applied to the functionalization of C(sp^2)–H bonds, facilitating the formation of new C–C and C–heteroatom bonds with the assistance of exogenous functional groups.[134,135] In contrast, examples of C(sp^3)–H functionalization remain relatively scarce. The primary challenge in using copper for C(sp^3)–H bond functionalization lies in the difficulty of accessing copper(III) species, which is energetically demanding and often requires high reaction temperatures and elevated copper salt loadings.

3.1. C–C bond formation

In 2015, Ge *et al.* reported the 8-AQ-assisted Cu-promoted β-C(sp^3)–H bond functionalization of aliphatic amides with polyfluoroarenes through a CDC reaction (Scheme 51).[136]

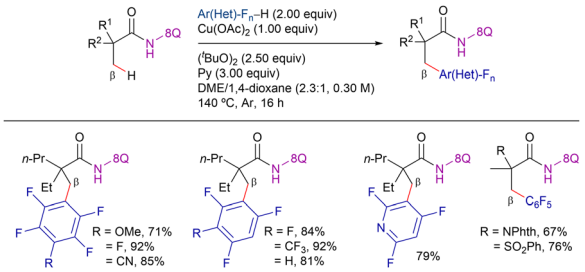

Scheme 51 Cu-promoted β-C(sp^3)–H arylation with polyfluorinated rings.

In their study, the authors discovered that pyridine was a crucial additive and di-*tert*-butyl peroxide was the optimal oxidant. However, stoichiometric $Cu(OAc)_2$ was required for this reaction. Under these conditions, the reaction exhibited good functional group tolerance and excellent site-selectivity. It favoured the functionalization of C(sp^2)–H bonds at the *ortho*-position relative to two fluorine atoms, as well as the C–H bonds of β-CH_3 groups over those of the β-CH_2 or γ-CH_3 groups in the amides.

Preliminary mechanistic studies indicated that C(sp^3)–H bond cleavage was irreversible but not the *r.d.s.* (KIE = 1.1), and the C(sp^2)–H activation of arenes appeared to be reversible, previous to the C(sp^3)–H activation and could take place at copper(I) or copper(II) species. Based on these results, the authors proposed the reaction mechanism depicted in Scheme 52. Initially, in the presence of pyridine, a reversible C(sp^2)–H bond cleavage mediated by copper(II) species leads to intermediate **XXXII**. Subsequently, *N,N*-coordination of the amide to the Cu–C(sp^2) complex **XXXII** forms the chelate **XXXIII**, from which a copper(II) or $(^tBuO)_2$ single-electron oxidation generates copper(III) intermediate **XXXIV**. Following C(sp^3)–H activation yields the five-membered metallacycle **XXXV**, from which final reductive elimination, along with nitrogen protonation releases the arylated product and copper(I) species. In principle, these copper(I) species would regenerate intermediate **XXXII** *via* two pathways: (a) initial $(^tBuO)_2$ oxidation followed by C(sp^2)–H activation, or (b) aromatic C–H activation and further oxidation.

Two years later, You *et al.* reported a copper-mediated oxidative heteroarylation of unactivated C(sp^3)–H bonds with azoles. The use of pyridine-*N*-oxide auxiliary facilitated the access to β-azolyl propanoic acid derivatives in good yields (Scheme 53).[85] The reaction proceeded in the presence of super stoichiometric amounts of $Cu(OAc)_2{\cdot}H_2O$ as promoter, using PivOH and K_2CO_3 as additives in *o*-xylene at 140 °C under a N_2 atmosphere for 24 h. In line with Ge's report, the reaction was limited to pivalamide derivatives with a quaternary α-carbon. Nonetheless, azoles such as oxazole, benzoxazole, thiazole, benzothiazoles, benzimidazole, purine, and even [1,2,4]triazolo[1,5-*a*]pyrimidine were well-tolerated under the optimized conditions. The practicability of the method was expanded by removing the auxiliary under basic conditions (Scheme 54).

H/D scrambling experiments revealed that while the C(sp^3)–H bond cleavage was an irreversible step, the C(sp^2)–H bond activation was reversible. The proposed mechanism is depicted in Scheme 55. First, a ligand exchange of 2-pivalamidopyridine 1-oxide with $Cu(OAc)_2{\cdot}H_2O$ forms complex **XXXVIII** (synthesized and characterized by X-ray diffraction). Next, complex **XXXVIII** reacts with benzoxazole to produce intermediate **XXXIX**. Next, the C–H cupration of a primary C(sp^3)–H bond forms the copper(III) complex **XLI**, with the involvement of additional $Cu(OAc)_2$ through disproportionation. Subsequently, **XLI** undergoes reductive elimination to generate a copper(I)-coordinated

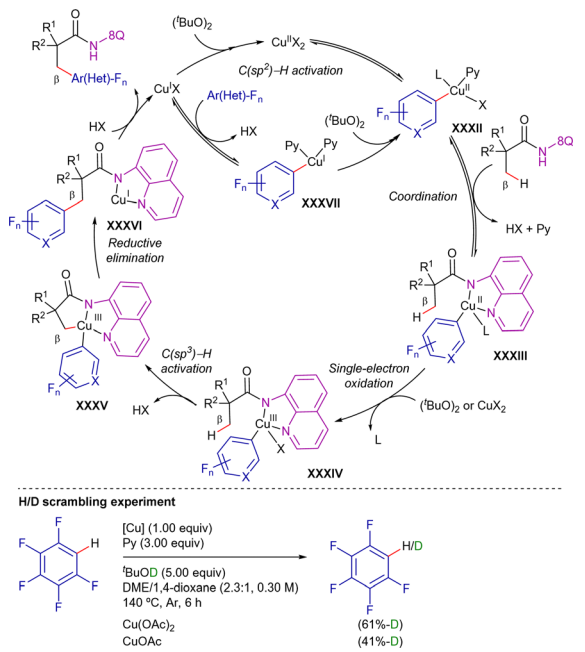

Scheme 52 Proposed mechanism for Cu-promoted CDC with polyfluorinated rings.

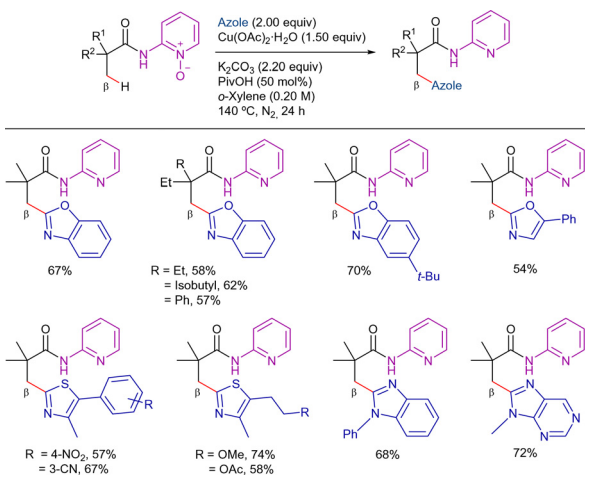

Scheme 53 Cu-promoted β-C(sp^3)–H arylation with azoles.

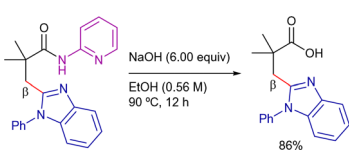

Scheme 54 Removal of the pyridine-2-amine auxiliary.

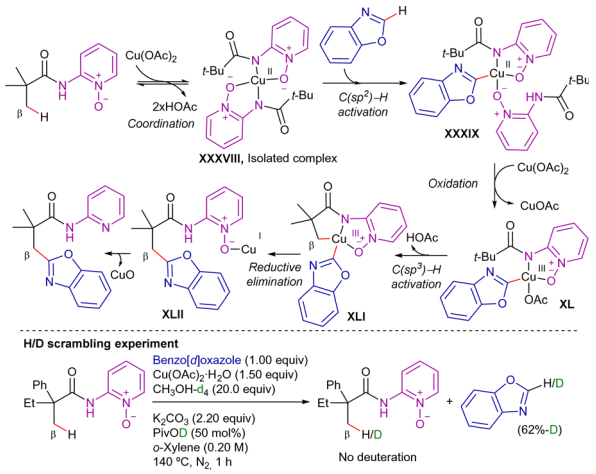

Scheme 55 Proposed reaction mechanism for Cu-promoted β-C(sp^3)-arylation with azoles.

intermediate **XLII**. Finally, the N–Oxide bond of intermediate **XLII** is reductively cleavaged by Cu(I), releasing the functionalized 2-pivalamidopyridine derivative and CuO (observed in the reaction mixture and tube wall). The formation of inert CuO would explain the requirement of super stoichiometric $Cu(OAc)_2 \cdot H_2O$ for this transformation.

Ge *et al.* disclosed the 8-AQ-assisted $Cu(OAc)_2$-promoted carbonylation of β-C(sp^3)–H bonds with nitromethane as the carbonyl equivalent (Scheme 56).[137] The optimized reaction conditions required the use of stoichiometric $Cu(OAc)_2$, $K_2S_2O_8$ as oxidant, $PhCO_2Na$ and Al_2O_3 as additives, along with DMPU in a solvent mixture 1,4-dioxane/isopropanol at 165 °C for 24 h. Using this system, the C(sp^3)–H functionalization showed high site selectivity by favouring the C–H bonds of α-methyl groups. In this study, initial mechanistic analysis indicated that the substrate first undergoes a dehydrogenative coupling with nitromethane, followed by a Nef-type reaction, leading to the formation of the carbonylation product (Scheme 57).[138] Deuterium labeling experiments unveiled that the C(sp^3)–H activation was reversible.

In 2016, Zhang's group reported a copper-catalyzed C(sp^3)–H alkynylation/annulation reaction between aliphatic amides and alkynyl carboxylic acids or terminal alkynes (Scheme 58).[139] In this system, TBAI was used as a phase-transfer catalyst system and Ag_2CO_3 played a crucial role by: (i) generating the

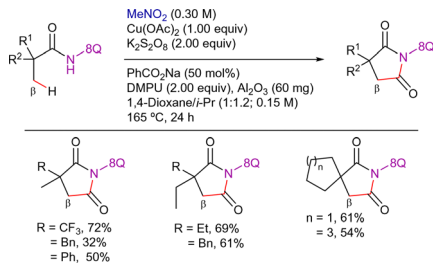

Scheme 56 Cu-promoted β-C(sp^3)–H carbonylative cyclization with nitromethane.

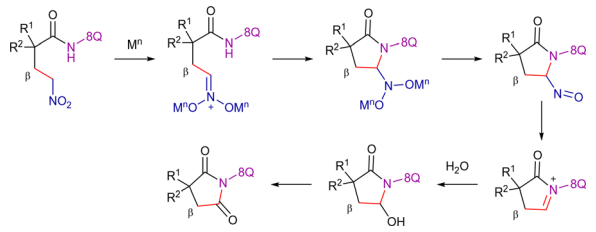

Scheme 57 Proposed Nef-type reaction.

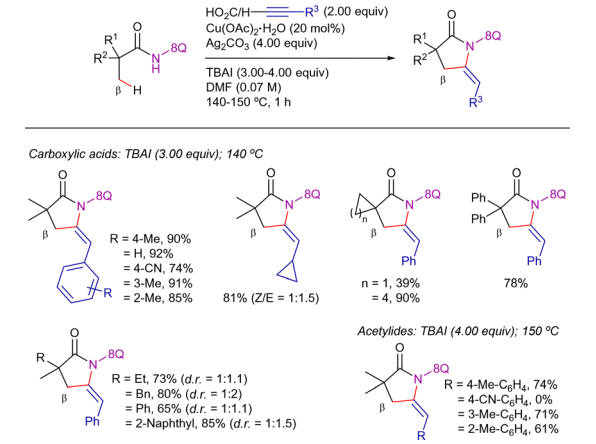

Scheme 58 Cu-cat. sequential β-C(sp^3)–H activation/annulation with alkynes.

active silver acetylide species *in situ*,[140–142] (ii) acting as oxidant, and (iii) promoting the cyclization of the alkynylated product, which leads to the thermodynamically favored (*E*)-ethylidene-pyrrolidinones. The reaction was carried out in DMF at 140–150 °C for 24 h. Interestingly, under the optimized conditions, terminal alkynes were less effective than the carboxylic acid analogues.

Under these conditions, the reaction was limited to pivalamide derivatives with a quaternary α-carbon. The postulated mechanism would be analogous to the one depicted in Scheme 22. The catalytic cycle would involve (i) copper(II)-mediated DG-assisted C–H activation to form a copper(II)-cyclometalated intermediate, (ii) copper(II) disproportionation to generate an alkyl-Cu(III) metallacycle, (iii) transmetalation with the silver/copper acetylide generated *in situ*, and (iv) C–C bond reductive elimination to generate the alkynylated product and copper(I) species. The silver(I) would re-oxidize the copper(I) to the catalytically active copper(II) species, closing the catalytic cycle, whereas the alkynylated product would evolve to the β-lactam through a Ag/TBAI mediated cyclization reaction.

3.2. C–Heteroatom bond formation

3.2.1. C–N bond formation. Since the discovery of the Ullmann and Golberg methods,[143,144] numerous strategies have appeared targeting the formation of C–N bonds under copper catalysis.[145–147] Among them, directed C–H functionalization has become a highly attractive approach. Most efforts relied on C(sp^2)–

H intermolecular amination/amidation with sulfoximines, amines, azides or cyanate salts and even the direct use of ammonia as coupling partners.[148] The effectiveness of copper in promoting C(sp^3)–N bond formations is more recent and limited.

In 2014, two protocols were independently reported for the synthesis of β-lactams through the 8-AQ-assisted copper-catalyzed intramolecular β-C(sp^3)–H oxidative amidation of carboxamides. The protocol of Kuninobu' and Kanai's groups involved $Cu(OAc)_2$ as catalyst and Ag_2CO_3 as oxidant in DCE at 140 °C (Scheme 59a),[149] while Ge's group used CuCl as the catalyst and duroquinone as oxidant, $PhCO_2Na$ as base, *ortho*-xylene as solvent at 160 °C (Scheme 59b).[150] In both protocols, similar reactivities and selectivities were observed. Additionally, both demonstrated that the 8-amino-5-methoxyquinoline DG was also efficient for this transformation and could be removed under oxidative conditions as shown in Scheme 35.

In both contributions, the initial C(sp^3)–H bond activation occurs *via* cyclocupration, leading to the formation of an alkyl–copper(II) species. This species is then oxidized by either another Cu-salt or oxidant, resulting in the formation of an alkyl–copper(III) species. Subsequent C–N bond formation *via* reductive elimination leads to the final product with concomitant generation of a copper(I) species, which would be reoxidized to copper(II). However, in some cases, the copper(II) might first coordinate the DG before being oxidized to copper(III). Subsequent cyclocupration forms the alkyl–copper(III) species.

In 2015, Yang' and You's groups described a more economical and practical protocol for the formation of β-lactam compounds using oxygen as the sole oxidant, observing complete β-CH_3 selectivity in most cases (Scheme 59c).[151] In this work, the authors proposed the plausible reaction mechanism shown in Scheme 60. Initially, copper(I) reacts with O_2 to generate a copper(II)-superoxide radical, which undergoes electron transfer oxidation and H-abstraction to yield a copper(II)-hydroperoxo species. The resulting copper(II) species then coordinates with the amide, forming the *N*,*N*-chelated copper complex **XLIII**, followed by C(sp^3)–H cupration to produce the cyclometallic intermediate **XLIV**. Subsequently, disproportionation generates copper(III) complex **XLV**. Finally,

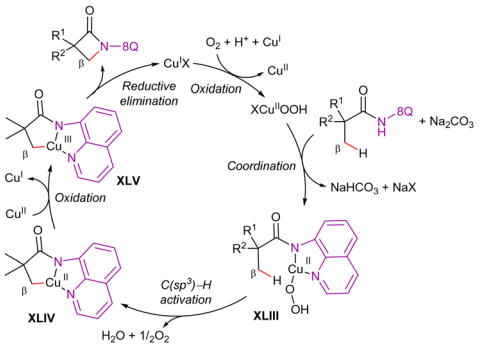

Scheme 60 Proposed catalytic cycle for Cu-cat. β-C(sp^3)–H amidation under O_2 atmosphere.

reductive elimination of the complex **XLV** releases the β-lactam and copper(I) species to close the catalytic cycle. It is worth noting that the direct oxidation of the copper(II) complex **XLIV** to the copper(III) species **XLV** by O_2 was not excluded as a possibility.

In 2016, two intermolecular versions for the coupling with secondary amines by using the 8-AQ as DG were disclosed independently by the groups of Qin and Yang. The method reported by the Qin's group, mediated by a $Cu(OAc)_2/O_2$ system at 130 °C, showed a useful substrate scope for α-quaternary carboxylic amides and cyclic secondary alkylamines (Scheme 61a).[152] On the other hand, the protocol disclosed by Yang's group was carried out at 150 °C under air and required the presence of Na_2HPO_4 (Scheme 61b).[153] This protocol was applied to a variety of cyclic and lineal secondary amines as well as to more challenging primary amines.

Mechanistic studies indicated that the C–H activation step would be irreversible and involved in the *r.d.s.* Furthermore, the addition of TEMPO or BHT inhibited the reaction, suggesting the involvement of radical species. In fact, in the work of Yang *et al.*, a coupling product between TEMPO and morpholine was isolated (Scheme 62).

On these bases, two reaction pathways have been proposed (Scheme 62): (a) copper(II) coordination to the carboxamide to generate intermediate **XLVI**, followed by the C–H activation

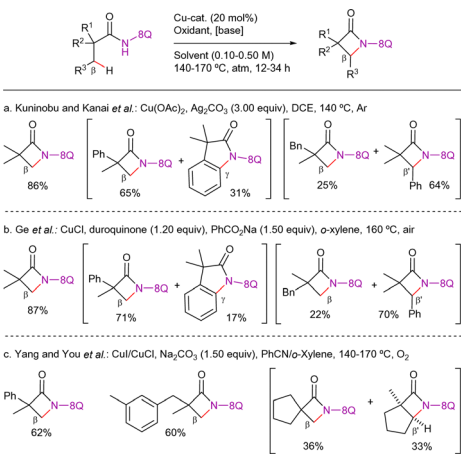

Scheme 59 Cu-cat. β-C(sp^3)–H amidation.

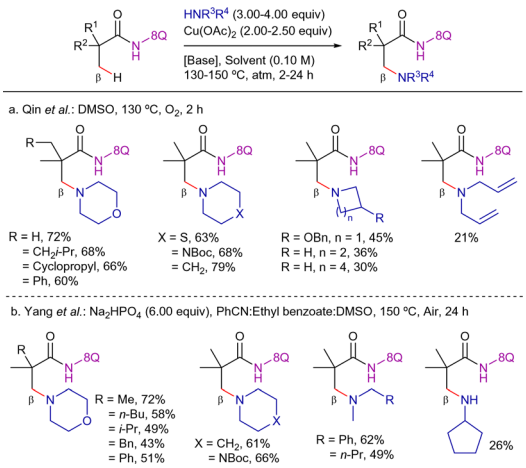

Scheme 61 Cu-cat. β-C(sp^3)–H intermolecular amination.

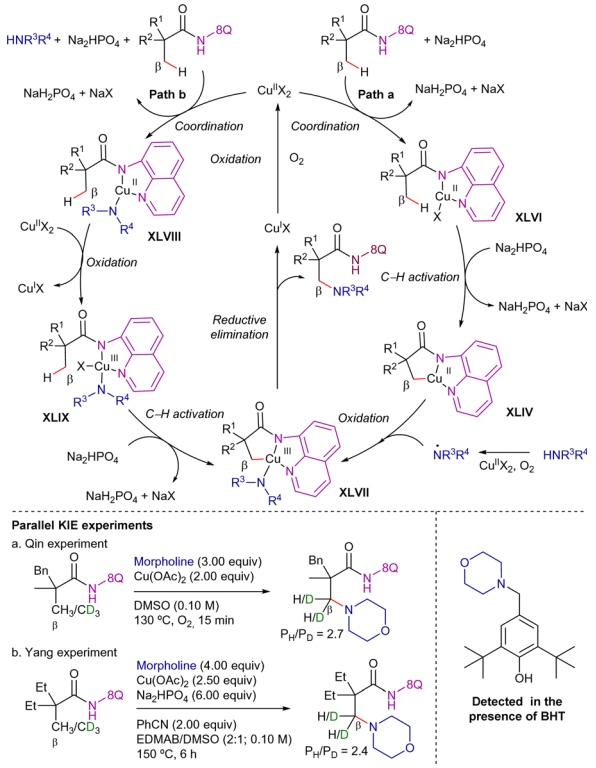

Scheme 62 Proposed catalytic cycle for Cu-cat. β-C(sp^3)–H intermolecular amination.

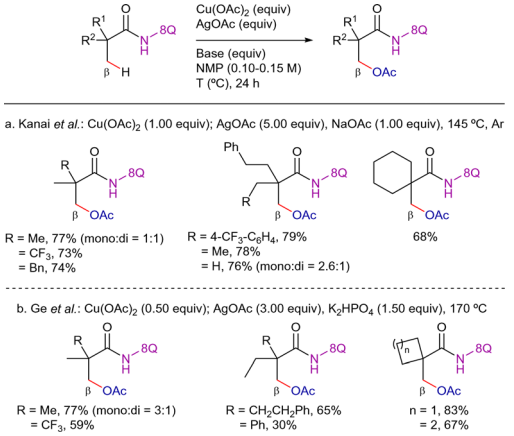

Scheme 63 Cu-mediated β-C(sp^3)–H acetoxylation.

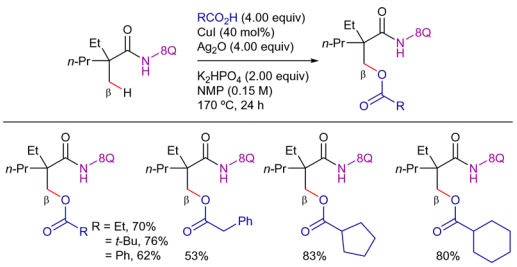

Scheme 64 Ge's *et al.* work on Cu-catalyzed β-C(sp^3)–H acyloxylation.

step to generate a copper(II)-cyclometallated complex **XLIV**. Then, nitrogen radical oxidative addition, generated by copper(II)-mediated amine oxidation, forms intermediate **XLVII** (path a); or (b) intermediate **XLVII** could also be formed by first amine and carboxamine coordination to copper(II) species to generate intermediate **XLVIII**, followed by disproportionation to produce the copper(III)-intermediate **XLIX**, and subsequent C–H activation (path b). Finally, from intermediate **XLVII**, a reductive elimination step forms the final product and copper(I) species, that would be re-oxidized by oxygen.

3.2.2. C–O bond formation. In 2014, Kuninobu and Kanai *et al.* reported the copper-catalyzed, 8-AQ-directed, β-methyl C(sp^3)–H acetoxylation of α-quaternary aliphatic amides (Scheme 63a).[154] Using $Cu(OAc)_2$ (1.00 equiv.) with AgOAc (5.00 equiv.) as an acetate source and oxidant, and NaOAc (1.00 equiv.) as base at 145 °C high group compatibility was observed. In parallel, Ge *et al.* developed an equally efficient substoichiometric method by using $Cu(OAc)_2$ (0.50 equiv.) as catalyst with 3.00 equiv. of AgOAc and 1.50 equiv. of K_2HPO_4 at 170 °C (Scheme 63b).[155]

Additionally, in the same work, Ge's group demonstrated that other acyloxy groups can be introduced at β-C(sp^3)–H bonds in the absence of acetoxy sources, under similar reaction conditions (Scheme 64).[155] More recently, Zhang *et al.* improved these conditions by reporting a copper-catalyzed, TBAB/TBAC-accelerated, C(sp^3)–H acyloxylation protocol (Scheme 65).[156] In this work, heteroaryl and alkenyl carboxylic acids were also suitable coupling partners. Regarding the mechanism, the use of TEMPO as radical scavenger suppressed the reaction, suggesting the involvement of radical species. In addition, deuterium labeling and KIE experiments indicated that the C(sp^3)–H activation was irreversible and involved in the *r.d.s.* (KIE = 2.8).

Likewise, Zhang and co-workers reported a copper-mediated oxidation of β-C(sp^3)–H bonds of propionamides with organosilanes (Scheme 66).[157] Vinyl and arylsilanes were suitable for this transformation, providing the desired product from moderate to good yields. A pathway involving a C–O coupling of the C(sp^3)–H bond with phenol generated from trimethoxy(phenyl)silane was

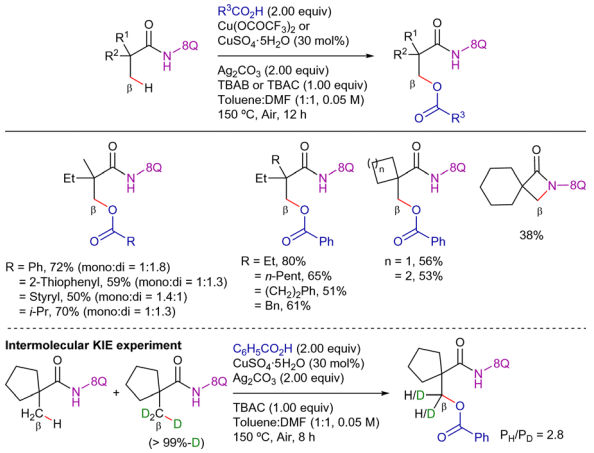

Scheme 65 Zhang's *et al.* work on Cu-catalyzed β-C(sp^3)–H acyloxylation.

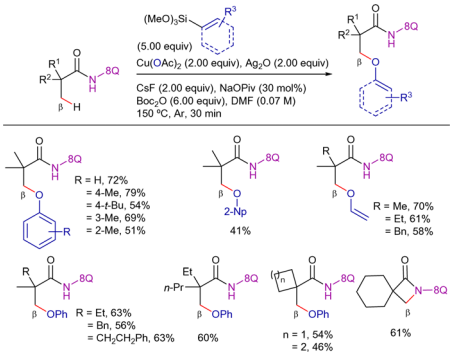

Scheme 66 Cu-promoted β-C(sp^3)–H aryl- and vinyloxylation with organosilanes.

ruled out since the phenol itself is not a suitable reaction partner. O^{18}-labeling experiments showed that $Cu(OAc)_2$ served as the source of the oxygen to generate the C(sp^3)–O bond during the aryloxylation process.

Based on these results, the proposed reaction pathway begins with the C(sp^3)–H bond activation and oxidation to an alkyl–copper(III) species. This species then undergoes C–O reductive elimination between the alkyl group and an acetate ligand to provide the newly inserted ester group and a copper(I) species ligated to the DG (intermediate **L** in Scheme 67). Oxidation of copper(I) to copper(II), presumably with Ag_2O and HOAc, generates intermediate **LI**, which allows the hydrolysis of the acetate inserted at the β-position, giving the copper(II) species **LII**. Oxidation *via* disproportionation and subsequent transmetalation gives intermediate **LIV**. Final reductive elimination between the alcohol and the aryl or alkenyl group provides the desired products.

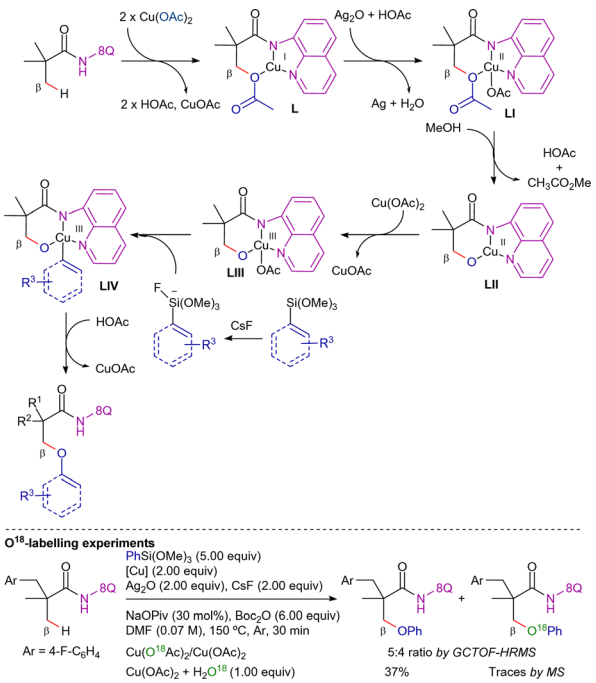

Scheme 67 Reaction mechanism for the aryl- and vinyloxylation with organosilanes.

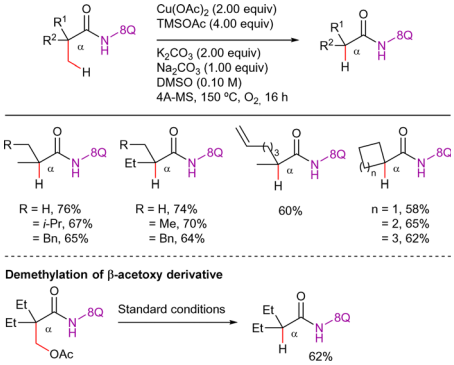

Scheme 68 Cu-promoted β-C(sp^3)–H demethylation.

An oxidative demethylation of α-quaternary propionamides was reported by the Fu's group using $Cu(OAc)_2$ (2 equiv.), TMSOAc (4 equiv.) as additive, K_2CO_3 (2 equiv.) and Na_2CO_3 (1 equiv.) as bases in DMSO at 150 °C under O_2 atmosphere, using 4Å molecular sieves (Scheme 68).[158] The authors suggested that this transformation might proceed *via* similar mechanism of initial β-C(sp^3)–H acetoxylation, next hydrolysis of the ester group and final oxidative decarboxylation. In fact, when a β-acetoxylated product was subjected to the reaction conditions, the formation of the demethylated product was observed.

4. Fe-catalysis

Iron is the second-most abundant metal in Earth's crust, after aluminium, and is relatively inexpensive compared to the precious metals often used in catalysis.[159] Moreover, iron can adopt oxidation states ranging from −2 to +5 (and in rare cases +6).[160–162] High-oxidation state iron catalysts (+3, +4, or even +5) are most commonly employed in nonactivated C(sp^3)–H bond functionalization reactions. Currently, iron-catalyzed C(sp^3)–H bond functionalization is primarily limited to C–C bond-forming processes, such as arylation and alkylation.

In 2013, Nakamura *et al.* reported the first 8-AQ-directed C(sp^3)–H arylation of α,α-disubstituted propamide derivatives with diaryl zinc reagents employing $Fe(acac)_3$ as catalyst. The use of 1,2-bis(diphenylphosphino)benzene (dppbz) as ligand and 1,2-dichloro-2-methylpropane (DCIB) as organic oxidant allowed the formation of arylated products in good yields (Scheme 69).[163] The experimental procedure of this reaction involves the previous mixture of ArMgBr (7.00 equiv.) and $ZnBr_2$·TMEDA (3 equiv.) to form *in situ* 3.00 equiv. of Ar_2Zn which probably act as nucleophiles in the reaction. The remaining 1.00 equiv. of ArMgBr most likely deprotonates the amide proton.

The arylation reaction was susceptible to steric effects in the aryl magnesium bromide reagent. Whereas with *para*- and *meta*-tolyl magnesium bromides, the arylated products were isolated in good yields, with *ortho*-tolyl derivative, the starting carboxamide was recovered unaltered.

The significantly greater reactivity of a methyl group compared to a benzylic group rules out a radical mechanism, while

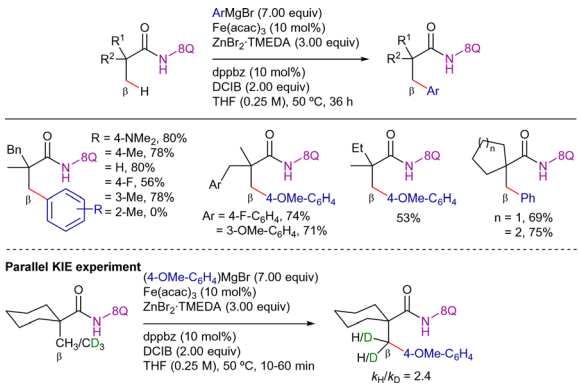

Scheme 69 8-AQ-assisted β-C(sp^3)–H arylation with Grignard reagents.

the strong dependence of the yield on the substrate's structure and the ligand indicates the involvement of organoiron intermediates in key steps. The KIE experiments suggested that the C–H bond cleavage is the *r.d.s.* of the reaction, with a primary KIE of 2.4 observed in parallel reactions and an intermolecular KIE of 4.0.

Further mechanistic studies performed by Chen's group revealed that the C(sp^3)–H activation step could be promoted by iron(II) or iron(III) species through a two-state reactivity (TSR) scenario. The low-spin iron(II) singlet state, initially an excited state, would transition to the quintet-spin ground state and facilitate the C–H bond cleavage.[164] From this point, inspired by the mechanistic knowledge on iron-catalyzed C(sp^2)–H arylation,[62,165] the authors proposed that the next step involves an aryl transmetalation, followed by the oxidation of Fe^{II} to Fe^{III} through a single-electron transfer (SET). The dichloroalkane would act as an oxidizing agent, facilitating the final C–C coupling and completing the C–H functionalization. Fe^{I} species would also be generated and reoxidized to the active Fe^{II} catalyst by another SET oxidation by DCIB. The ligand sphere of iron would thus be essential in the TSR mechanism by stabilization of the reactive low-spin state that mediates the C–H activation.

In 2014, Ackermann's group demonstrated that a triazole-based DG also afforded excellent results in the iron-catalyzed arylation of unactivated C(sp^3)–H bonds with Ar_2Zn (Scheme 70).[166] The reaction conditions were very similar, with an increase in the catalyst loading and reaction temperature. Removal of the DG was achieved using concentrated HCl at 130 °C.

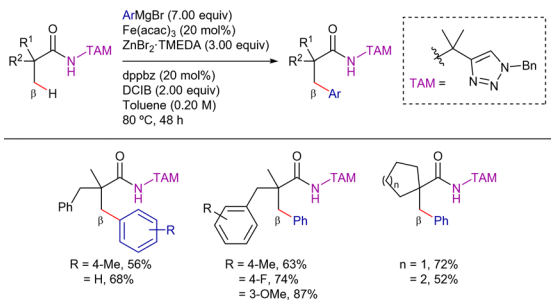

Scheme 70 β-C(sp^3)–H arylation with Ar_2Zn using a triazole type-DG.

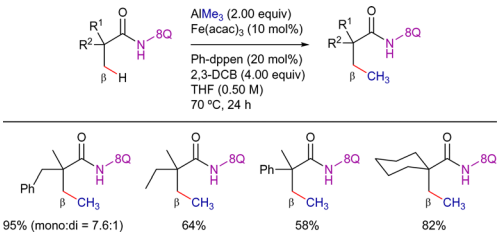

Scheme 71 β-C(sp^3)–H alkylation with $AlMe_3$.

In 2015, Nakamura's group reported the direct methylation of a C(sp^3)–H bond with a $AlMe_3/Fe^{III}$ system by using the 8-AQ as DG (Scheme 71).[167] In this work, $AlMe_3$ was used as the methyl donor and 2,3-dichlorobutane (2,3-DCB) as oxidant, along with (*Z*)-1-phenyl-1,2-bis(diphenylphosphino)ethene (Ph-dppen) as ligand. The reaction was applied to a variety of α,α-disubstituted propanamide substrates.

Alternatively, Ackermann's group developed a complementary methodology for the β-C(sp^3)–H alkylation with $ZnCl_2$·TMEDA using TAM as DG (Scheme 72).[168] In this work, optimal results were achieved at near ambient temperature with $FeCl_3$ as catalyst and DCIB as a mild oxidant. The strong selectivity for functionalizing the methyl C–H bond over the weaker benzylic C–H bond suggested an organometallic C–H metalation mechanism.

On the other hand, in 2017, Nakamura's group expanded the methodology to aryl-, heteroaryl-, and alkenyl boron reagents as coupling partners (Scheme 73).[169] The success of this reaction relied on the use of 8-AQ as DG, $Fe(acac)_3$ as catalyst and a Zn^{II}-salt as a co-catalyst, along with a diphosphine ligand bearing a conjugated backbone [(*Z*)-1,2-bis-(diphenylphosphino)ethene or its electron-rich congener, (*Z*)-1,2-bis[bis(4-methoxyphenyl)-phosphine]ethene].

Based on experimental mechanistic studies, the authors postulated the mechanism shown in Scheme 74. Zinc-assisted deprotonation gives the zinc amide **LV**, and then boron/iron transmetalation gives the organoiron(III) intermediate **LVI**. Conversion of **LVI** to the β-arylated product *via* a C–H oxidative addition mechanism (*via* an iron(V) species **LVII**) would be unlikely. Alternatively, the C–H activation through σ-bond metathesis forming intermediate **LVIII** is postulated. Ferracycle **LVIII** then reacts with another phenyl group from phenylboronate and undergoes reductive elimination to form the new C–C bond product, generating the organoiron(I) intermediate

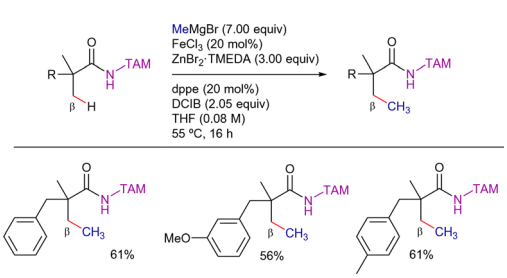

Scheme 72 β-C(sp^3)–H alkylation with MeMgBr/$ZnBr_2$ using a triazole type-DG.

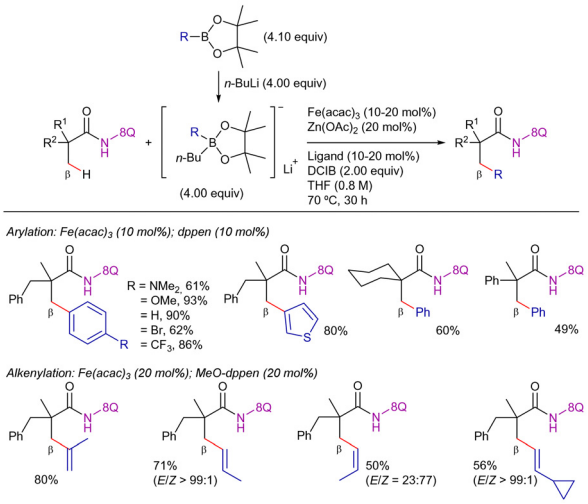

Scheme 73 β-C(sp^3)–H arylation and alkenylation with organoboron reagents.

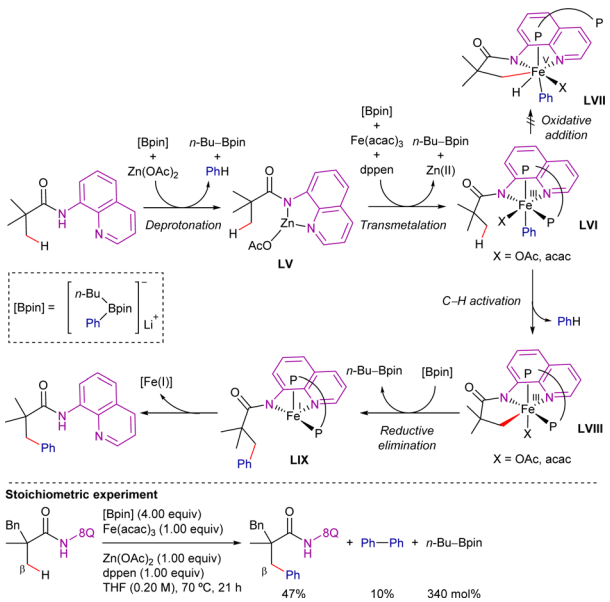

Scheme 74 Proposed mechanism for C(sp^3)–H arylation with organoboron reagents.

LIX. This seemingly unstable iron(I) species may be stabilized through electron delocalization over the conjugated ligand backbone. Finally, the product is released by protonolysis, generating iron(I) species that can be easily oxidized in the presence of O_2.

5. Co-catalysis

Cobalt has achieved a privileged status as catalyst due to its low cost, high abundance and variable oxidation states (+1, +2, +3 and +4). Since the first cobalt-catalyzed work of Kharasch and Fields on the homocoupling of Grignard reagents,[170] several efficient cross-couplings,[171] hydroformylations,[172] and many other reactions have been reported.[56,173–175]

In the field of cobalt-catalyzed C–H functionalization reactions, two categories can be defined based on the oxidation state of the catalysts:[176–179] a low-valent approach, where the active catalyst is a cobalt(0) or cobalt(I) species,[180,181] and a high-valent approach, where the active catalysts typically feature a cobalt-center in the +3 oxidation state.[182–186] Nonetheless, advancements in DG-assisted cobalt-catalyzed C(sp^3)–H functionalization have predominantly been achieved through high-valent cobalt catalysis.[61] These transformations primarily rely on bench-stable Cp*Co(III) complexes in combination with monodentate coordinating DGs.[187,188] Alternatively, they can be facilitated *via* the *in situ* oxidation of cobalt(II) catalyst precursors, enabled by bidentate chelation assistance, particularly from 8-AQ, picolinamide, and pyridine-2-sulfonamide. In particular, when cobalt(II) precursors are employed, two plausible operative pathways can be considered. One option is that the catalytic cycle begins with the coordination of the substrate to the cobalt(II) salt, forming a cobalt(II)-substrate complex, which is subsequently oxidized to a cobalt(III) species that undergoes C–H activation. Alternatively, a second option is that the cobalt(II) catalyst is initially oxidized to a cobalt(III) salt, followed by substrate coordination. Literature evidence supports both pathways, and the most likely operative mechanism depends on the specific reaction conditions and/or the substrate used in the transformation.

The following are relevant contributions in this area grouped by the type of bond formed.

5.1. C–C bond formation

5.1.1. Alkenylation processes. In 2015, Zhang *et al.* reported an optimal protocol for the synthesis of 5-(*E*)-ethylidene-pyrrolidin-2-ones *via* a 8-AQ-assisted cobalt-catalyzed C(sp^3)–H alkynylation/cyclization process from α,α-disubstituted propanamides and terminal alkynes (Scheme 75).[189] The best results

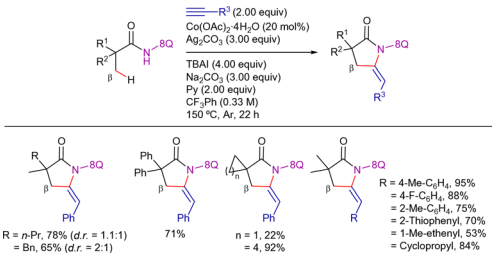

Scheme 75 Sequential β-C(sp^3)–H alkynylation/annulation with terminal alkynes.

were obtained using $Co(OAc)_2{\cdot}4H_2O$ as catalyst precursor, Ag_2CO_3 as oxidant, Na_2CO_3 as base, and Py and TBAI as additives, in CF_3Ph at 150 °C for 22 h. Substrates having *pro*-chiral β-CH_3 positions led to a mixture of diastereomers. Aryl, alkenyl, and alkyl acetylenes were suitable coupling partners, providing the desired products with moderate to good yields.

In line with the previously mentioned reports using nickel- and copper-catalysis,[89,139] the authors suggested that this transformation goes through an oxidative alkynylation process and subsequent Ag/TBAI-mediated intramolecular annulation reaction (Scheme 76). The authors detected the alkynylated intermediate **c** in the reaction mixture through GC-MS analysis at short reaction times and demonstrated its conversion into the corresponding 5-(*E*)-ethylidene-pyrrolidin-2-one derivative under the reaction conditions. They proposed that an alkynyl–cobalt(IV) or alkynyl–cobalt(III) intermediate undergoes reductive elimination to generate intermediate **c**. Additionally, an alkynyl radical intermediate was suggested based on a control

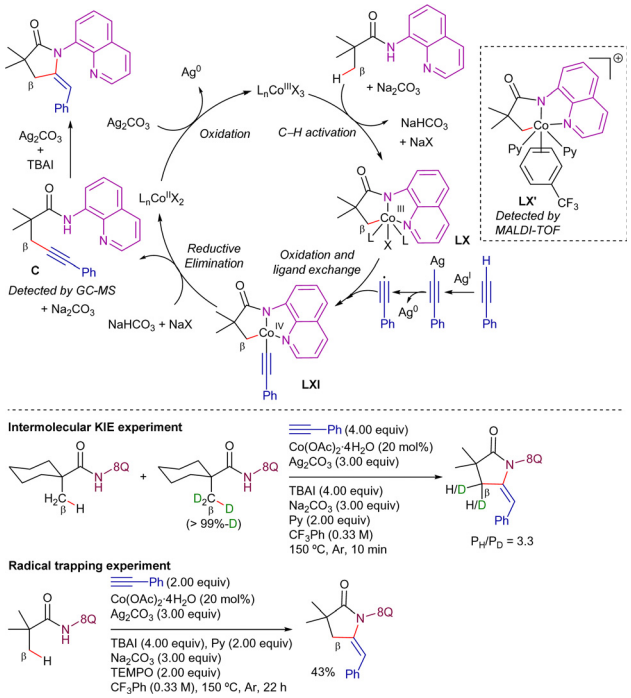

Scheme 76 Sequential β-C(sp^3)–H alkynylation/annulation process. Proposed mechanism.

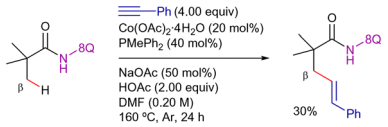

Scheme 77 β-C(sp^3)–H alkenylation with terminal alkynes.

experiment using 2,2,6,6-tetramethylpiperidin-1-yl)oxyl (TEMPO) as a radical inhibitor. However, since the reaction proceeded with moderate yield even in the presence of TEMPO and no TEMPO adduct was detected, the involvement of an alkynyl radical remains uncertain. Notably, radical-trapping experiments in transition-metal catalysis should be interpreted cautiously, as radical-trapping reagents may also interact with transition-metal species.[190]

On the other hand, the use of aromatic solvents was essential for this transformation, and the solvated metallacycle intermediate **LX′** was identified *via* MS (MALDI-TOF) analysis of the reaction solution. Therefore, both pyridine and $PhCF_3$ may play a role in the formation of the metallacycle intermediate. Additionally, since no deuterium scrambling is observed, the C–H activation step is irreversible and presumably the *r.d.s.* (competitive KIE experiment with a value of P_H/P_D = 3.3).

Relying on related work, the authors suggest that TBAI may act as a phase-transfer catalyst.

Interestingly, Zhang *et al.* also reported one example demonstrating the viability of carrying the 8-AQ-assisted cobalt-catalyzed C(sp^3)–H alkenylation of the pivalamide derivative with phenyl acetylene. The reaction was carried out using NaOAc (50 mol%) and HOAc (2 equiv.) as additives (Scheme 77).[88] Although no mechanistic studies have been conducted on this outcome, the observed reactivity could be rationalized by a pathway involving C–H activation, followed by a plausible migratory insertion and subsequent protonolysis to yield the alkenylated product. Without a silver(I) salt in the medium, the alkynyl–cobalt(III) intermediate does not form, thereby preventing the formation of the alkynylated intermediate.

Recently, Hamlin and Dixon *et al.* have described an efficient protocol for the enantioselective Co-catalyzed β-C(sp^3)–H alkenylation of benzyl thioamide derivatives with but-2-ynoate ester coupling partners (Scheme 78).[191] The mild reaction conditions were compatible with a broad range of α-dimethyl-substituted thioamide partners, delivering the alkenylated products as

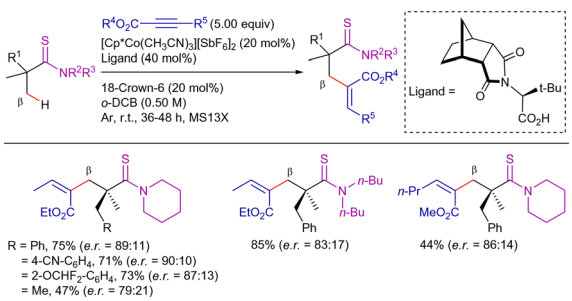

Scheme 78 Enantioselective β-C(sp^3)–H alkenylation with internal alkynes.

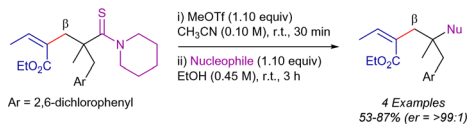

Scheme 79 Conversion of the thioamide into different functional groups.

single regioisomers in excellent yields (up to 85%) and high enantiomeric excess [up to 91 : 9 enantiomeric ratio (*er*), or >99 : 1 *er* after a single recrystallization]. Post-synthetic modifications allowed the conversion of the thioamide group into a wide range of functional groups using MeOTf and different nucleophiles (Scheme 79).

As illustrated in Scheme 80, DFT calculations suggest that the active species, $Cp^*Co(O_2CR)^+$, is generated through the interaction of Cp*Co(III) with the L-*tert*-leucine-derived chiral acid ligand under the reaction conditions. The catalytic cycle then begins with the coordination of the thioamide substrate to the proposed active catalyst, forming complex **LXII**. The C–H activation step is initiated *via* a κ^2–κ^1 displacement of the carboxylate by the β-hydrogen of the substrate (**LXIII**), proceeding through a CMD mechanism to afford intermediate **LXIV**. The steric bulk of the acid co-catalyst with the benzyl group is likely a key factor in governing stereoselectivity at this stage. Subsequent migratory insertion of the alkyne yields intermediate **LXV**, which, upon protonolysis, leads to the formation of the desired alkenylated product while regenerating the active $Cp^*Co(O_2CR)^+$ species. The regioselectivity of the migratory insertion step is also influenced by steric repulsions with the benzyl group at the corresponding transition state.

On the other hand, Sundararaju's group developed a highly regioselective and stereoselective method for the γ-alkenylation of 8-methylquinoline derivatives with alkynes under mild conditions.[192] The reaction employed a $Cp^*Co(CO)I_2$ catalyst precursor (5 mol%), AgOTf and $AdCO_2H$ as additives (10 mol% each), and TFE as solvent at 80 °C (Scheme 81). Under these conditions, the *cis*-addition of the C(sp^3)–H bond to the alkyne proceeded in good yields. The reaction tolerated a wide range of substituted quinolines and symmetrical alkyl internal alkynes.

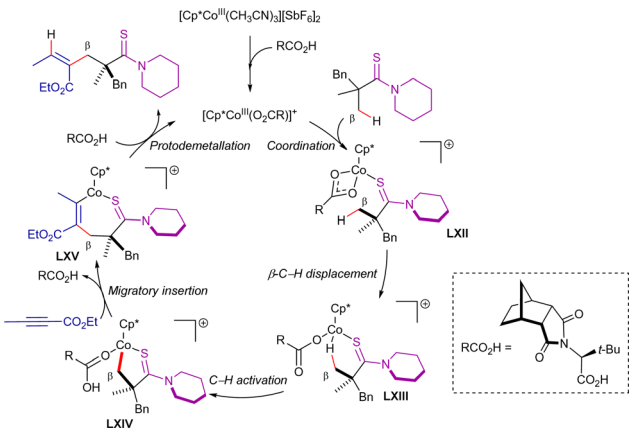

Scheme 80 Enantioselective β-C(sp^3)–H alkenylation with internal alkynes. Proposed mechanism.

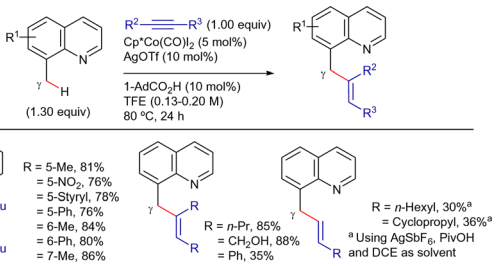

Scheme 81 Cp^*Co^{III}-cat. γ-C(sp^3)–H alkenylation with alkynes.

Unfortunately, aryl alkynes were less effective and mixtures of regioisomers were obtained using unsymmetrical alkynes. Terminal alkynes could also be used by changing to $AgSbF_6$ and PivOH as additives, and DCE as solvent, albeit the products were isolated in low yields.

Intermolecular competitive experiments revealed that the reaction was favoured with electron-rich substituents at the quinoline ring and alkyl substitution at the internal alkyne. Deuterium labeling experiments suggested an irreversible cyclometalation pathway which, as determined by DFT calculations, appears to occur *via* an outer-sphere C–H activation rather than an inner-sphere pathway. The proposed reaction mechanism is depicted in Scheme 82. First, halogen abstraction from $[Cp^*Co(CO)I_2]$ with AgOTf and ligand exchange generates the catalytically active cationic cobalt(III) species that then undergoes coordination to the 8-methylquinoline derivative to generate intermediate **LXVI**. Subsequent external base-assisted cyclometalation *via* a CMD mechanism leads to the cationic intermediate **LXVII**. From intermediate **LXVII**, coordination of the alkyne in a preorganized orientation followed by its insertion into the C(sp^3)–Co bond leads to the cationic 7-membered intermediate **LXIX**. Finally, after a protodemetalation step, the final alkenylated product is released and the catalytically active cobalt(III)-species is regenerated.

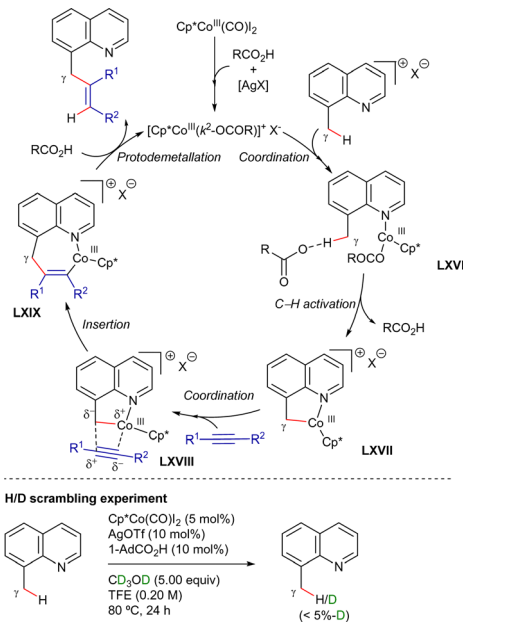

Scheme 82 γ-C(sp^3)–H alkenylation with alkynes. Proposed mechanism.

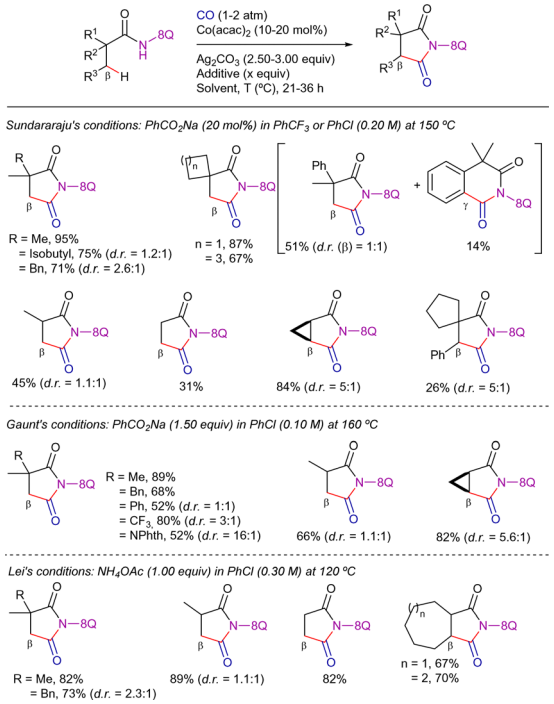

Scheme 83 Sequential β-C(sp^3)–H carbonylation/annulation.

5.1.2. Carbonylation processes. The 8-AQ-assisted Co(acac)$_2$-catalyzed C(sp^3)–H carbonylative cyclization of aliphatic amides was independently reported by Sundararaju's,[193] Gaunt's,[194] and Lei's[195] groups (Scheme 83). In all these contributions, the reaction proceeded under atmospheric pressures of CO (1–2 atm), using operationally simple conditions and accommodating a variety of versatile functional groups. Similar yields were obtained in the functionalization of α,α-disubstituted propanamide derivatives regardless of the method, but for α-substituted or linear α-propanamide substrates, Lei's reaction conditions were more efficient in most cases. All protocols showed that secondary *β*-positions could also be functionalized effectively in cyclic carboxamides.

A parallel KIE experiment conducted by Sundararaju's group revealed a k_H/k_D value of 1.42, suggesting that C–H activation is not the *r.d.s.* Both Sundararaju's and Lei's groups reported that the addition of TEMPO significantly reduced reaction yields, implying the potential involvement of a SET pathway. However, no TEMPO adducts were identified, making the characterization of radical intermediates challenging, as previously mentioned. Furthermore, Lei's group conducted an X-ray absorption spectroscopy (XAS) analysis, which suggested that the oxidation of cobalt(II) to cobalt(III) is more likely to occur after cobalt(II) coordinates to the amide derivative. On these bases, although a plausible mechanism was still unclear at that stage, Lei and Sundararaju considered the possibilities shown in Scheme 84. Initial coordination of cobalt(II) to the propanamide substrate, followed by NH deprotonation (possibly by silver carbonate) and subsequent oxidation to cobalt(III) promoted by silver(I) leads to intermediate **LXX**. Subsequent carboxylate/carbonate assisted CMD provides cobaltacycle **LXXI**. Coordination of CO to the cobalt(III) intermediate **LXXI**, followed by its insertion into the

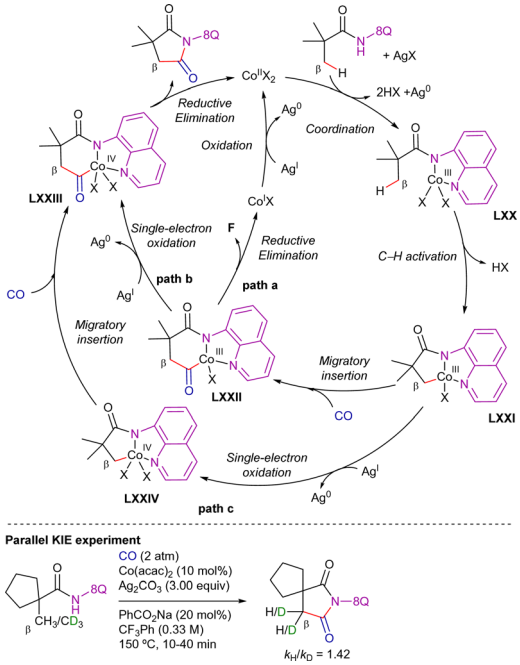

Scheme 84 Proposed mechanism for the Co-cat. β-C(sp^3)–H cyclative carbonylation.

Co–C bond generates intermediate **LXXII**. From here, the final product succinimide could be generated by means of: (i) a reductive elimination step, also generating cobalt(I) species which would be re-oxidized by silver (path a), or (ii) one electron oxidation to generate the cobalt(IV) intermediate **LXXIII**, which would then undergo the reductive elimination to give the final succinimide product, regenerating cobalt(II) species (path b). Besides these options, the authors also considered that intermediate **LXXI** could undergo one electron oxidation to the cobalt(IV) intermediate **LXXIV**, and then insertion of CO into the Co–C bond to lead to intermediate **LXXIII** (path c), which would subsequently undergo reductive elimination to generate the final product and cobalt(II) species.

More recently, Sundararaju's group developed a complementary two-chamber method in which the CO atmosphere was created by CO_2 reduction in the presence of disilanes, achieving similar yields to those of previous protocols (Scheme 85).[196]

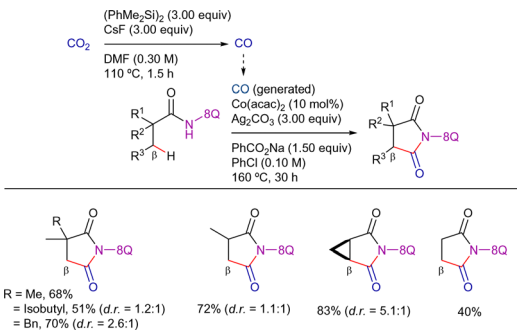

Scheme 85 Sequential β-C(sp^3)–H carbonylation/annulation with CO_2 as CO-source.

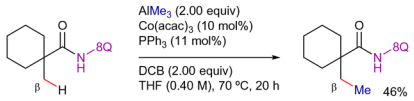

Scheme 86 β-C(sp^3)–H methylation with trimethylaluminum.

5.1.3. Alkylation processes. In 2016, Xu *et al.* reported one example of cobalt(III)-catalyzed β-C(sp^3)–H alkylation of 1-methyl-*N*-(quinolin-8-yl)cyclohexane-1-carboxamide using trimethylaluminum as methyl donor (Scheme 86).[197] Although the yield was rather low, this was the first precedent of a cobalt-catalyzed alkylation process.

In the next year, Shi's group reported a $Co(OAc)_2{\cdot}4H_2O$-catalyzed, 8-AQ-directed double C(sp^3)–H activation strategy for the synthesis of bicyclo[4.1.0]heptane and bicyclo[3.1.0]hexane derivatives by using α-substituted 2-methylhept-6-enamide or 2-methylhex-5-enamide derivatives as starting materials (Scheme 87).[198] The formation of larger bicyclo[5.1.0]octanes was not possible.

Since no deuterium scrambling is observed, the authors suggest that the C–H activation step is irreversible and presumably the *r.d.s.* As shown in Scheme 88, this reaction was

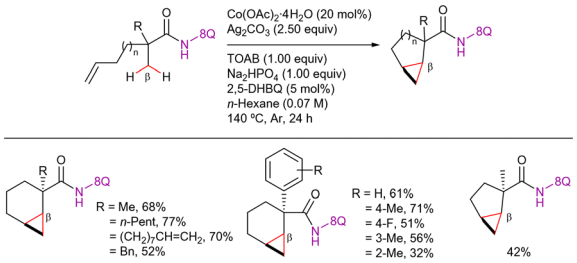

Scheme 87 Double β-C(sp^3)–H bond functionalization.

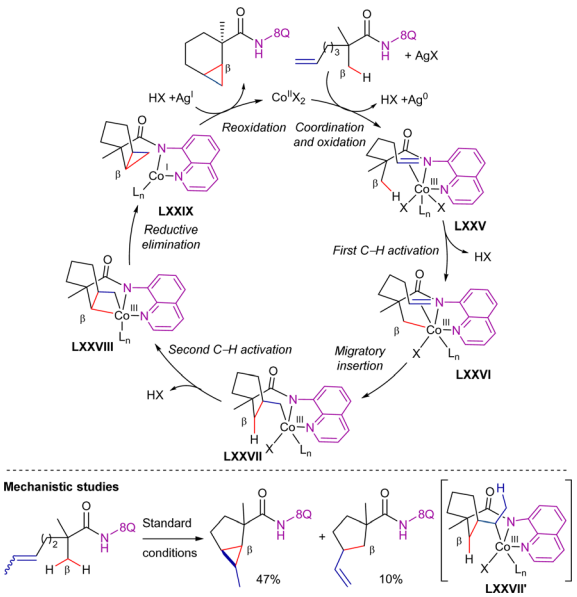

Scheme 88 Double β-C(sp^3)–H functionalization. Proposed mechanism.

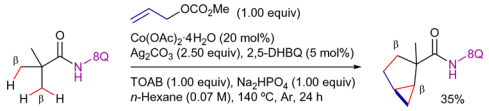

Scheme 89 Triple β-C(sp^3)–H functionalization.

proposed to start with the coordination of the cobalt(II)-species to the 8-AQ and the double bond of the substrate, followed by silver(I)-mediated single-electron oxidation to generate the cobalt(III)-species **LXXV**. Then, subsequent irreversible activation of the methyl C(sp^3)–H bond generates intermediate **LXXVI**, which, after alkene migratory insertion, leads to intermediate **LXXVII**. From this point, methylene C(sp^3)–H activation at the same *β*-position gives the formation of the four-membered cobaltacycle intermediate **LXXVIII**. Subsequent reductive elimination and decomplexation would release the bicyclo[n.1.0]alkane product and cobalt(I) species, that would be reoxidized by silver(I)-species to regenerate the active cobalt(II)-species, closing the catalytic cycle. To support this mechanism the authors analyzed the reactivity of a 2-methylhept-5-enamide derivative that presented two allylic hydrogens. In this case, a mixture of the desired bicyclo[3.1.0]hexane derivative along with a monocyclic vinylcyclopentane derivative was obtained. The formation of the later was explained *via* β-hydride elimination from intermediate **LXXVII′** (analogue of intermediate **LXXVII**).

Interestingly, the authors also reported the synthesis of a bicyclo[3.1.0]hexane from pivalamide and allyl methyl carbonate, under slightly modified reaction conditions. This reaction presumably proceeds through a C(sp^3)–H allylation/cyclopropanation sequence, which involves the cleavage of three C(sp^3)–H bonds (Scheme 89).

In parallel, Shi's group showed that the γ-alkylation of 8-methylquinolines was feasible by employing diazo compounds as coupling partners (Scheme 90).[199] The reaction presumably proceeded through primary C(sp^3)–H cobaltation/carbene insertion. C5, C6 and C7 substituted quinolines were equally reactive, tolerating the presence of electron donor and electron-withdrawing groups. Remarkably, halogen and Bpin substitution remained intact after the transformation, providing flexible handles for further orthogonal functionalization. Both the

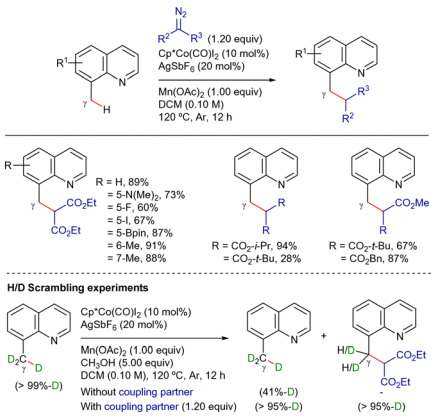

Scheme 90 γ-C(sp^3)–H alkylation with diazo compounds.

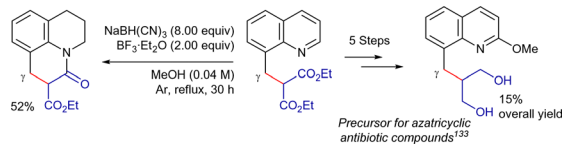

Scheme 91 Synthetic applications of γ-alkylated 8-methylquinoline derivatives.

symmetrical and unsymmetrical diazomalonates were compatible. However, low yield was observed when di-*tert*-butyl diazomalonate was employed. The alkylated products served as precursors for the synthesis of tricyclic products under reductive conditions or as key intermediates for the synthesis of azatricyclic antibiotics (Scheme 91).[200]

Regarding the mechanism, deuterium labeling experiments indicated that the cyclometalation step was reversible (observing deuterium scrambling) but the subsequent carbene formation/insertion seemed faster than the back reaction. Furthermore, parallel and competitive KIE experiments provided values of 6.7 and 8.1, respectively, indicating that the cleavage of the C–H bond was likely involved in the *r.d.s.*

Later, Ackermann's group showed that the cobalt(III)-catalyzed γ-C(sp^3)–H bond mono-methylation of 8-methylquinoline was viable using the commercially available trimethylboroxine as methyl source (Scheme 92).[201]

On the other hand, Sun *et al.* reported a novel way to introduce maleimides at the γ-CH_3 position of 8-methylquinoline derivatives under cobalt(III)-catalysis using a combination of AgOTf and $Zn(OAc)_2$ as additives (Scheme 93).[202] The reaction mechanism, depicted in Scheme 94, involves the formation of the catalytically active cobalt(III)-species and coordination with the quinoline substrate to form cationic cobalt(III)-species. Next, C–H activation and subsequent migratory insertion of the maleimide into the Co–C bond generates a 7-membered cationic cyclometallated complex which by protodemetalation releases the final product, regenerating the active catalyst. Mechanistic studies showed that benzyl activation was reversible in the absence of maleimide.

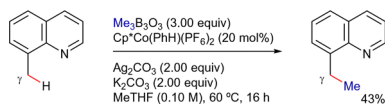

Scheme 92 γ-C(sp^3)–H alkylation with trimethylboroxine.

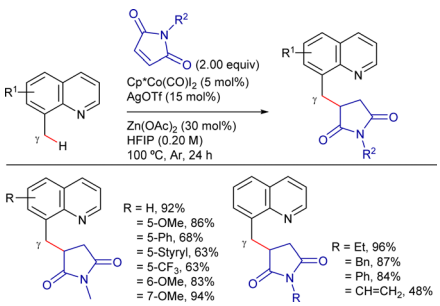

Scheme 93 γ-C(sp^3)–H alkylation with maleimides.

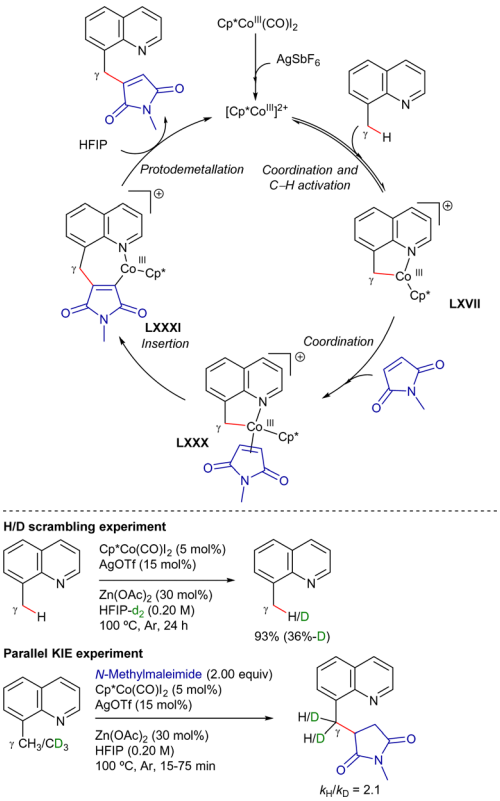

Scheme 94 γ-C(sp^3)–H alkylation with maleimides. Proposed mechanism.

However, no deuteration at the benzyl position of quinoline was observed in its presence, indicating that functionalization of the C–Co bond formed after the C–H activation step is faster than its protodemetalation. A KIE value of 2.1 indicated that cleavage of the methyl C–H bond was potentially involved in the *r.d.s.*

A complementary protocol for the coupling between 8-methylquinoline and maleimide derivatives was reported by Sharma *et al.*[203] In this case, a carboxylic acid was used as additive and TFE as solvent (Scheme 95). Albeit the reaction yields were slightly lower, the scope was broad, being possible to apply the method to mono- and di-substituted quinoline substrates with diverse alkyl, unsaturated and halogen substitution at any position. Moreover, the method worked well with a wide range of *N*-protecting groups at the maleimide and more

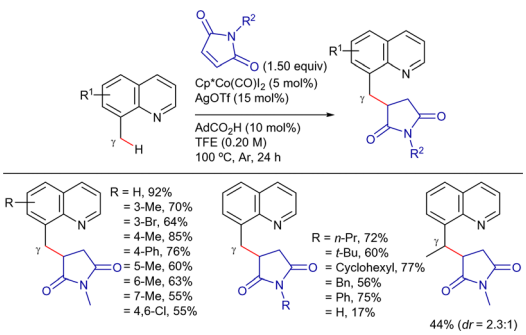

Scheme 95 γ-C(sp^3)–H alkylation with maleimides.

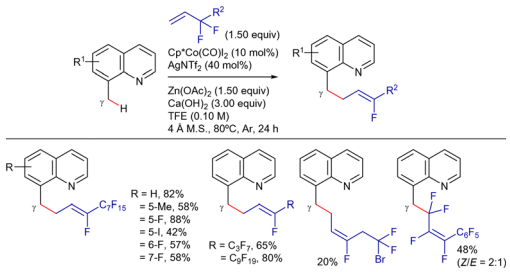

Scheme 96 Cp*Co^{III}-cat. γ-C(sp^3)–H allylation with polyfluorinated olefins.

interestingly, the direct use of the NH free maleimide was also tolerated albeit provided the product in low yield. 8-Ethylquinoline was also compatible with the method, giving the alkylated products with moderate yields and diastereoselectivities. Since no deuterium scrambling is observed, the catalytic cycle proposed by the authors would be like the one previously proposed by Sun[202] but, in this case the C–H activation step is irreversible and presumably the *r.d.s.* (k_H/k_D value of 2.1).

On the other hand, Kong, Chang, and Li described a method for the regio- and stereoselective benzylic allylation of 8-methylquinolines with (per)fluoroalkyl olefins, which involves benzylic C–H activation followed by C–F bond cleavage. (Scheme 96).[204] Interestingly, a calcium additive was employed as halide scavenger to facilitate the formation of the active metal species. Regarding the organofluorine coupling partner, mono-substituted olefins were tolerated regardless of the length of the fluorine chain. The method was less effective with tetrasubstituted or less activated olefins.

Based on previous works, the authors proposed that the catalytic cycle starts by first formation of the active Cp*CoX$_2$ (X = OAc or NTf$_2$) followed by coordination to the quinoline substrate and subsequent C–H activation to generate the five-membered metallacycle **LXVII** (Scheme 97). Next, olefin coordination and migratory insertion lead to the 7-membered cobaltacycle **LXXXIII**. Finally, β-F elimination *via* a *syn*-coplanar transition state delivers the final product with concomitant

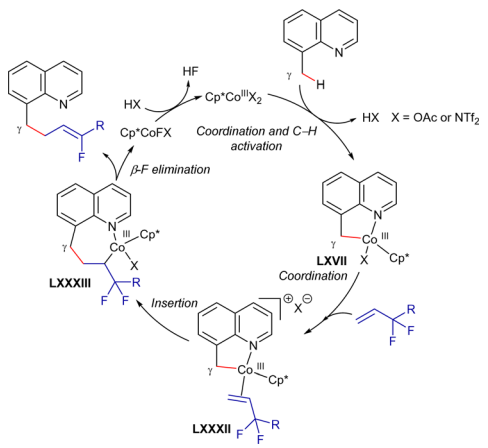

Scheme 97 γ-C(sp^3)–H allylation with polyfluorinated olefins. Proposed mechanism.

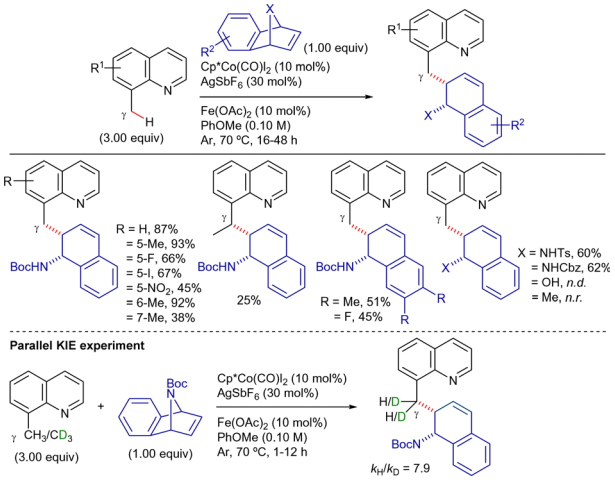

Scheme 98 γ-C(sp^3)–H alkylation with azabenzonorbornadienes.

generation of a cobalt(III) fluoride species. Anion exchange would regenerate the active cobalt(III) species.

Later, Zhou, Fan and co-workers showed that azabenzonorbornadienes were compatible coupling partners for the benzylic functionalization of 8-methylquinolines under an Ag/Cp*Co^{III} catalytic system.[205] Remarkably, the method proceeds at only 70 °C (Scheme 98). Electron-donating groups at the C5 position of the quinoline substrate provided the ring-opening products in better yields than electron-withdrawing substituents. However, the method was more sensitive to steric effects, observing a lower yield when a methyl group was at the C7 position rather than at the C6 or C5 ones. Interestingly, methylene benzylic positions were also reactive, providing the desired product in low yields. In contrast, the reaction did not proceed with any or *N*-protecting group at the azabenzonorbornadienes substrate, being not possible to use oxabenzonorbornadiene and benzonorbornadiene.

Deuterium scrambling experiments indicated that the C–H bond cleavage was reversible (observing deuterium incorporation in the absence of the azabenzonorbornadiene). However, the evolution of the five-membered metallated intermediate to the final product was presumably faster than the back reaction. Nonetheless, a parallel KIE experiment revealed a k_H/k_D value of 7.9, suggesting that C–H activation is involved in the *r.d.s.*

4.2. C–N bond formation

In 2015, Ge *et al.* disclosed the cobalt-catalyzed site-selective dehydrogenative cyclization of propionamide and butyramide derivatives using the 8-AQ as DG (Scheme 99).[206] The reaction favoured the functionalization of β-methyl groups over β-methylene and γ- or δ-methyl groups, providing the β-lactam derivatives with high regioselectivity. Interestingly, the authors also observed a preference for the functionalization of γ-benzylic over β-methyl and methylene C–H bonds, thus obtaining the γ-lactams as the major products.

Based on mechanistic studies, two distinct pathways were proposed to explain the formation of the four- and five-membered ring products. On the one hand, it seemed unlikely that the formation of β-lactams was a radical-mediated process

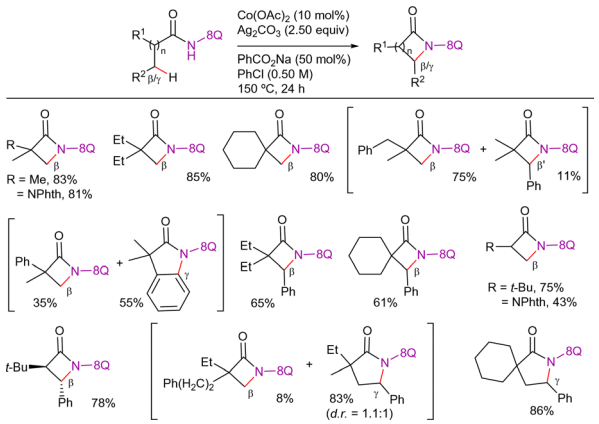

Scheme 99 β/γ-C(sp^3)–H intramolecular amidation.

due to the high selectivity for β-methyl bonds over β-benzyl C–H bonds and the good yields obtained in the presence of TEMPO. Thus, the formation of β-lactams implies the formation of the cobalt(III) complex **LXXXIV** by coordination of the amide to the cobalt species and a subsequent ligand exchange under basic conditions (Scheme 100). Cyclometalation *via* a benzoate-assisted CMD mechanism produces intermediate **LXXXV**. Oxidation of **LXXXV** with Ag_2CO_3 gives the cobalt(IV) complex **LXXXVI**, which leads to the β-lactam compound upon reductive elimination. The newly generated cobalt(II) species could then

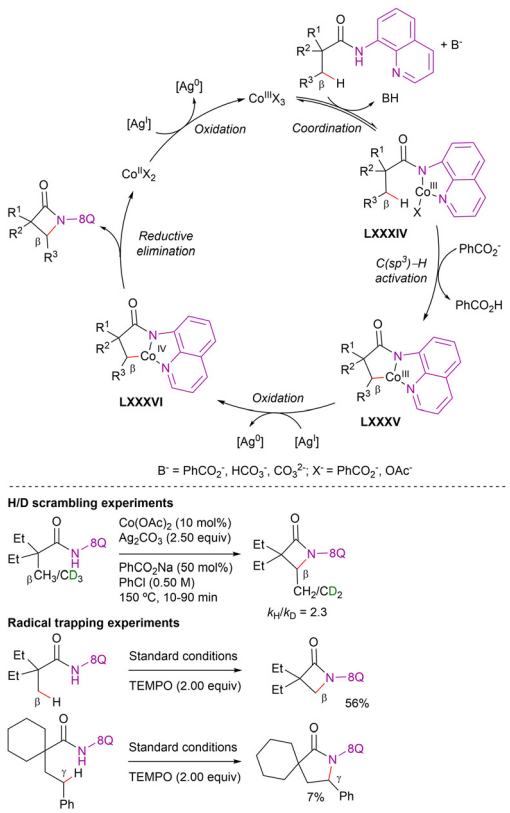

Scheme 100 β-C(sp^3)–H intramolecular amidation. Proposed catalytic cycle.

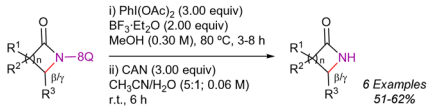

Scheme 101 Removal of the DG under oxidative conditions.

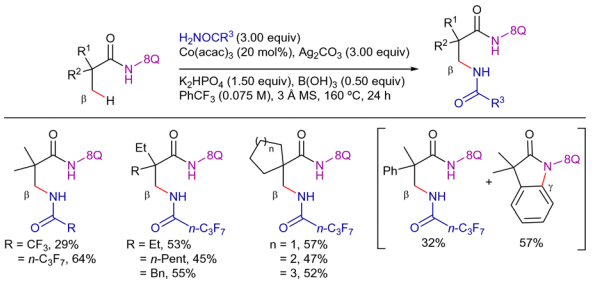

Scheme 102 β-C(sp^3)–H intermolecular amidation.

be re-oxidized to cobalt(III) by silver(I) furnishing the catalytic cycle. Alternatively, the authors also considered that the cyclometalation of the amide can be at cobalt(II) species, forming intermediate **LXXXVI** by further oxidation. The KIE experiments revealed that the C–H cleavage was presumably irreversible (KIE value of 2.3).

In contrast, in the case of the formation of γ-lactam derivatives, a radical or cationic species seemed to be involved in the catalytic cycle due to the predominant preference for γ-benzylic over β-methyl C–H bonds. Moreover, in the case of γ-lactams the addition of TEMPO considerably reduced the yield, which suggested the participation of radical species or a SET pathway.

The applicability of the method was further enhanced by converting the 8-AQ into the 8-amino-5-methoxyquinoline group to access the free NH lactam products under oxidative conditions (Scheme 101).

Additionally, in the above-mentioned contribution, Ge *et al.* also reported the cobalt(III)-catalyzed β-C(sp^3)–H intermolecular amidation using electron-deficient amides as coupling partners (Scheme 102).[206] In general, the desired products were obtained in modest yields, observing complete selectivity towards β-methyl positions over β-methylene and γ-methyl ones. In this case, the activation of γ-C(sp^2)–H bonds competed, obtaining the corresponding γ-lactam as the major product.

It is interesting to enote that the synthesis of lactams has also been achieved *via* Pd-, Cu- and Ni-catalysis.[207] However, Ni- (Section 2.2.1)[102,103] and Cu-catalyzed (Section 3.2.1)[149–151] processes were restricted to the synthesis of β-lactams substrates from α,α-disubstituted propanamide derivatives. On the other hand, Pd-catalyzed synthesis of β-lactams was restricted to α-unsubstituted and α,β-cyclic substrates, and the synthesis of γ-lactams was only feasible from β-substituted substrates.[208] Therefore, the cobalt-catalyzed method provided a complementary approach to access monocyclic and spiro β- or γ-lactams.

In 2017, Seayad, Dixon, and their team developed the thioamide-directed Co-catalyzed amidation of C(sp^3)–H bonds, utilizing (hetero)aryl- and alkyl-substituted dioxazolones (Scheme 103).[209] The

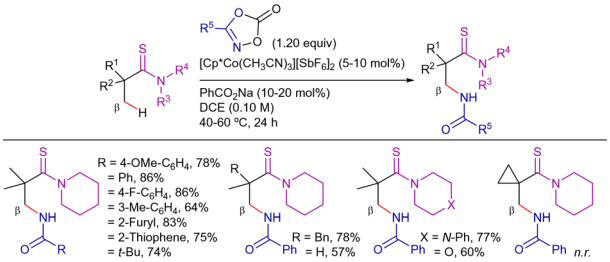

Scheme 103 β-C(sp^3)–H amidation with dioxazolones in carboxylic acid derivatives.

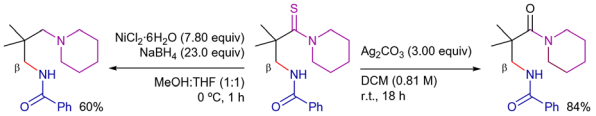

Scheme 104 Post-synthetic modifications of the thioamide group.

method was suitable for α-quaternary and tertiary substrates. Moreover, a broad range of thioamides containing N-heterocycles such as piperazine and morpholine were tolerated and provided the corresponding products in good yields. Notably, reduction of the thioamide group was achieved using a $Ni^{II}/NaBH_4$ system or converted into an amide group using Ag_2CO_3 (Scheme 104).

The authors proposed that the [Cp*Co(III)]-catalyzed thioamide-directed C–H amidation reaction follows the mechanism shown in Scheme 105. Notably, *ab initio* calculations suggest that the C–H activation step proceeds *via* an external concerted metalation-deprotonation (CMD) mechanism rather than an internal CMD pathway. The calculated energy difference between the external and internal CMD transition states was 35 kJ mol^{-1}.

In 2019, Matsunaga's group reported the enantioselective C(sp^3)–H amidation of thioamides with dioxazolones employing a Cp*Co/chiral carboxylic acid (CCA) system (Scheme 106a).[210] In particular, *N*-protected *tert*-leucine derivatives induced high enantioselectivities. The reactivity and selectivity were both

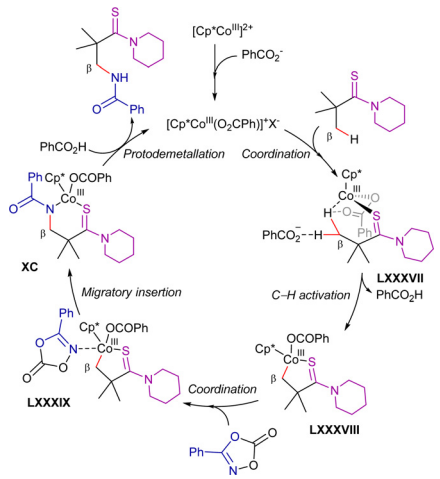

Scheme 105 β-C(sp^3)–H amidation with dioxazolones. Proposed mechanism.

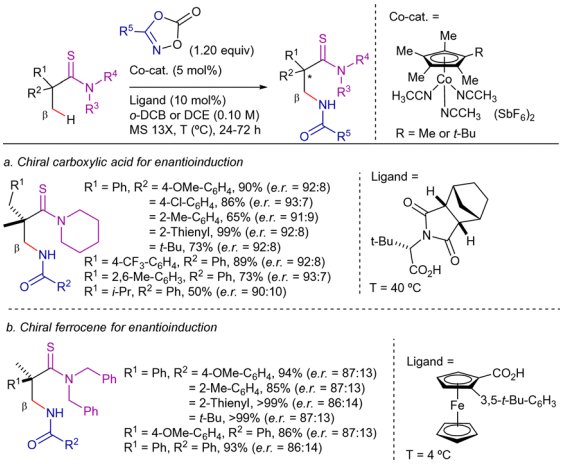

Scheme 106 Enantioselective β-C(sp^3)–H amidation with dioxazolones.

further improved by combining sterically hindered cobalt catalyst with the MS13X zeolite.

Later, Matsunaga' group introduced the 2-aryl ferrocene carboxylic acids as a new type of efficient chiral ligands for this transformation. Good reactivity and enantioselectivity were obtained for a wide range of structural diverse amino acids (Scheme 106b).[211] Deuterium labeling and DFT calculations revealed that the C–H activation step was presumably irreversible, and it was involved in the enantio-determining step.

In 2019, Loh *et al.* reported the Cp*Co^{III}-catalyzed, thioamide-directed amination of C(sp^3)–H bonds using anthranils as amine electrophiles (Scheme 107).[212] Using 7.5% of $[Cp^*Co(CH_3CN)_3][SbF_6]_2$ and 1 equiv. of 1-$AdCO_2H$ as additive, the method allowed the introduction of 2-formyl, -acetyl and -benzoyl anilines at the *β*-position of thioamide derivatives.

Disclosing a similar reactivity, more recently, Li *et al.* published a complementary method by using 20 mol% of $[Cp^*Co(CH_3CN)_3][SbF_6]_2$ as catalyst and *i*-$PrCO_2Na$ as basic additive (Scheme 108).[213]

In 2016, Sundararaju *et al.* reported a methodology for the γ-amidation of 8-methylquinoline derivatives with (hetero)aryl dioxazolones under cobalt(III)-catalysis, employing $AgSbF_6$ and NaOPiv as additives in DCE at 100 °C (Scheme 109).[214] The reaction was selective and tolerated a variety of functional groups. However, the method was less effective with 3-nonyl-

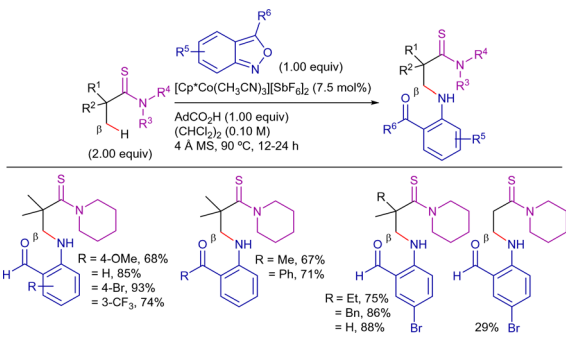

Scheme 107 β-C(sp^3)–H amidation with anthranils.

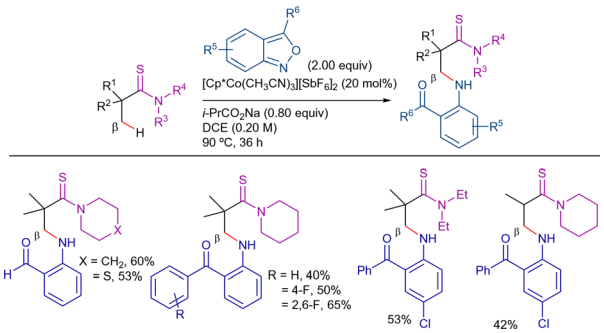

Scheme 108 β-C(sp^3)–H amidation with anthranils.

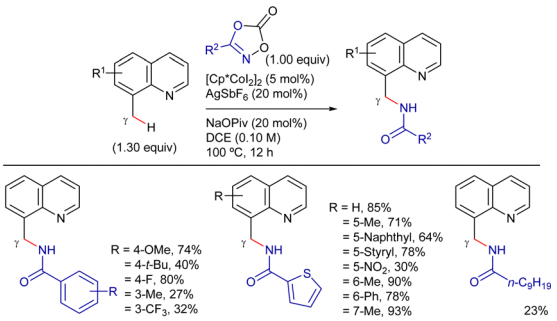

Scheme 109 γ-C(sp^3)–H intermolecular amidation.

1,4,2-dioxazol-5-one, providing the γ-amidated product in low yield. Diversification of the amidated quinoline derivatives was achieved under a $Ni^{II}/NaBH_4$ catalytic system (Scheme 110).

In 2022, Niu *et al.* developed two efficient methodologies for the synthesis of indoline and benzoxazine derivatives *via* cobalt(II)-catalyzed PA-directed selective C(sp^3)–H functionalization processes (Schemes 111 and 112).[215] A key feature in these protocols is the use of a hydroxylamine-based oxidant.

On the one hand, as can be seen in Scheme 111, the synthesis of indolines required only 5 mol% of $Co(OAc)_2 \cdot 4H_2O$, demonstrating the efficiency of this cobalt-system

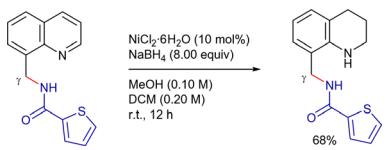

Scheme 110 Diversification of the amidated products.

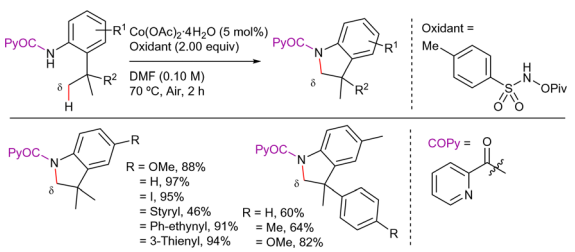

Scheme 111 δ-C(sp^3)–H intramolecular amidation in aniline structures.

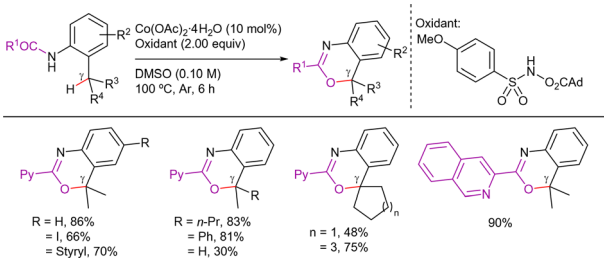

Scheme 112 γ-C(sp^3)–H intramolecular oxidation in aniline structures.

compared to Pd- or Cu- catalysis.[216,217] A wide variety of *para*-substituted aniline and 4-methyl-2-(2-arylpropan-2-yl)aniline derivatives were well tolerated and afforded the corresponding indoline products in good yields by the direct functionalization of the δ-CH_3 positions. Remarkably, substrates having alkenyl, alkynyl, alkyl, phenyl, naphthyl and heteroaryl groups were compatible with the reaction conditions.

On the other hand, as can be seen in Scheme 112, the synthesis of 4*H*-3,1-benzoxazine products occurred through direct activation of secondary and tertiary γ-C(sp^3)–H bonds in *ortho*-substituted anilines. Interestingly, the reaction was effective with cycloalkyl framework substrates, leading to the desired spirocyclic products in good yields. Moreover, this method proved effective with *para*-substituted picolinamide derivatives and isoquinoline structures.

According to the authors, both procedures occur through the catalytic cycles depicted in Scheme 113. Both reactions

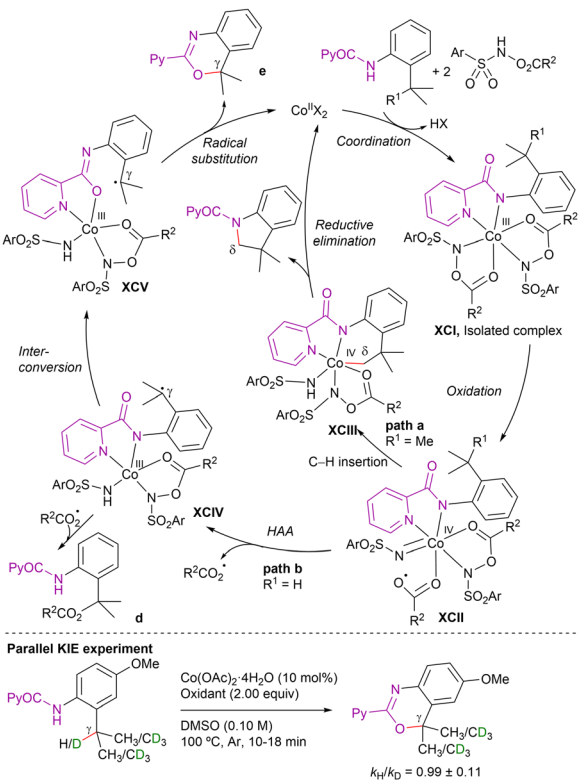

Scheme 113 Formation of indoline and benzoxazine derivatives. Proposed mechanisms.

begin with the oxidation of the cobalt(II)-salt to the cobalt(III)-species **XCI** (this complex was isolated when R^1 = H, CCDC 2116720). Intermediate **XCI** is oxidized intramolecularly to afford cobalt(IV)-imido intermediate **XCII**. From this stage, the reaction proceeds *via* two distinct pathways, depending on the R^1 group. If R^1 is a methyl group, the cobalt(IV) species **XCII** undergoes intramolecular C–H insertion, followed by reductive elimination, yielding the indoline product and regenerating the cobalt(II) species (path a). While, if R^1 group is H, the reaction proceeds *via* intramolecular hydrogen atom abstraction (HAA) from cobalt(IV) species **XCII** to deliver the radical intermediate **XCIV**, leading to the radical-adduct **d**. This adduct was isolated in some examples as by-product. Nonetheless, intermediate **d** cannot be transformed to product **e** by intramolecular nucleophilic substitution, ruling out this pathway. In contrast, isomerization of **XCIV** generates intermediate **XCV**, which undergoes radical substitution to deliver the target product **e**.

In both the synthesis of indoline derivatives and benzoxazines, no deuterium scrambling was observed, leading the authors to suggest that the C–H activation step is irreversible. However, the parallel kinetic isotope effect (KIE) value of 0.99 ± 0.11 obtained for benzoxazine synthesis indicates that C–H bond cleavage is unlikely to be involved in the rate-limiting step in this case.

In 2022, Song *et al.* reported the synthesis of indole derivatives starting from (2-pyridyl)sulfonanilide derivatives (Scheme 114).[218] This reaction also worked with a hydroxylamine-based compound ($ArSO_2NHOR$) as oxidant. The method showed good functional group tolerance under the optimal conditions, tolerating the presence of halogen groups that could be used in post-synthetic modifications. Substrates with both electron-rich and electron-deficient substituents reacted effectively, yielding the desired products in moderate to good yields. Additionally, substrates containing secondary C–H bonds were also compatible with this protocol.

Regarding the mechanism, as no deuterium scrambling was observed, the authors proposed that the C–H activation step is irreversible. Furthermore, the reaction was inhibited upon the addition of TEMPO, and when BHT was introduced into the catalytic system, a TsNH-BHT adduct was detected. Based on these findings, the authors suggested that a single-electron transfer (SET) step is involved in the transformation. Based on these studies, the authors suggested the mechanism outlined in Scheme 115. First, in the presence of the (2-pyridyl)sulfonanilide derivative and TsNHOPiv, the cobalt(II) catalyst evolves into the

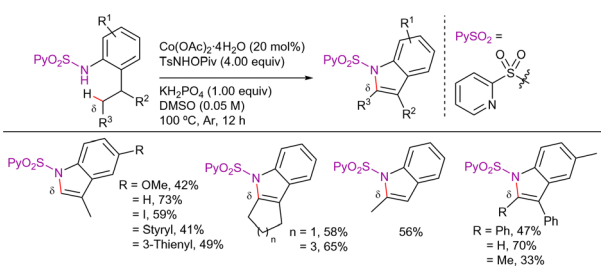

Scheme 114 SO_2Py-directed β-C(sp^3)–H intramolecular amidation.

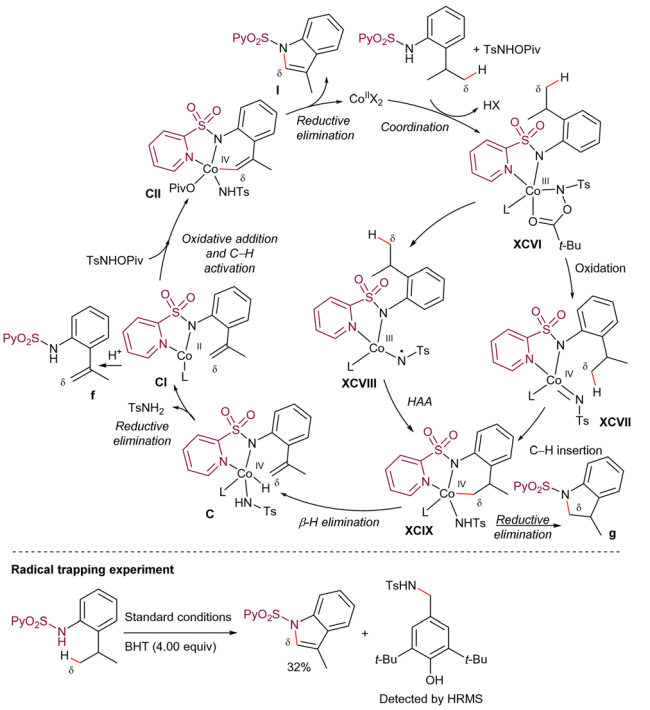

Scheme 115 Formation of indoline and benzoxazine derivatives. Proposed mechanisms.

cobalt(III) species **XCVI**, which by intramolecular one-electron oxidation would form the cobalt(IV) imide intermediate **XCVII**. Then, the intermediate **XCVII** undergoes a C(sp^3)–H insertion forming the cobalt(IV) imide **XCIX**. However, there is an alternative pathway which would involve **XCVI** becoming **XCIX** *via* the cobalt(III) intermediate **XCVIII** aminyl radical. This would involve a homogeneous intramolecular N–O bonding reaction followed by one-electron oxidation processes and hydrogen atom abstraction (HAA).

In any case, from the cobaltacycle, **XCIX** a β-H elimination step leads to intermediate **C**, and a reductive elimination results in intermediate **CI** and $TsNH_2$. Subsequently, oxidation of **CI** to cobalt(IV) species by oxidative addition of TsNHOPiv, followed by C(sp^2)–H activation produces intermediate **CII**. This intermediate **CII** undergoes reductive elimination to afford the desired product along with cobalt(II) species.

Alternatively, the authors also suggest that protonation of intermediate **CI** generates the dehydrogenation byproduct **f** (isolated product in some examples). Then, a Heck-type mechanism involving amino-metalation of the double bond and subsequent β-hydride elimination would lead to the indole product. Besides these options, the authors also considered an alternative path through a reductive elimination step from intermediate **XCIX** to generate indoline **g** and further oxidation to form product **I**. However, oxidation of indoline **g** was not observed under the optimized conditions.

Summary and outlook

The synthetic efficiency achieved in the directed functionalization of inactive C(sp^3)–H bonds has established DG-assisted

cyclometalation as one of the most optimal approaches to diversify organic molecules. To date, this area has mainly been governed by the use of 4d and 5d metals as catalysts. However, in recent decades, the impetus to move from precious metals to cost-effective, cheaper and earth-abundant first-row transition metals has driven new developments in nickel, iron, copper and cobalt catalysis.

(A) Nickel catalysis has enabled the selective β-C(sp^3)–H functionalization of carboxylic acid derivatives using 8-AQ and related DGs. Various oxidation states of Ni facilitate diverse bond-forming reactions (C–C, C–N, C–S, C–Se, and C–O) *via* Ni^{II}/Ni^{II} or Ni^{II}/Ni^{IV} pathways. However, Ni catalysts generally exhibit lower reactivity toward inert C(sp^3)–H bonds compared to Pd and often require harsh conditions. Key challenges include oxidation state control, mechanistic complexity, and the development of milder catalytic systems. A unified mechanistic framework remains elusive, and advances in more versatile and traceless DGs and enantioselective transformations are needed for broader applicability.

(B) Copper(II)-salts, in conjunction with 8-AQ as a DG, have been employed in the β-functionalization of aliphatic carboxylic acid derivatives, enabling arylation, alkenylation, carbonylation, amidation, and acyl-, aryl-, and vinyloxylation reactions. However, these transformations often necessitate stoichiometric copper due to its multifaceted roles throughout the catalytic cycle and the challenges associated with stabilizing high-valent copper(III) species. The development of sustainable catalytic cycles, particularly those leveraging O_2 or electrochemical approaches, represents a promising yet underexplored avenue. Additionally, the design of chiral ligands capable of achieving high enantioselectivity in these transformations remains a significant challenge.

(C) Iron catalysis remains relatively underexplored but has demonstrated remarkable versatility in β-arylation, alkenylation, and methylation of aliphatic carboxylic acids using various organometallic reagents. These transformations, facilitated by directing groups such as 8-aminoquinoline (8-AQ) or triazoles, often proceed under significantly milder conditions compared to other 3d transition metals. Nonetheless, the transient nature of iron intermediates complicates mechanistic elucidation, requiring a combination of computational studies, kinetic experiments, and spectroscopic techniques to unravel reaction pathways. Understanding and harnessing iron's multiple oxidation states, particularly Fe^{II}/Fe^{III} and Fe^{III}/Fe^{V}, is crucial for designing well-defined catalytic cycles. This knowledge will undoubtedly aid in advancing Fe-catalyzed enantioselective C(sp^3)–H functionalization, a field that, like nickel and copper, remains largely unexplored.

(D) The d^6-electron configuration of cobalt(III) complexes has been crucial in the recent development of numerous directed C–H transformations. Monodentate strongly coordinating DGs have been typically used in Cp*Co(III)-catalyzed reactions, while bidentate DGs (specially, 8-aminoquinoline and picolinamide) have commonly been exploited with cobalt(II)-salts under oxidative conditions. Most processes were directed at *β*-position in carboxylic acid derivatives, achieving also the functionalization at *γ*- and *δ*-position in aniline derivatives. In addition, a handful of enantioselective Cp*Co(III)-catalyzed C–H functionalization procedures have been reported using chiral carboxylic acids as chiral additives to promote the enantioselective C–H activation step. The field of enantioselective C–H functionalization holds immense potential in organic synthesis, drug discovery and medicinal chemistry.

(E) Overall, considering the sustainable and cost-effective nature of 3d metal-catalyzed C–H activation, substantial progress in this rapidly evolving field is expected. The primary challenges that remain include: (i) the widespread use of 8-AQ as a DG, which often requires harsh conditions for its removal, highlighting the need for more versatile or traceless alternatives, and (ii) the dependence on substantial steric activation, such as the Thorpe–Ingold effect, to facilitate C–H activation in most substrates. Undoubtedly, future progress will be driven by a deeper mechanistic understanding, particularly concerning oxidation state control, ligand effects, and reaction intermediates, ultimately leading to more efficient and widely applicable methodologies.

Furthermore, the integration of emerging technologies, such as photochemistry and electrochemistry, is expected to drive advancements in sustainable C–H functionalization by reducing reliance on stoichiometric metal oxidants. While these approaches have already shown significant impact in C(sp^2)–H functionalization, their application to C(sp^3)–H functionalization remains relatively underdeveloped, requiring further investigation.[219]

We hope that this review can provide new perspectives in the catalytic 3d-catalyzed C(sp^3)–H functionalization to expand the practicability of these metals in chelation-assisted strategies.

Data availability

No primary research results, software or code have been included and no new data were generated or analysed as part of this review.

Conflicts of interest

There are no conflicts to declare.

Acknowledgements

We thank FEDER/Ministerio de Ciencia, Innovación y Universidades–Agencia Estatal de Investigación (Grants PGC2018-098660-B-I00 and PID2021-1248553NB-100) for financial support. We also thank the MINECO for the financial support for the RED2022-134331-T.

Notes and references

1 J. A. M. Simoes and J. L. Beauchamp, *Chem. Rev.*, 1990, **90**, 629–688.
2 Y.-R. Luo, *Handbook of Bond Dissociation Energies in Organic Compounds*, CRC Press, 2002.

3 X.-S. Xue, P. Ji, B. Zhou and J.-P. Cheng, *Chem. Rev.*, 2017, **117**, 8622–8648.
4 K. M. Altus and J. A. Love, *Commun. Chem.*, 2021, **4**, 173.
5 J. Tsuji, *Transitions Metal Reagents and Catalysts: Innovations in Organic Synthesis*, Wiley-VCH, Weinheim, 2000.
6 D. J. Abrams, P. A. Provencher and E. J. Sorensen, *Chem. Soc. Rev.*, 2018, **47**, 8925–8967.
7 O. Baudoin, *Angew. Chem., Int. Ed.*, 2020, **59**, 17798–17809.
8 L. Guillemard, N. Kaplaneris, L. Ackermann and M. J. Johansson, *Nat. Rev. Chem.*, 2021, **5**, 522–545.
9 R. Jana, H. M. Begam and E. Dinda, *Chem. Commun.*, 2021, **57**, 10842–10866.
10 J. H. Docherty, T. M. Lister, G. Mcarthur, M. T. Findlay, P. Domingo-Legarda, J. Kenyon, S. Choudhary and I. Larrosa, *Chem. Rev.*, 2023, **123**, 7692–7760.
11 J.-Q. Yu and Z. Shi, *C–H Activation, Topics in Current Chemistry*, Springer-Verlag, 2010, 292.
12 D. Balcells, E. Clot and O. Eisenstein, *Chem. Rev.*, 2010, **110**, 749–823.
13 H. M. L. Davies and D. Morton, *ACS Cent. Sci.*, 2017, **3**, 936–943.
14 Y. Wei, P. Hu, M. Zhang and W. Su, *Chem. Rev.*, 2017, **117**, 8864–8907.
15 M. Bietti, *Angew. Chem., Int. Ed.*, 2018, **57**, 16618–16637.
16 T. Rogge, N. Kaplaneris, N. Chatani, J. Kim, S. Chang, B. Punji, L. L. Schafer, D. G. Musaev, J. Wencel-Delord, C. A. Roberts, R. Sarpong, Z. E. Wilson, M. A. Brimble, M. J. Johansson and L. Ackermann, *Nat. Rev. Methods Primers*, 2021, **1**, 43.
17 D. Maiti, *Handbook of C–H Functionalization of C–H Functionalization*, John Wiley & Sons, Inc., 2022.
18 N. Holmberg and D. A. Nicewicz, *Chem. Rev.*, 2022, **122**, 1925–2016.
19 S. K. Sinha, S. Guin, S. Maiti, J. P. Biswas, S. Porey and D. Maiti, *Chem. Rev.*, 2022, **122**, 5682–5841.
20 Q. Sun, X. Xu and X. Xu, *ChemCatChem*, 2022, **14**, e202201083.
21 Y. He, Z. Huang, K. Wu, J. Ma, Y.-G. Zhou and Z. Yu, *Chem. Soc. Rev.*, 2022, **51**, 2759–2852.
22 Y. Zhang, T. Zhang and S. Das, *Chem*, 2022, **8**, 3175–3201.
23 T. Punniyamurthy and A. Kumar, *Transition-Metal-Catalyzed C–H Functionalization of Heterocycles*, John Wiley & Sons, Inc., 2023.
24 J. Grover, A. T. Sebastian, S. Maiti, A. C. Bissember and D. Maiti, *Chem. Soc. Rev.*, 2025, **54**, 2006–2053.
25 P. Belloti, H.-M. Huang, T. Faber and F. Glorius, *Chem. Rev.*, 2023, **123**, 4237–4352.
26 J. J. Li, *C–H Activation in Organic Synthesis*, CRC Press, 1st edn, 2015.
27 I. J. S. Fairlamb and A. R. Kapdi, in *Directed C–H Bond Functionalization Strategies for Synthesis*, ed. A. R. Kapdi and D. Maiti, Elsevier Inc., 2017, pp. 9–48.
28 C. Sambiagio, D. Schönbauer, R. Blieck, T. Dao-Huy, G. Pototschnig, P. Schaaf, T. Wiesinger, M. F. Zia, J. Wencel-Delord, T. Besset, B. U. W. Maes and M. Schnürch, *Chem. Soc. Rev.*, 2018, **47**, 6603–6743.
29 S. Rej, Y. Ano and N. Chatani, *Chem. Rev.*, 2020, **120**, 1788–1887.
30 M. Kapoor, A. Singh, K. Sharma and M. H. Hsu, *Adv. Synth. Catal.*, 2020, **362**, 4513–4542.
31 K. Murali, L. A. Machado, R. L. Carvalho, L. F. Pedrosa, R. Mukherjee, E. N. S. Júnior and D. Maiti, *Chem. - Eur. J.*, 2021, **27**, 12453–12508.
32 T. Sarkar, T. A. Shah, P. K. Maharana, K. Talukdar, B. K. Das and T. Punniyamurthy, *Chem. Rec.*, 2021, **21**, 3758–3778.
33 S. Rej, A. Das and N. Chatani, *Coord. Chem. Rev.*, 2021, **431**, 213683.
34 B. Desai, M. Patel, B. Z. Dholakiya, S. Rana and T. Naveen, *Chem. Commun.*, 2021, **57**, 8699–8725.
35 J. Zhang, X. Lu, C. Shen, L. Xu, L. Ding and G. Zhong, *Chem. Soc. Rev.*, 2021, **50**, 3263–3314.
36 R. H. Crabtree, *Chem. Rev.*, 1985, **85**, 245–269.
37 A. A. Mishra, D. Subhedar and B. M. Bhanage, *Chem. Rec.*, 2019, **19**, 1829–1857.
38 P. W. Tan and J. Seayad, *Tetrahedron Lett.*, 2019, **60**, 151338.
39 J. Das, S. Guin and D. Maiti, *Chem. Sci.*, 2020, **11**, 10887–10909.
40 B. Liu, A. M. Romine, C. Z. Rubel, K. M. Engle and B.-F. Shi, *Chem. Rev.*, 2021, **121**, 14957–15074.
41 B. Li, M. Elsaid and H. Ge, *Chem*, 2022, **8**, 1254–1360.
42 J. Das, W. Ali and D. Maiti, *Trends Chem.*, 2023, **5**, 551–560.
43 F. Doraghi, M. M. A. Ashtiani, M. Ameli, B. Larijani and M. Mahdavi, *Chem. Rec.*, 2024, **24**, e202400116.
44 J. C. K. Chu and T. Rovis, *Angew. Chem., Int. Ed.*, 2018, **57**, 62–101.
45 B.-B. Zhan, M.-X. Jiang and B.-F. Shi, *Chem. Commun.*, 2020, **56**, 13950–13958.
46 S. Shabani, Y. Wu, H. G. Ryan and C. A. Hutton, *Chem. Soc. Rev.*, 2021, **50**, 9278–9343.
47 I. F. Yu, J. W. Wilson and J. F. Hartwig, *Chem. Rev.*, 2023, **123**, 11619–11663.
48 C. He, W. G. Whitehurst and M. J. Gaunt, *Chem*, 2019, **5**, 1031–1058.
49 H. Ha, J. Lee, M. H. Park, B. Jung and M. Kim, *Bull. Korean Chem. Soc.*, 2020, **41**, 582–587.
50 G. Saini and M. Kapur, *Chem. Commun.*, 2021, **57**, 1693–1714.
51 A. Das and B. Maji, *Chem. – Asian J.*, 2021, **16**, 397–408.
52 S. A. Babu, Y. Aggarwal, P. Patel and R. Tomar, *Chem. Commun.*, 2022, **58**, 2612–2633.
53 B.-B. Zhan, L. Jin and B.-F. Shi, *Trends Chem.*, 2022, **4**, 220–232.
54 W. Ali, G. A. Oliver, D. B. Werz and D. Maiti, *Chem. Soc. Rev.*, 2024, **53**, 9904–9953.
55 M. Sadeghi, *ACS Catal.*, 2024, **14**, 15356–15373.
56 P. Gandeepan, T. Müller, D. Zell, G. Cera, S. Warratz and L. Ackermann, *Chem. Rev.*, 2019, **119**, 2192–2452.
57 S. St John-Campbell and J. A. Bull, *Adv. Synth. Catal.*, 2019, **361**, 3662.
58 L. Woźniak and N. Cramer, *Trends Chem.*, 2019, **1**, 471–484.
59 J. Loup, U. Dhawa, F. Pesciaioli, J. Wencel-Delord and L. Ackermann, *Angew. Chem., Int. Ed.*, 2019, **58**, 12803–12818.
60 L. Ackermann, *Acc. Chem. Res.*, 2020, **53**, 84–104.

61 B. Desai, A. Uppuluru, A. Dey, N. Deshpande, B. Z. Dholakiya, A. Sivaramakrishna, T. Naveen and K. Padala, *Org. Biomol. Chem.*, 2023, **21**, 673–699.
62 J. Mo, A. M. Messinis, J. Li, S. Warratz and L. Ackermann, *Acc. Chem. Res.*, 2024, **57**, 10–22.
63 C. Johnson, S. Li, R. Arora, B. Mirabi and M. Lautens, *Synlett*, 2024, 851–861.
64 P. Xu and S. Zhao, *ChemistrySelect*, 2024, **9**, e202305125.
65 J. Son, *Beilstein J. Org. Chem.*, 2021, **17**, 1733–1751.
66 T. Aneeja, M. Neetha, C. M. A. Afsina and G. Anilkumar, *Catal. Sci. Technol.*, 2021, **11**, 444–458.
67 G. Anusree, P. S. Devi and G. Anilkumar, *Adv. Synth. Catal.*, 2019, **366**, 1–38.
68 V. M. Chernyshev and V. P. Ananikov, *ACS Catal.*, 2022, **12**, 1180–1200.
69 J. P. Kleiman and M. Dubeck, *J. Am. Chem. Soc.*, 1963, **85**, 1544–1545.
70 S. M. Khake and N. Chatani, *Trends Chem.*, 2019, **1**, 524–539.
71 Y.-H. Liu, Y.-N. Xia and B.-F. Shi, *Chin. J. Chem.*, 2020, **38**, 635–662.
72 N. Chatani, *Acc. Chem. Res.*, 2023, **56**, 3053–3064.
73 F. Požgan, U. Grošelj, J. Svete, B. Štefane and H. H. Al Mamari, *Molecules*, 2024, **29**, 1917.
74 Y. Aihara and N. Chatani, *J. Am. Chem. Soc.*, 2014, **136**, 898–901.
75 M. Li, J. Dong, X. Huang, K. Li, Q. Wu, F. Song and J. You, *Chem. Commun.*, 2014, **50**, 3944–3946.
76 D. Lapointe and K. Fagnou, *Chem. Lett.*, 2010, **39**, 1118–1126.
77 H. M. Omer and P. Liu, *J. Am. Chem. Soc.*, 2017, **139**, 9909–9920.
78 S. Singh, K. Surya and R. B. Sunoj, *J. Org. Chem.*, 2017, **82**, 9619–9626.
79 J. Liu and S. A. Johnson, *Organometallics*, 2021, **40**, 2970–2982.
80 X. Wang, L. Zhu, S. Chen, X. Xu, C.-T. Au and R. Qiu, *Org. Lett.*, 2015, **17**, 5228–5231.
81 M. Iyanaga, Y. Aihara and N. Chatani, *J. Org. Chem.*, 2014, **79**, 11933–11939.
82 E. L. Nolan, I. M. Blythe, F. Qu, J. W. Kampf and M. S. Sanford, This proposal is comparable with the detailed organometallic studies conducted by M. Sanford on the aminoquinoline-directed Ni-catalyzed C−H functionalization of 2,3,4,5-tetrafluoro-N-(quinolin-8-yl)benzamide using diarylio-donium reagents. These studies implicated a $Ni^{II/III/IV}$ catalytic cycle in which the diaryliodonium promotes a double single-electron oxidation process involving aryl radical intermediates in the transformation, *J. Am. Chem. Soc.*, 2024, **146**, 18128–18135.
83 M. W. Milbauer, J. W. Kampf and M. S. Sanford, *J. Am. Chem. Soc.*, 2022, **144**, 21030–21034.
84 X. Wang, P. Xie, R. Qiu, L. Zhu, T. Liu, Y. Li, T. Iwasaki, C.-T. Au, X. Xu, Y. Xia, S.-F. Yin and N. Kambe, *Chem. Commun.*, 2017, **53**, 8316–8319.
85 G. Tan, L. Zhang, X. Liao, Y. Shi, Y. Wu, Y. Yang and J. You, *Org. Lett.*, 2017, **19**, 4830–4833.
86 M. Li, Y. Yang, D. Zhou, D. Wan and J. You, *Org. Lett.*, 2015, **17**, 2546–2549.
87 S. Maity, S. Agasti, A. M. Earsad, A. Hazra and D. Maiti, *Chem. – Eur. J.*, 2015, **21**, 11320–11324.
88 C. Lin, Z. Chen, Z. Liu and Y. Zhang, *Org. Lett.*, 2017, **19**, 850–853.
89 C. Lin, J. Zhang, Z. Chen, Y. Liu, Z. Liu and Y. Zhang, *Adv. Synth. Catal.*, 2016, **358**, 1778–1793.
90 C. Lin, Y. Xu, Q. Teng, J. Lin, F. Gao and L. Shen, *Synlett*, 2020, 889–894.
91 Y.-J. Liu, Z.-Z. Zhang, S.-Y. Yan, Y.-H. Liu and B.-F. Shi, *Chem. Commun.*, 2015, **51**, 7899–7902.
92 X. Wu, Y. Zhao and H. Ge, *J. Am. Chem. Soc.*, 2015, **137**, 4924–4927.
93 X. Wu, Y. Zhao and H. Ge, *J. Am. Chem. Soc.*, 2014, **136**, 1789–1792.
94 T. Uemura, M. Yamaguchi and N. Chatani, *Angew. Chem., Int. Ed.*, 2016, **55**, 3162–3165.
95 X. Li, J.-M. Lv, D. Hu and I. Abe, *RSC Chem. Biol.*, 2021, **2**, 166–180.
96 P. T. Boeck, R. Yadav, B. S. Sumerlin and A. S. Veige, *Macromolecules*, 2024, **57**, 71–77.
97 J. P. Brand and J. Waser, *Chem. Soc. Rev.*, 2012, **41**, 4165–4179.
98 A. S. Sarala, S. Bhowmick, R. L. de Carvalho, S. A. Al-Thabaiti, M. Mokhtar, E. N. da S. Júnior and D. Maiti, *Adv. Synth. Catal.*, 2021, **363**, 4994–5027.
99 F.-X. Luo, Z.-C. Cao, H.-W. Zhao, D. Wang, Y.-F. Zhang, X. Xu and Z.-J. Shi, *Organometallics*, 2017, **36**, 18–21.
100 N. Kerru, L. Gummidi, S. Maddila, K. K. Gangu and S. B. Jonnalagadda, *Molecules*, 2020, **25**, 1909.
101 M. V. K. Rao, S. Kareem, S. R. Vali and V. S. Reddy, *Org. Biomol. Chem.*, 2023, **21**, 8426–8462.
102 X. Wu, Y. Zhao and H. Ge, *Chem. – Eur. J.*, 2014, **20**, 9530–9533.
103 Y. Aihara and N. Chatani, *ACS Catal.*, 2016, **6**, 4323–4329.
104 P. Roy, J. R. Bour, J. W. Kampf and M. L. Sanford, *J. Am. Chem. Soc.*, 2019, **141**, 17382–17387.
105 Y. B. Kim, J. Won, J. Lee, J. Kim, B. Zhou, J.-W. Park, M.-H. Baik and S. Chang, *ACS Catal.*, 2021, **11**, 3067–3072.
106 M. R. Ringenberg, D. L. Gray and T. B. Rauchfuss, *Organometallics*, 2011, **30**, 2885–2888.
107 Q. Chen, X.-H. Fan, L.-P. Zhang and L.-M. Yang, *RSC Adv.*, 2014, **4**, 53885–53890.
108 A. A. Antonov and K. P. Bryliakov, *Appl. Organomet. Chem.*, 2022, **36**, e6499.
109 C. Wang, L. Zhang and J. You, *Org. Lett.*, 2017, **19**, 1690–1693.
110 L. L. Hegedus and R. W. McCabe, *Catalyst Poisoning*, ed. M. Dekker, New York, 1984.
111 D. Rampon, D. Seckler, E. Q. da Luz, D. B. Paixão, A. M. Larroza, P. H. Schneider and D. Alves, *Org. Biomol. Chem.*, 2022, **20**, 6072–6177.
112 C. Lin, W. Yu, J. Yao, B. Wang, Z. Liu and Y. Zhang, *Org. Lett.*, 2015, **17**, 1340–1343.
113 X. Wang, R. Qiu, C. Yan, V. P. Reddy, L. Zhu, X. Xu and S.-F. Yin, *Org. Lett.*, 2015, **17**, 1970–1973.

114 S.-Y. Yan, Y.-J. Liu, B. Liu, Y.-H. Liu, Z.-Z. Zhang and B.-F. Shi, *Chem. Commun.*, 2015, **51**, 7341–7344.
115 X. Ye, J. L. Pettersen and X. Shi, *Chem. Commun.*, 2015, **51**, 7863–7866.
116 J. L. G. Ruano, A. Parra and J. Alemán, *Green Chem.*, 2008, **10**, 706–711.
117 J.-M. Li, Y. Yu, J. Weng and G. Lu, *Org. Biomol. Chem.*, 2018, **16**, 6047–6056.
118 D. D. Beattie, A. C. Grunwald, T. Perse, L. L. Schafer and J. A. Love, *J. Am. Chem. Soc.*, 2018, **140**, 12602–12610.
119 B. E. Nadeau, D. D. Beattie, E. K. J. Lui, M. Tewkesbury, J. A. Love and L. L. Schafer, *Organometallics*, 2023, **42**, 2326–2334.
120 C. C. Roberts, E. Chong, J. W. Kampf, A. J. Canty, A. Ariafard and M. S. Sanford, *J. Am. Chem. Soc.*, 2019, **141**, 19513–19520.
121 G. Anilkumar and S. Saranya, *Copper Catalysis in Organic Synthesis*, Wiley-VCH, Weinheim, 2020.
122 F. Ullmann and J. Bielecki, *Ber. Dtsch. Chem. Ges.*, 1901, **34**, 2174–2185.
123 F. Wang, P. Chen and G. Liu, *Acc. Chem. Res.*, 2018, **51**, 2036–2046.
124 S. Thapa, B. Shrestha, S. K. Gurung and R. Giri, *Org. Biomol. Chem.*, 2015, **13**, 4816–4827.
125 S. Radhika, N. A. Harry, M. Neetha and G. Anilkumar, *Org. Biomol. Chem.*, 2019, **17**, 9081–9094.
126 I. P. Beletskaya and A. V. Cheprakov, *Coord. Chem. Rev.*, 2004, **248**, 2337–2364.
127 P. Rajeshwaran, J. Trouvé, K. Youssef and R. Gramage-Doria, *Angew. Chem., Int. Ed.*, 2022, **61**, e202211016.
128 T. Aneeja, M. Neetha, C. M. A. Afsina and G. Anilkumar, *RSC Adv.*, 2020, **10**, 34429–34458.
129 H. Y. Kim and K. Oh, *Org. Biomol. Chem.*, 2021, **19**, 3569–3583.
130 Z. Zhang, P. Chen and G. Liu, *Chem. Soc. Rev.*, 2022, **51**, 1640–1658.
131 R. Trammell, K. Rajabimoghadam and I. García-Bosch, *Chem. Rev.*, 2019, **119**, 2954–3031.
132 L.-J. Cheng and N. P. Mankad, *Chem. Soc. Rev.*, 2020, **49**, 8036–8064.
133 L. Marais, H. C. M. Vosloo and A. J. Swarts, *Coord. Chem. Rev.*, 2021, **440**, 213958.
134 J. Liu, G. Chen and Z. Tan, *Adv. Synth. Catal.*, 2016, **358**, 1174–1194.
135 I. M. Blythe, J. Xu, J. S. F. Odell, J. W. Kampf, M. A. Bowring and M. S. Sanford, Nowadays, there is little knowledge about the organometallic intermediates involved in directed Cu-catalyzed C–H functionalization reaction. Nonetheless, the group of Sanford described the isolation of key intermediates in the Cu-mediated 8-AQ-directed C(sp^2)–H functionalization of polyfluorinated benzamide derivatives. This study showed that anionic copper complexes are involved in the transformation stabilize Cs^+ counterion. Moreover, while the C–H activation step occurs at copper(II)-species *via* CMD mechanism assisted by carbonate basic additive, the subsequent steps involved copper(III) σ-aryl complexes, *J. Am. Chem. Soc.*, 2023, **145**, 18253–18259.
136 X. Wu, Y. Zhao and H. Ge, *Chem. Sci.*, 2015, **6**, 5978–5983.
137 X. Wu, J. Miao, Y. Li, G. Li and H. Ge, *Chem. Sci.*, 2016, **7**, 5260–5264.
138 W. E. Noland, *Chem. Rev.*, 1955, **55**, 137–155.
139 J. Zhang, D. Li, H. Chen, B. Wang, Z. Liu and Y. Zhang, *Adv. Synth. Catal.*, 2016, **358**, 792–807.
140 U. Halbes-Letinois, J.-M. Weibel and P. Pale, *Chem. Soc. Rev.*, 2007, **36**, 759–769.
141 G. Fang and X. Bi, *Chem. Soc. Rev.*, 2015, **44**, 8124–8173.
142 P. Sivaguru, S. Cao, K. R. Babu and X. Bi, *Acc. Chem. Res.*, 2020, **53**, 662–675.
143 F. Ullmann, *Ber. Dtsch. Chem. Ges.*, 1903, **36**, 2382–2384.
144 I. Goldberg, *Ber. Dtsch. Chem. Ges.*, 1906, **39**, 1691–1692.
145 X. Yan, X. Yang and C. Xi, *Catal. Sci. Technol.*, 2014, **4**, 4169–4177.
146 A. Ribaucourt and J. Cossy, *ACS Catal.*, 2020, **10**, 10127–10148.
147 J.-P. Wan and Y. Jing, *Beilstein J. Org. Chem.*, 2015, **11**, 2209–2222.
148 J.-L. Ma, X.-M. Zhou, P.-H. Guo, H.-C. Cheng and H. B. Ji, *Chin. J. Chem.*, 2022, **40**, 1204–1223.
149 Z. Wang, J. Ni, Y. Kuninobu and M. Kanai, *Angew. Chem., Int. Ed.*, 2014, **53**, 3496–3499.
150 X. Wu, Y. Zhao, G. Zhang and H. Ge, *Angew. Chem., Int. Ed.*, 2014, **53**, 3706–3710.
151 C. Wang, Y. Yang, D. Qin, Z. He and J. You, *J. Org. Chem.*, 2015, **80**, 8424–8429.
152 Q. Gou, Y.-W. Yang, Z.-N. Liu and J. Qin, *Chem. – Eur. J.*, 2016, **22**, 16057–16061.
153 C. Wang and Y. Yang, *Tetrahedron Lett.*, 2017, **58**, 935–940.
154 Z. Wang, Y. Koninobu and M. Kanai, *Org. Lett.*, 2014, **16**, 4790–4793.
155 X. Wu, Y. Zhao and H. Ge, *Chem. – Asian J.*, 2014, **9**, 2736–2739.
156 F. Wang, X. Li, Z. Li, S. Zhou and W. Zhang, *ACS Omega*, 2019, **4**, 331–343.
157 J. Zhang, H. Chen, B. Wang, Z. Liu and Y. Zhang, *Org. Lett.*, 2015, **17**, 2768–2771.
158 J.-H. Liu, M. Cui, X.-Y. Lu, Z.-Q. Zhang, B. Xiao and Y. Fu, *Chem. Commun.*, 2016, **52**, 1242–1245.
159 N. E. Idoine, E. R. Raycraft, S. F. Hobbs, P. Everett, E. J. Evans, A. J. Mills, D. Currie, S. Horn and R. A. Shaw, *World mineral production 2018-22*, British Geological Survey, Keyworth, 2024.
160 I. Bauer and H.-J. Knölker, *Chem. Rev.*, 2015, **115**, 3170–3387.
161 A. Fürstner, *ACS Cent. Sci.*, 2016, **2**, 778–789.
162 S. Cattani and G. Cera, *Chem. – Asian J.*, 2024, **19**, e202300897.
163 R. Shang, L. Ilies, A. Matsumoto and E. Nakamura, *J. Am. Chem. Soc.*, 2013, **135**, 6030–6032.
164 Y. Sun, H. Tang, K. Chen, L. Hu, J. Yao, S. Shaik and H. Chen, *J. Am. Chem. Soc.*, 2016, **138**, 3715–3730.
165 T. E. Boddie, S. H. Carpenter, T. M. Baker, J. C. DeMuth, G. Cera, W. W. Brennessel, L. Ackermann and M. L. Neidig, *J. Am. Chem. Soc.*, 2019, **141**, 12338–12345.

166 Q. Gu, H. H. Al Mamari, K. Graczyk, E. Diers and L. Ackermann, *Angew. Chem., Int. Ed.*, 2014, **53**, 3868–3871.
167 R. Shang, L. Ilies and E. Nakamura, *J. Am. Chem. Soc.*, 2015, **137**, 7660–7663.
168 K. Graczyk, T. Haven and L. Ackermann, *Chem. – Eur. J.*, 2015, **21**, 8812–8815.
169 L. Ilies, Y. Itabashi, R. Shang and E. Nakamura, *ACS Catal.*, 2017, **7**, 89–92.
170 M. S. Kharasch and E. K. Fields, *J. Am. Chem. Soc.*, 1941, **63**, 2316–2320.
171 G. Cahiez and A. Moyeux, *Chem. Rev.*, 2010, **110**, 1435–1462.
172 F. Hebrard and P. Kalck, *Chem. Rev.*, 2009, **109**, 4272–4282.
173 M. M. Tohidi, B. Paymard, S. R. Vasquez-García and D. Fernández-Quiroz, *Tetrahedron*, 2023, **136**, 133352.
174 P. Gandeepan and C.-H. Cheng, *Acc. Chem. Res.*, 2015, **48**, 1194–1206.
175 H. Pellissier and H. Clavier, *Chem. Rev.*, 2014, **114**, 2775–2823.
176 M. Moselage and L. Ackermann, *ACS Catal.*, 2016, **6**, 498–525.
177 T. Gensch, M. N. Hopkinson, F. Glorius and J. Wencel-Delord, *Chem. Soc. Rev.*, 2016, **45**, 2900–2936.
178 Y. Zheng, C. Zheng, Q. Gu and S.-L. You, *Chem. Catal.*, 2022, **2**, 2965–2985.
179 J. Bora, M. Dutta and B. Chetia, *Tetrahedron*, 2023, **132**, 133248.
180 K. Gao and N. Yoshikai, *Acc. Chem. Res.*, 2014, **47**, 1208–1219.
181 D. Tilly, G. Dayaker and P. Bachu, *Catal. Sci. Technol.*, 2014, **4**, 2756–2777.
182 R. Mei, U. Dhawa, R. C. Samanta, W. Ma, J. Wencel-Delord and L. Ackermann, *ChemSusChem*, 2020, **13**, 3306–3356.
183 L. Lukasevics, A. Cizikovs and L. Grigorjeva, *Chem. Commun.*, 2021, **57**, 10827–10841.
184 S. Sunny and R. Karvembu, *Adv. Synth. Catal.*, 2021, **363**, 4309–4331.
185 D. Chandra, Manisha and U. Sharma, *Chem. Rec.*, 2022, **22**, e202100271.
186 E. L. Nolan, F. Qu and M. S. Sanford, To date, it remains unclear whether cobalt(II) centers are directly involved in the C–H activation step. Nonetheless, M. Sanford just reported that the dehydrogenative dimerization of 2,3,4,5-tetrafluoro-*N*-(quinolin-8-yl)benzamide occurs through a first cyclometalation with $Co(OAc)_2$, forming an NNC cobalt(II) pincer complex. Single-electron oxidation with AgOAc generates a cobalt(III) intermediate, which undergoes a second directed $C(sp^2)$–H activation, yielding a bis-cyclometalated octahedral cobalt(III) complex. This cobalt(III) species remains inert to thermal C–C bond-forming reductive elimination, even when heated at 160 °C for 48 hours. However, treatment with ferrocenium oxidants at room temperature induces oxidative carbon–carbon coupling, presumably *via* a cobalt(IV) intermediate, *Organometallics*, 2024, **43**, 2165–2168.
187 T. Yoshino, S. Satake and S. Matsunaga, *Chem. – Eur. J.*, 2020, **36**, 7346–7357.
188 T. Yoshino and S. Matsunaga, in *C–H Functionalization Catalyzed by Cobalt(III)/Cp* and Related Complexes*, ed. N. Yoshikai, Georg Thieme Verlag KG, 1st edn, 2023.
189 J. Zhang, H. Chen, C. Lin, Z. Liu, C. Wang and Y. Zhang, *J. Am. Chem. Soc.*, 2015, **137**, 12990–12996.
190 J.-H. Wu and H.-Q. Yu, *Environ. Sci. Technol.*, 2024, **58**, 18496–18507.
191 L. Staronova, K. Yamazaki, X. Xu, H. Shi, F. M. Bickelhaupt, T. A. Hamlin and D. J. Dixon, *Angew. Chem., Int. Ed.*, 2024, **63**, e202316021.
192 M. Sen, B. Emayavaramban, N. Barsu, J. R. Premkumar and B. Sundararaju, *ACS Catal.*, 2016, **6**, 2792–2796.
193 N. Barsu, S. K. Bolli and B. Sundararaju, *Chem. Sci.*, 2017, **8**, 2431–2435.
194 P. Williamson, A. Galván and M. J. Gaunt, *Chem. Sci.*, 2017, **8**, 2588–2591.
195 L. Zeng, S. Tang, D. Wang, Y. Deng, J.-L. Chen, J.-F. Lee and A. Lei, *Org. Lett.*, 2017, **19**, 2170–2173.
196 N. Barsu, D. Kalsi and B. Sundararaju, *Catal. Sci. Technol.*, 2018, **8**, 5963–5969.
197 H. Wang, S. Zhang, Z. Wang, M. He and K. Xu, *Org. Lett.*, 2016, **18**, 5628–5631.
198 Z.-Z. Zhang, Y.-Q. Han, B.-B. Zhan, S. Wang and B.-F. Shi, *Angew. Chem., Int. Ed.*, 2017, **56**, 13145–13149.
199 S.-Y. Yan, P.-X. Ling and B.-F. Shi, *Adv. Synth. Catal.*, 2017, **359**, 2912–2917.
200 H. Christian, R. Georg, S. Jean-Philippe and Z. A. Cornelia, *U.S. Pat.*, 2010/331318 A1, 2010.
201 S. D. Friis, M. J. Johansson and L. Ackermann, *Nat. Chem.*, 2020, **12**, 511–519.
202 X.-X. Chen, J.-T. Ren, J.-L. Xu, H. Xie, W. Sun, Y.-M. Li and M. Sun, *Synlett*, 2018, 1601–1606.
203 R. Kumar, R. Kumar, D. Chandra and U. Sharma, *J. Org. Chem.*, 2019, **84**, 1542–1552.
204 N. Li, Y. Wang, L. Kong, J. Chang and X. Li, *Adv. Synth. Catal.*, 2019, **361**, 3880–3885.
205 H. Tan, R. Khan, D. Xu, Y. Zhou, X. Zhang, G. Shi and B. Fan, *Chem. Commun.*, 2020, **56**, 12570–12573.
206 X. Wu, K. Yang, Y. Zhao, H. Sun, G. Li and H. Ge, *Nat. Commun.*, 2015, **6**, 6462.
207 S. Dutta, S. Chatterjee, S. A. Al-Thabaiti, S. Bawaked, M. Mokhtar and D. Maiti, *Chem. Catal.*, 2022, **2**, 1046–1083.
208 Y. N. Timsina, B. F. Gupton and K. C. Ellis, *ACS Catal.*, 2018, **8**, 5732–5776.
209 P. W. Tan, A. M. Mak, M. B. Sullivan, D. J. Dixon and J. Seayad, *Angew. Chem., Int. Ed.*, 2017, **56**, 16550–16554.
210 S. Fukagawa, Y. Kato, R. Tanaka, M. Kojima, T. Yoshino and S. Matsunaga, *Angew. Chem., Int. Ed.*, 2019, **58**, 1153–1157.
211 D. Sekine, K. Ikeda, S. Fukagawa, M. Kojima, T. Yoshino and S. Matsunaga, *Organometallics*, 2019, **38**, 3921–3926.
212 R.-H. Liu, Q.-C. Shan, X.-H. Hu and T.-P. Loh, *Chem. Commun.*, 2019, **55**, 5519–5522.
213 L. Liu, Z. Zhang, Y. Wang, Y. Zhang and J. Li, *Synthesis*, 2020, 3881–3890.

214 N. Barsu, Md. A. Rahman, M. Sen and B. Sundararaju, *Chem. – Eur. J.*, 2016, **22**, 9135–9138.
215 H. Zhang, M.-C. Sun, D. Yang, T. Li, M.-P. Song and J.-L. Niu, *ACS Catal.*, 2022, **12**, 1650–1656.
216 J. J. Neumann, S. Rakshit, T. Droge and F. Glorius, *Angew. Chem., Int. Ed.*, 2009, **48**, 6892–6895.
217 F. Pan, B. Wu and Z.-J. Shi, *Chem. – Eur. J.*, 2016, **22**, 6487–6490.
218 H. Zhang, D. Yang, X.-F. Zhao, J.-L. Niu and M.-P. Song, *Org. Chem. Front.*, 2022, **9**, 3723–3729.
219 U. Dhawa, N. Kaplaneris and L. Ackermann, *Org. Chem. Front.*, 2021, **8**, 4886–4913.

